HZDR-004

Wissenschaftlich-Technische Berichte
HZDR-004 2011 · ISSN 2191-8708

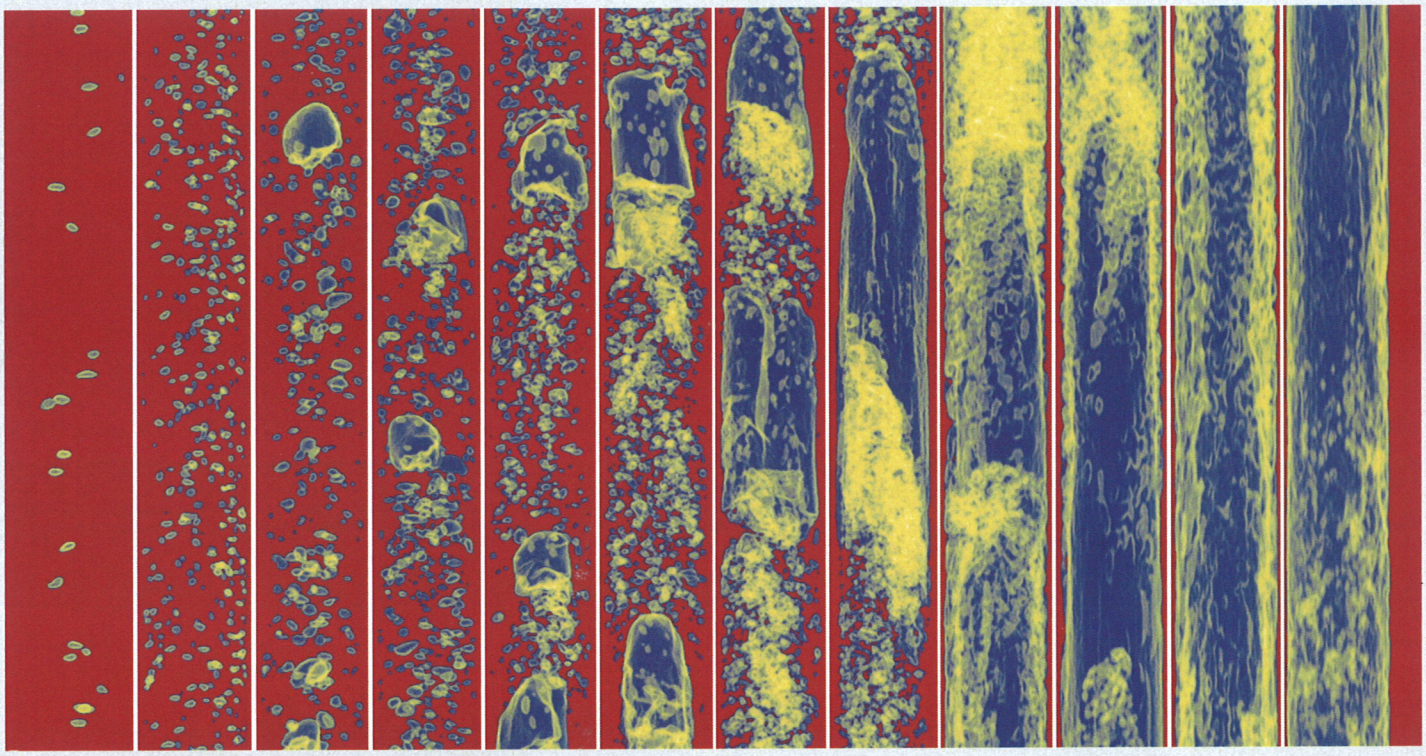

ANNUAL REPORT 2010

INSTITUTE OF SAFETY RESEARCH

HZDR

HELMHOLTZ
ZENTRUM DRESDEN
ROSSENDORF

Wissenschaftlich-Technische Berichte
HZDR-004
2011

HZDR

HELMHOLTZ ZENTRUM DRESDEN ROSSENDORF

Annual Report 2010

Institute of Safety Research

Editors:
Dr. Gunter Gerbeth
Dr. Frank Schäfer

Cover Picture: Visualisation of two phase flow structures in a vertical pipe.
The figure shows co-current upwards air-water flow in a titanium-pipe with an inner diameter of 54 mm measured by ultrafast X-ray tomography. While the liquid flow rate is kept constant, the gas flow rate increases from left to right.

Helmholtz-Zentrum Dresden-Rossendorf
Institut für Sicherheitsforschung

Postfach 51 01 19
D-01314 Dresden
Bundesrepublik Deutschland

komm. Direktor Dr. Gunter Gerbeth
Telefon + 49 (3 51) 2 60 34 80
Telefax + 49 (3 51) 2 60 34 40
E-Mail g.gerbeth@hzdr.de
WWW http://www.hzdr.de/FWS

CONTENTS

Preface

The Institute of Safety Research (ISR) was over the past 20 years one of the six Research Institutes of Forschungszentrum Dresden-Rossendorf e.V. (FZD), which in 2010 belonged to the Wissenschaftsgemeinschaft Gottfried Wilhelm Leibniz. Together with the Institutes of Radiochemistry and Radiation Physics, ISR implements the research programme „Nuclear Safety Research“ (NSR), which was during last years one of the three scientific programmes of FZD. NSR involves two main topics, i.e. “Safety Research for Radioactive Waste Disposal” and “Safety Research for Nuclear Reactors”. The research of ISR aims at assessing and enhancing the safety of current and future reactors, the development of advanced simulation tools including their validation against experimental data, and the development of the appropriate measuring techniques for multi-phase flows and liquid metals.

The subtopic “Materials and Components Safety” is focused on the experimental investigation and modelling of the irradiation induced ageing of reactor construction materials. Monte-Carlo transport calculations are used to characterize the neutron irradiation in terms of flux and dose. Authentic irradiated specimens from decommissioned reactor pressure vessels and irradiated model alloys are subjected to fracture mechanical tests in dedicated hot cells. The irradiated reactor pressure vessel steels are investigated by advanced techniques in order to detect and characterize the neutron induced defects on the nano and sub-nano meter scale. On one hand, these experimental data along with the mechanical test results are used to gain basic understanding of the ageing mechanisms. On the other hand, these data constitute the reference for the multi-scale modelling of the ageing effects ranging from molecular dynamics and rate theory up to fracture mechanical calculations. This subtopic relies on close collaboration with the Institute of Ion Beam Physics and Materials Research inside FZD regarding the modelling efforts. The research work is embedded in EURATOM projects on the ageing of reactor materials like NULIFE, PERFORM60, and LONGLIFE. The latter is coordinated by FZD.

The subtopics “Thermal Fluid Dynamics of Multi-Phase Flows” and “Magneto-Hydrodynamics (MHD)” deal with the thermal hydraulics of light water reactors (LWR) and liquid metal flows. The thermal hydraulics studies aim at the development of a new generation of thermal hydraulic simulation tools that are capable of describing transient multi-phase flows relying on models which consider the local flow characteristics. These tools have to be validated against experimental data of sufficient resolution in space and time to allow for appropriate comparison with the calculations. For that reason, the transient two-phase flow test facility TOPFLOW is an essential element of FZDs reactor safety research. Due to its industry relevant scale, its sophisticated experimental techniques, as e.g. the pressurised chamber, and above all because of the advanced instrumentation, TOPFLOW represents a unique facility worldwide. The development of measuring techniques for multi-phase flows, up to fast tomographic imaging, is constitutional part of our reactor safety research.
Generation IV fast nuclear reactors use liquid metal coolants like sodium or lead, transmutation facilities or neutron spallation sources are supposed to work with a liquid lead-bismuth target. Adequate instrumentation for such liquid metal flows is decisive for the basic safety concept of these reactors. The new multi-purpose sodium platform DRESDYN, of which the design has been started in 2010, will offer the unique chance for the development of the above mentioned technologies. The results obtained at DRESDYN will also be used to develop and validate adequate simulation tools for liquid metal flows. DRESDYN will also be designed to astrophysical laboratory experiments, related for instance to the self-excitation of cosmic magnetic fields and to the role of magnetic fields in the stability of cosmic flows. The platform offers the unique chance to combine both types of experiments in one and the same

experimental environment. The MHD research is implemented in close collaboration with partners from TU Dresden, TU Bergakademie Freiberg, and IFW Dresden in frame of the Collaborative Research Centre SFB 609 funded by DFG.
Both, the activities on LWR thermal hydraulics and on liquid metals are integrated into key European projects such as NURISP, ADRIANA, CP-ESFR or THINS.

The subtopic "Accident Analysis of Nuclear Reactors" makes use of the results generated by the materials and thermal hydraulics research of the reactor safety programme in order to create new quality simulation tools for current and future reactors and to analyse the safety of these reactors. In the centre of this subtopic, our in house three-dimensional reactor dynamics code DYN3D is continuously developed with regard to the

- implementation of neutron transport options into the diffusion based code,
- the availability of multi-scale options in neutronics calculations,
- the integration into a multi-physics environment,
- the link to sensitivity and uncertainty analysis tools, and
- code versions for GEN-IV reactors.

These efforts are embedded into the European initiative NURESIM (Nuclear Reactor Simulation) on the creation of a uniform simulation platform for nuclear reactors. DYN3D is one of the reference codes within this platform. DYN3D can refer to a growing user community. The support of these users, in particular of the Eastern European users applying DYN3D to the safety analysis of Russian reactors, is part of the subtopic. There is clearly a growing interest of industry in getting access to DYN3D.
Moreover, the subtopic addresses experimental and theoretical mixing studies in the context of LWR boron dilution and cold water scenarios as well as experiments and simulations on the possible clogging of LWR sump screens and of the fuel assembly spacer grids by insulation material released in a loss of coolant accident.
The activities in accident analysis are parts of large international (EU, OECD, AER, etc.) and national research projects. Recently, there is a clear tendency to shift the emphasis in the subtopic from LWRs to high-temperature and GEN-IV reactors.

ISR is financed through the basic funding of FZD, as well as by external funds from public research grants and from contracts with industry. In 2010, 49% (4.695 k€) of our total expenditure were covered by such external funds with 26% from research grants of the Federal Government, 8% originated from Deutsche Forschungsgemeinschaft, 4% from EU, and 11% from research contracts with industry (see Fig. 1). The deployment of the total budget on the different projects and the user facility TOPFLOW is illustrated in Fig. 2.

Together with the Dresden Technical University, the Zittau University of Applied Sciences, and VKTA (Verein für Kernverfahrenstechnik und Analytik) Rossendorf, the ISR represents the East German Centre of Competence in Nuclear Technology (Kompetenzzentrum Ost für Kerntechnik) which in turn is a member of the German Alliance for Competence in Nuclear Technology (Kompetenzverbund Kerntechnik). As such, ISR also takes care to keep and promote the expertise in nuclear engineering.

Since autumn 2010 significant changes took place at ISR and FZD. At first, the long-term and founding director of ISR, Prof. Dr. Frank-Peter Weiß left ISR with the beginning of November 2010 and became the CEO of the German Gesellschaft für Anlagen- und Reaktorsicherheit. I took over the acting directorship with the expectation that a new director of ISR will be selected via the usual appointment procedure. With the begin of 2011, FZD became a member of the German Helmholtz society (HGF) and changed his name to "Helmholtz-Zentrum Dresden-Rossendorf (HZDR)". HGF is clearly a much better host for nuclear safety research as this subject is within HGF a dedicated programme in frame of the

research field Energy. As already well-prepared over the years, the cooperation with KIT and FZJ will be further intensified and coordinated under the HGF roof.

In March 2011 the Fukushima nuclear accident took place and in the following few months Germany decided to finally escape from the use of nuclear power until 2022. This so-called "Energiewende", which was already longer planned but became now more definitive, is strongly based on the decision that renewable energy sources, mainly wind and solar, shall take over a significantly larger part of the German energy supply. No doubt, the handling of such highly fluctuating sources will be a challenging task for the next decade. Not less challenging will be the question how the requested CO_2 reduction shall be realized on the background of the decided programme to install new coal or gas based power stations. Furthermore, the announced goals of energy reduction (20% until 2020, 50% until 2050) appear as even more challenging in view of the fact that major strategic developments (photovoltaic, e-mobility, new transmission lines) represent, at least for a transitional period of several years, dedicated activities of increased power consumption.

After Fukushima the role of nuclear safety research in Germany was intensively discussed among the related authorities. Fortunately, there was a clear and complete agreement that the escape from nuclear power generation shall not be accompanied by an escape from the related safety research. In August 2011 it was fixed in frame of the 6th energy research programme of the German government that research works on nuclear safety research shall be continued in Germany approximately on the existing level. Know-how conservation as well as education and training of young people are particularly mentioned as important topics for NSR.

The general change connected with the German Energiewende has triggered a decision of the HZDR's Board of Directors to re-organize the works in the two institutes of Safety Research and Radiochemistry in such a way that both institutes will be closed at the end of 2011, but the two new institutes of Fluiddynamics and Ressource-Ecology will be created. The latter institute will involve the previous activities of "Accident Analysis of Nuclear Reactors" with an increasing focus on the subject of Transmutation. The fluiddynamic investigations will partly remain in the NSR programme, but will also belong to the new HGF programme of "Materials, Energy- and Resource-Efficiency". The NSR activities on materials research will in future belong to the institute of Ion Beam Physics and Materials Research. There is a clear agreement at HZDR that the programme works on NSR will be continued on the presently existing level, in particular in close cooperation with the partners of the HGF research programme and the Kompetenzzentrum Ost für Kerntechnik.

Due to this restructuring at HZDR, the present annual report of the Institute of Safety Research will be the last one. ISR has developed over the past 20 years to a well-recognized partner in the national and international nuclear safety research, which was only possible due to the encouraging work of all staff members and, in particular, the guidance of the previous director, Prof. Dr. Frank-Peter Weiß. I would like to thank all staff members of the institute for their engagement and high quality work.

Gunter Gerbeth

Rossendorf, November 17, 2011

Fig. 1: Funding sources 2010

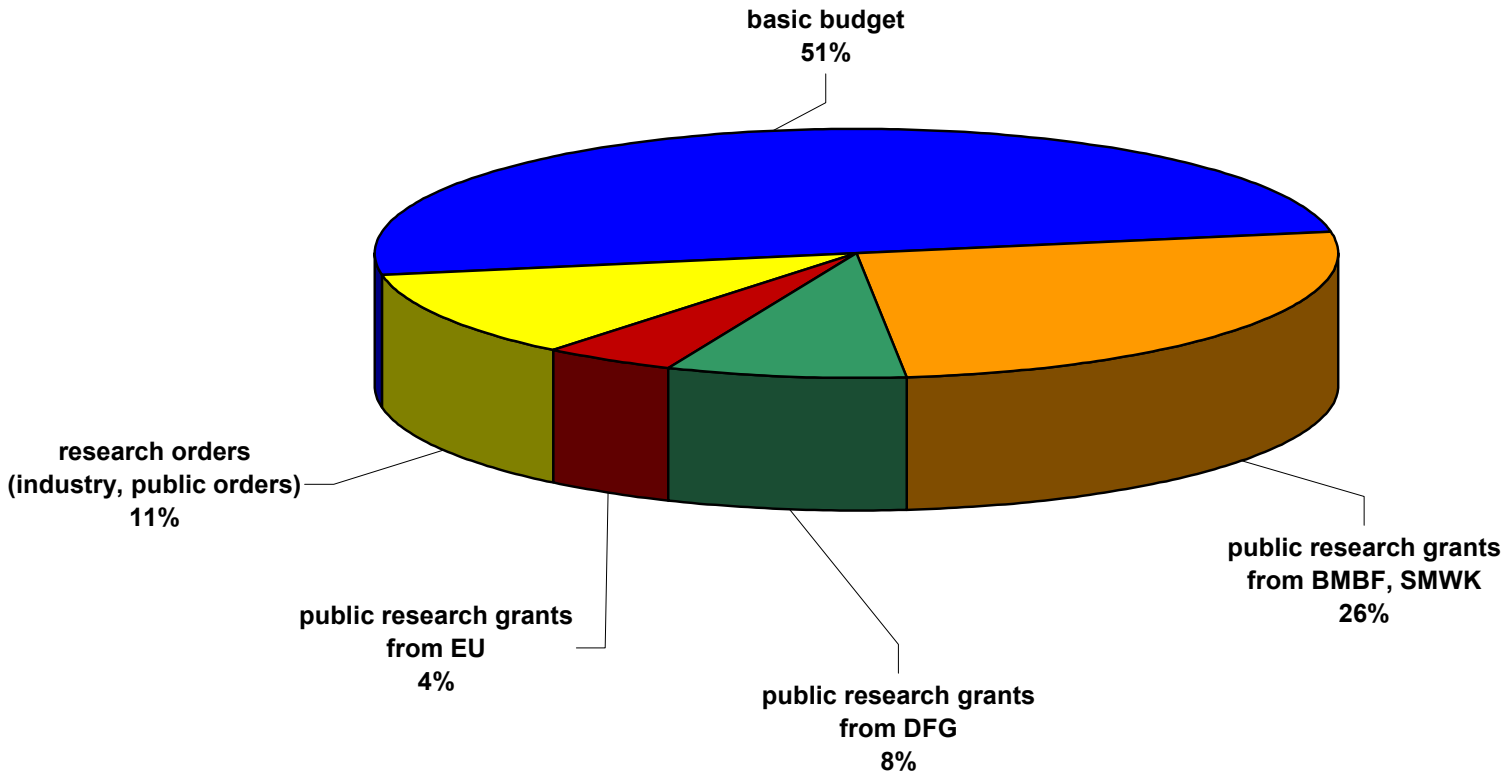

Fig. 2: Deployment of funding on the subtopics and the user facility TOPFLOW in 2010

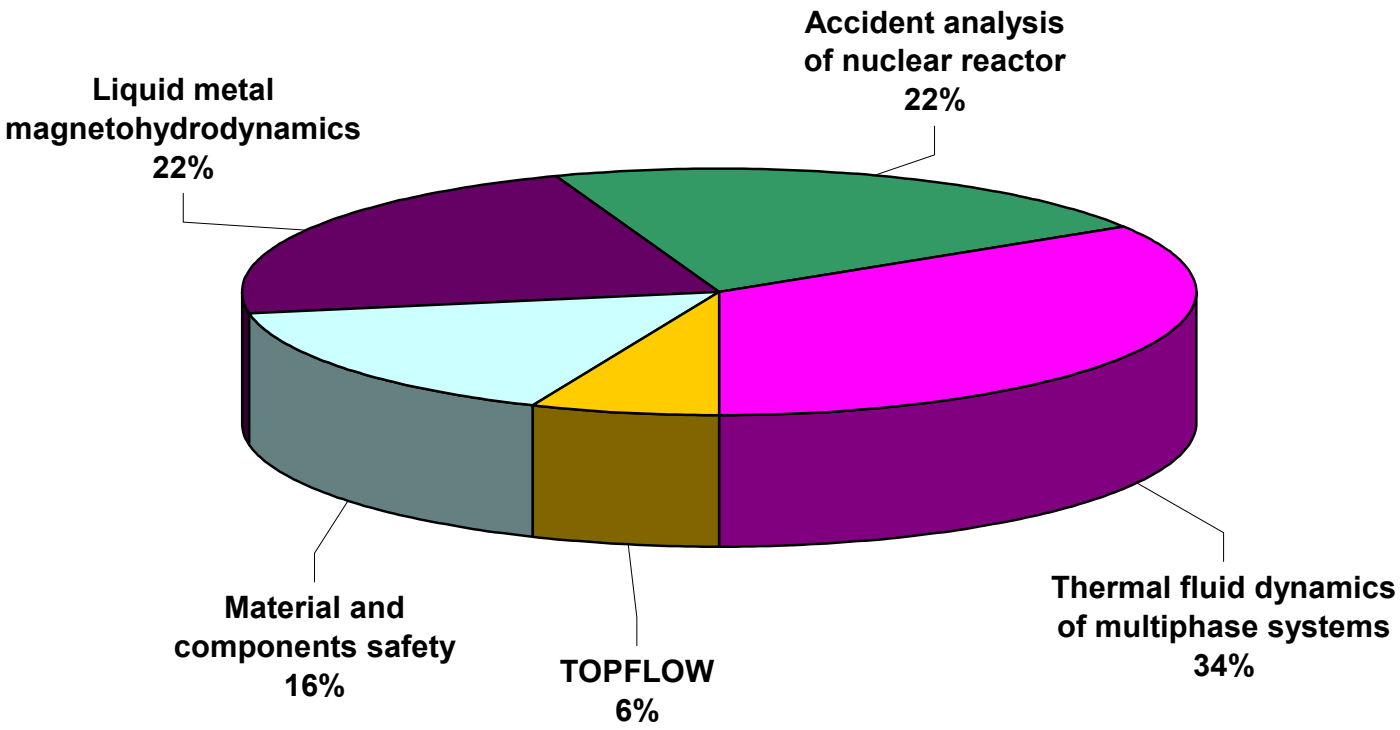

Selected reports

ULTRAFAST THREE-DIMENSIONAL LIMITED-ANGLE X-RAY COMPUTED TOMOGRAPHY

Martina Bieberle, Frank Barthel, Hans-Jürgen Menz[1], Hans-Georg Mayer[1], and Uwe Hampel

1. Introduction

Recent years have seen considerable progress in fast imaging techniques. Most notably, high-speed cameras have evolved towards imaging devices which are able to acquire hundred thousands of images [1]. In many scientific and engineering problems, however, radiation based imaging techniques are needed, which can give insight into the structure of opaque bodies. Since fast X-ray radiography [2] is only able to provide superimposed images, a focus of research lies on the acceleration of computed tomography methods. Especially in the field of flow imaging, a number of new techniques have been developed for example by using multiple gamma ray [3] or X-ray sources [4]. Also, magnetic resonance imaging [5] is able to provide high-resolution images at comparatively moderate speed (100 s^{-1}) However, none of today's tomographic imaging modalities is able to visualize processes at rates above 100 frames per second with high spatial resolution in three spatial dimensions. Nevertheless, this is highly desirable for flow measurements because phase-boundaries and flow structures will not be bound to a frozen axial movement in the main flow direction.

Recently, we introduced ultrafast electron beam X-ray computed tomography to flow measurement [6]-[8]. This technology allows cross-sectional imaging of objects with up to 10 000 frames per second speed. Now we demonstrate the opportunity to obtain volumetric image data [9] with a spatial resolution in the range of one millimetre and a temporal resolution of more than 500 volumes per second using an experimental tomography setup.

2. Electron beam X-ray CT

2.1. Setup

The principle of three-dimensional ultrafast electron beam X-ray CT is illustrated in Fig. 1. An electron beam of 150 kV acceleration voltage and 7 mA beam current is focused onto an elongated tungsten target which has a step-like geometry. An electromagnetic deflection system scans the electron beam with a frequency of 2 kHz across the 160 mm long tungsten target such that the focal spot sweeps successively from top to bottom across each of the 8 milled target steps. The sweep time per step is 250 µs and thus a volumetric image rate of 500 volumes per second is reached. From the moving focal spot, X-rays are emitted, which pass the object in front of the target and are registered by an X-ray detector arc on the opposite side (256 pixel, 1.5 × 1.5 mm² pixel size, 1 MHz sampling rate). The whole setup, including the object of investigation, is operated in a vacuum chamber.

The acquisition of projections differs from conventional X-ray CT in that way, that the angular range of projections is confined to the end points of the focal spot path on the target (limited angle CT). Projections from all possible angles around the object as required for conventional CT cannot be acquired due to restrictions imposed by three-dimensional imaging with a fixed detector. A full angle CT would require an angular overlap of target and

[1] Institute of Nuclear Energy Technology and Energy Systems, Stuttgart University

detector which is not feasible. As a consequence it is no longer practicable to reconstruct images with analytical image reconstruction techniques. Instead iterative algorithms are appropriate. From the viewpoint of three-dimensional tomography the used projection scheme is similar to classical cone-beam tomography [10]. The difference lies mainly in the inverse arrangement of a single detector arc and multiple source paths instead of a single source path and an array of detector elements.

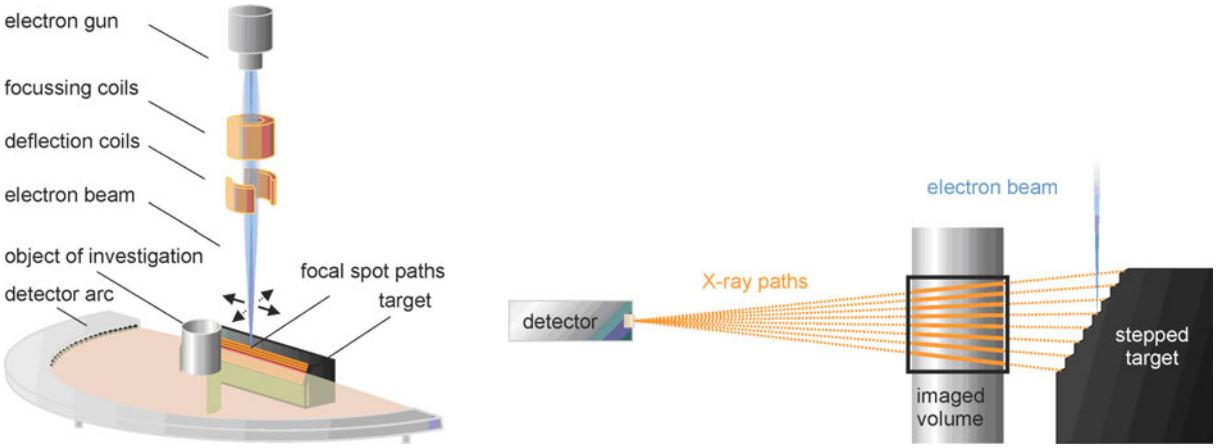

Fig. 1: Experimental setup of ultrafast 3D electron beam X-ray computed tomography

2.2. Data processing

The inverse problem requires iterative image reconstruction, which means, that the projection measurement is modeled by the linear equation system $\mathbf{p} = \mathbf{A} \cdot \boldsymbol{\mu}$, which considers the integral attenuation values p_k of an X-ray path k as a sum of individual voxel contributions

$$p_k = -\log\left(I / I_0\right)_k = \sum_n a_{kn} \mu_n \,. \tag{1}$$

Therein, I and I_0 denote the attenuated and reference X-ray intensities for the ray, μ_n the attenuation coefficient in the volume element n and a_{kn} the geometric contribution of voxel n to X-ray k. The number of X-rays (or projection values) is given by the number of source positions times the number of detector elements and the number of voxels is given by the size and resolution of the 3D volume to be reconstructed. The algebraic reconstruction technique (ART) [11] as one of the most accepted iterative reconstruction methods with the iteration formula

$$\boldsymbol{\mu}^{(i+1)} = \max\left(0, \boldsymbol{\mu}^{(i)} + \lambda \frac{p_k - \mathbf{a}_k \cdot \boldsymbol{\mu}^{(i)}}{\left\|\mathbf{a}_k\right\|^2} \cdot \mathbf{a}_k^{\mathrm{T}}\right) \tag{2}$$

has been implemented to solve (1).
For the study of binary distributions, as for example in two-phase flows, in which the attenuation coefficients of the single phases are known *a priori*, an alternative reconstruction algorithm has been implemented. It aims at a direct reconstruction of phase boundaries from the projection data. This algorithm is derived from the level set method [12], which was originally developed to model moving interfaces. The new level set reconstruction (LSR) algorithm directly recovers the phase boundaries from the tomographic projections by treating the phase boundary as the zero level set of an underlying function φ. This level set function is iteratively deformed by a force function F, satisfying in each step the level set equation

$$\frac{\partial \varphi}{\partial t} + F\left|\nabla \varphi\right| = 0\,. \tag{3}$$

Following the ART concept, the discrete values for the force function F are chosen as the sum of the normalized deviations between the measured attenuation values p_k and the ones determined by the binary distribution $\boldsymbol{\mu}^{(i)}$, which in turn is defined by the current boundary $(\varphi = 0)$, that is

$$\mathbf{F}^{(i)} = \sum\nolimits_k \left[\left(\mathbf{a}_k \boldsymbol{\mu}^{(i)} - p_k \right) \cdot \frac{\mathbf{a}_k}{\left\| \mathbf{a}_k \right\|^2} \right]. \tag{4}$$

The LSR algorithm converges towards a solution which defines a binary distribution with the same projection values as the measured projection data. Thus, this algorithm combines different advantages. First, the phase assignment is directly integrated in the reconstruction process, i.e. no further processing is necessary. At the same time, the limited-angle artifacts are effectively suppressed, since the lack of information from the inaccessible viewing angles is compensated by the *a priori* information about the attenuation coefficient of the involved phases. Finally, the level set approach leads smooth boundaries and thus prevents noise in the projection data from reducing the image quality exceedingly.

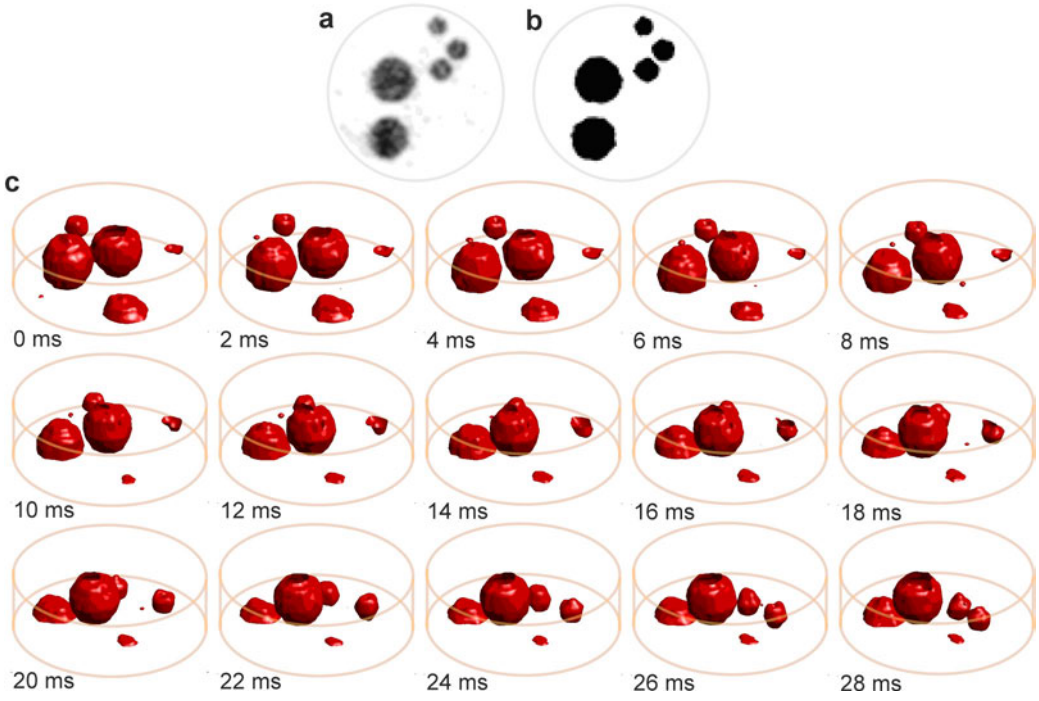

Fig. 2: Tomography results of fluidized particles of diameter 2 mm, 5 mm and 10 mm: reconstructed cross-section using ART (a) and LSR (b), sequence of rendered volume images (c)

3. Experiments

In order to test the capability of ultrafast x-ray tomography to image dynamic three-dimensional material distributions, different experiments have been carried out. A modified commercial electron beam welding system served as an X-ray scanning system. It provides all

necessary features such as a high power electron beam with vacuum and deflection system. The X-ray detector was specifically designed for this application and purpose-built reconstruction software was applied.

3.1. Fluidized particles

In a first experiment, the movement of fluidized large particles in an upward gas flow was studied. Polyoxymethylene balls of 2 mm, 5 mm and 10 mm diameter served as particles for fluidization inside an aerated vertical pipe of 38 mm inner diameter. The balls could freely move within a small axial section defined by two wire mesh barriers. A reference measurement (I_0 in eq. (1)) with no balls in the scanned volume and flow measurements (I) with balls at an adjusted air flow rate were acquired.

The measured data was pre-processed and reconstructed using ART and LSR, respectively. The results of the two alternative reconstruction techniques described above are presented in Fig. 2a and b in form of cross-sectional images. Furthermore, a sequence of rendered 3D images of the reconstructed distributions is shown (Fig. 2c). As can be seen, the irregular movements of the balls are fully captured without any motion artefacts. Particle velocities were determined by simple displacement analysis, which recovered a maximum of 1.4 m/s. The shapes of the particles are not distorted as it is known from limited-angle CT owing to the level-set-reconstruction. The particle sizes have been extracted from the 3D images and a standard deviation of 0.19 mm from the nominal radius of the balls was found for the level set reconstruction.

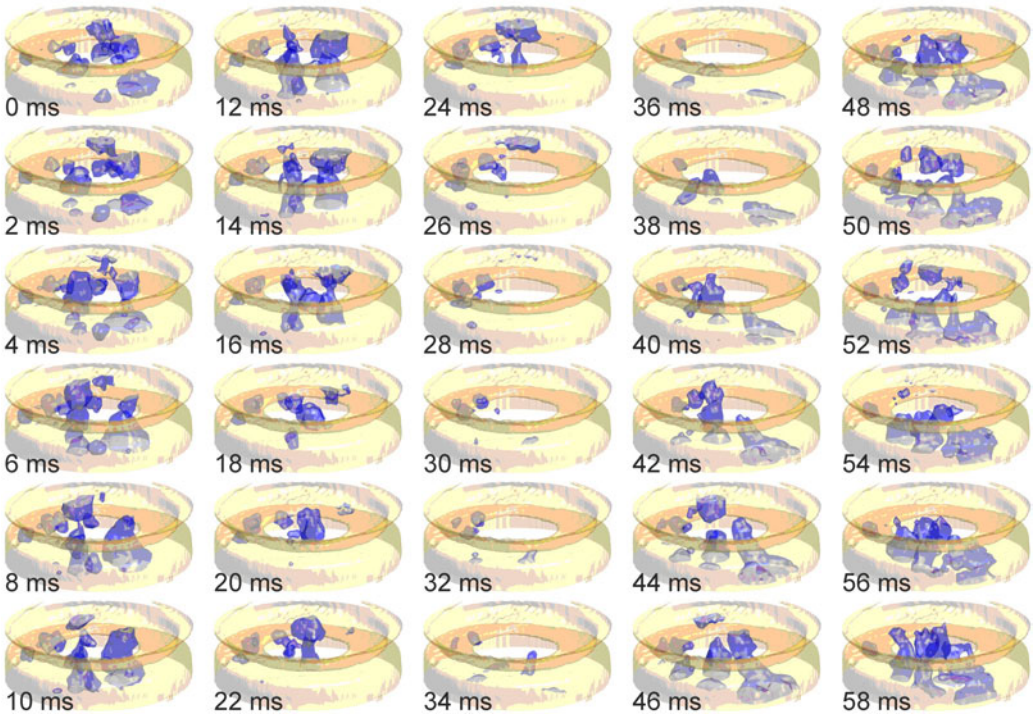

Fig. 3: Tomography results of a bubbly water-air two-phase flow passing an 18 mm diameter orifice in a 38 mm diameter pipe

3.2. Water-air two-phase flow

In a second experiment, a water-air two-phase flow within an upward pipe of 38 mm diameter was studied. In order to examine a real three-dimensional phenomenon of practical relevance, an orifice that reduces the pipe diameter by a factor of about two was placed within the pipe and the two-phase flow passing this obstacle was observed. Gas has been injected 22 mm below the orifice and different liquid and air flow rates have been studied over a period of one second each. Fig. 3 shows part of a sequence acquired at a liquid flow rate of 20 l/min (0.30 m/s superficial liquid velocity) and a gas flow rate of 10 l/min (0.15 m/s superficial gas velocity). Each frame shows the extracted phase boundaries in combination with the contours of the orifice. The sequence visualizes gas bubbles which are captured within the stagnation zones upstream of the orifice as well as bubbles which are elongated by the flow acceleration while passing the orifice. This impressively demonstrates the capability of this ultrafast X-ray tomography to recover the three-dimensional structure of a complex two-phase flow, which cannot be achieved with any other measurement technique at such temporal and spatial resolution by now. Furthermore, due to the high imaging speed, gas bubbles could be tracked over several volume frames and even their dynamic deformation by different forces within the flow can be studied. In this way, this simple experiment provides already valuable information for the modelling of bubble forces in disperse gas-liquid flows and the validation of direct numerical simulation of complex flows.

4. Conclusions

A new ultrafast three-dimensional X-ray tomography method has been presented and its capability to visualize highly dynamic flow situations with distinct three-dimensional structure has been demonstrated. In a fluidized particle experiment, the free three-dimensional motion of polyoxymethylene particles has been captured and the sizes as well as the velocities of the particles have been determined. In a two-phase flow experiment visualizing the phase boundaries of the flow while passing through an orifice an even more complex flow could be studied. We consider the experiments presented as an initial step into a new world of ultrafast three-dimensional X-ray tomography. This new method can be very valuable for the modelling of complex multiphase flow and stimulate further experimental studies. As a proof-of-principle it shall furthermore open the door towards more dedicated scanner developments.

References

[1] R. D. Brown, Z. Warhaft, G. A. Voth (2009), Acceleration statistics of neutrally buoyant spherical particles in intense turbulence, Phys. Rev. Lett. 103, 194501.

[2] Y. J Wang, X. Liu, K.-S. Im, W.-K. Lee, J. Wang, K. Fezzaa, D. L. S. Hung, J. R. Winkelmann (2008), Ultrafast X-ray study of dense-liquid-jet flow dynamics using structure-tracking velocimetry, Nature Phys. 4, 305-309.

[3] G. A. Johansen, T. Frøystein, B. T. Hjertaker, Ø. Olsen (1996), A dual sensor flow imaging tomographic system, Meas Sci Technol 7, 297–307.

[4] K. Hori, T. Fujimoto, K. Kawanashi, H. Nishikawa H (2000), Development of an ultra fast X-ray computed tomography scanner system: application for measurement of instantaneous void distribution of gas–liquid two-phase flow, Heat Trans Asian Res 29(3), 155-165.

[5] C. R. Müller, J. F. Davidson, J. S. Dennis, P. S. Fennell, L. F. Gladden, A. N. Hayhurst, M. D. Mantle, A. C. Rees, A. J. Sederman (2006), Real-Time Measurement of Bubbling Phenomena in a Three-Dimensional Gas-Fluidized Bed Using Ultrafast Magnetic Resonance Imaging, Phys. Rev. Lett. 96, 154504.

[6] M. Bieberle, F. Fischer, E. Schleicher, D. Koch, K. S. do Couto Aktay, H.-J. Menz, H.-G. Mayer, U. Hampel (2007), Ultra fast limited-angle type X-ray tomography, Appl. Phys. Lett. 91, 123516.
[7] M. Bieberle, F. Fischer, E. Schleicher, D. Koch, H.-J. Menz, H.-G. Mayer, U. Hampel (2009), Experimental two-phase flow measurement using ultra fast limited-angle-type electron beam X-ray computed tomography, Exp. Fluids 47(3), 369-78.
[8] M. Bieberle, F. Fischer, E. Schleicher, H.-J. Menz, H.-G. Mayer, U. Hampel (2010), Ultrafast cross-sectional imaging of gas-particle flow in a fluidized bed, AIChE Journal 56(8), 2221-25.
[9] M. Bieberle, F. Barthel, H.-J. Menz, H.-G. Mayer, U. Hampel (2011), Ultrafast three-dimensional X-ray computed tomography, Appl. Phys. Lett. 98, 034101.
[10] L. A. Feldkamp, L. C. Davis, J. W. Kress (1984), Practical cone-beam algorithm, J. Opt. Soc. Am. A 1, 612-19.
[11] R. Gordon, R. Bender, G. T. Herman (1970), Algebraic reconstruction techniques (ART) for three-dimensional electron microscopy and X-ray photography, J Theor Biol 29, 471-481.
[12] J. A. Sethian (1999), Level Set Methods and Fast Marching Methods, Cambridge University Press, Cambridge.

Acknowledgements

This work was supported by Deutsche Forschungsgemeinschaft (DFG) grant no. HA 3088/3-1 and KO 2942/3-1.

AUTONOMOUS SENSOR PARTICLES FOR PARAMETER TRACKING IN LARGE REACTOR VESSELS

Sebastian Reinecke, Martin Tschofen, Uwe Pöpping, and Uwe Hampel

1. Introduction

The acquisition of spatial parameter distributions in large-scale vessels, such as large tanks, reactors, fermenters, etc., is of great interest for the investigation and optimization of industrial processes. This is especially the case for fermentation biogas reactors, where a number of process parameters, such as the temperature profile, distribution of pH, local growth rate of the biomass, gas-liquid fraction in the substrates as well as flow characteristics, such as velocity profiles, dead zone locations and short-circuits of liquids, are of interest to engineers and operators. Knowledge of a few basic physical parameters, such as temperature and local velocities, allows us to draw conclusions with regard to the efficiency of the mixing and heating regimes. However, in most industrial applications and especially in fermentation gas production, the measurement and monitoring of significant parameters in reactor vessels is hampered by limited access to the process itself, because sensor mounting or cable connections are not feasible or desired. Furthermore, state of the art instrumentation of such reactors is commonly limited to few spatial positions. On the other hand, measurement techniques giving spatial parameter distributions, such as tomographic, infrared, or optical imaging techniques, are mostly not feasible due to the size of vessels or the opaque nature of the mixed liquors and vessel walls. Thus, there is a need for advanced and distributed measurement techniques and process monitoring in large-scale vessels and containers (for more details we refer to [1]). For the reasons given above, remote sensing and autonomous sensor concepts have gained increasing attention in recent years. The ongoing miniaturization of sensors and the increasing capability of highly integrated circuits have enabled the design of multi-parameter systems for the acquisition, storage and communication of physical, chemical or biological process parameters that can be combined in a small-scale and compact system design [2].

A swarm of autonomous sensor particles and a corresponding base station has been designed and tested. Validation experiments have been carried out, where the sensor swarm has been applied to the flow conditions of fermentation reactors. Analysis of the acquired data delivers conclusive information about spatially distributed process parameter and the internal reactor conditions in general. Although the intended application of the sensor swarm is in a large-scale process such as a stirred fermentation biogas reactor, generally it is not limited to this type of process.

2. System Hardware Design

The system incorporates a swarm of numerous autonomous sensor particles and a corresponding base station (see Fig. 1a and 1b). A block diagram of the system is shown in Fig. 1a and 1b depicts a photograph of the measurement system used during the trials. Each sensor particle comprises of a robust and neutrally buoyant capsule (diameter 45 mm and total height 73 mm), which is equipped with measurement electronics and three miniaturized sensors, capturing the basic physical process parameters, namely temperature, pressure as well as three-axis particle acceleration namely for temperature, pressure (i.e. immersion depth) and acceleration (see Fig. 1a and 2a). These parameters are already quite instructive for the evaluation of local flow (mixing) and fermentation conditions. To fit to typical biogas

fermenter conditions the measuring ranges of these sensors were chosen as follows: pressure from 100 kPa to 200 kPa, temperature from 10 °C to 70 °C and acceleration from -2g to +2g. In the future, however, this set of sensors shall be complemented by other sensors, such as pH/OPR sensors, biochemical sensors or gas sensors. Each sensor particle has a digital interface to be connected to the base station, which is used to set acquisition parameters and synchronize the swarm. Download of the measured data proceeds offline using the base station after recovering the swarm from the process.

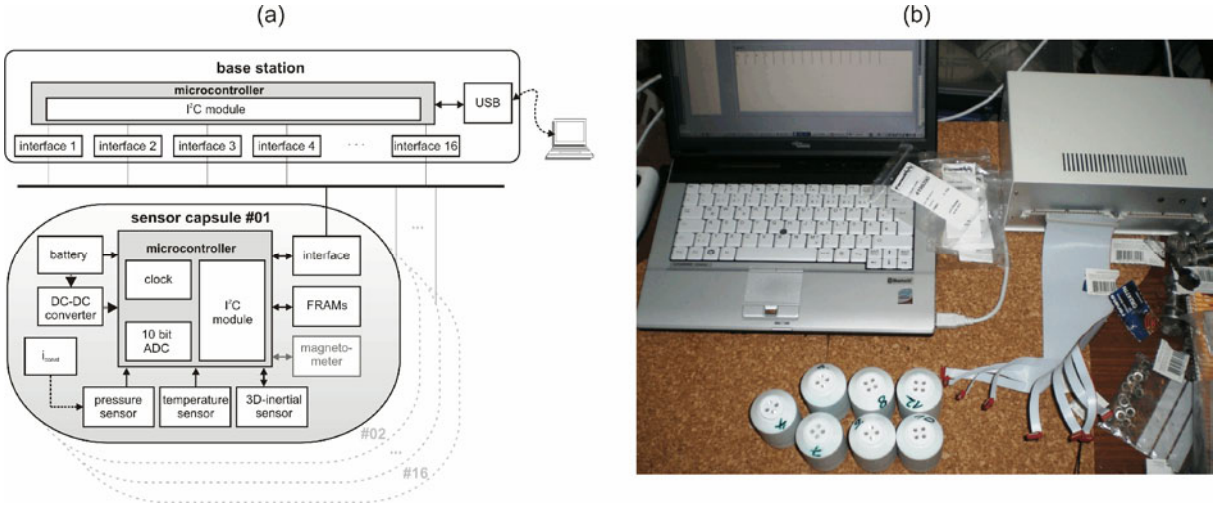

Fig. 1: Block diagram of the base station with 16 individual connections and the autonomous sensor particle's electronics (a) and photograph of the measurement system used during the trials, comprising a PC, the base station with cable connections and 7 fabricated sensor particles (b)

The current design of the sensor particle is based on the first particle prototype [3] and is explicitly described in [4]. An adjustable payload can be placed in the capsule head to give a balance between buoyancy and gravitation with respect to the process substrate (see Fig. 2a). This enables free movement of the capsule to follow even slow moving flows. Moreover, the capsules' low volume makes it almost unpersuasive towards large-scale processes and thus the capsule can be regarded as a flowing particle or precisely a sensor particle. In order to realize long term self-powered operation of the sensor particle a Li/MnO_2 primary battery is used as on-board energy storage. This battery is connected to a step-up converter delivering a constant supply voltage. Moreover as discussed in [5] buffering capacitors are applied in parallel to reduce battery stresses coming from current peaks during changes in the operational mode of the sensor particle and from switching of circuit components during operation. A central processing unit, namely a low power microcontroller, is employed to control the autonomous operation cycle of the particle, which proceeds over a user defined interval in the following way: the particle (i) awakes for an active period from sleep mode, (ii) takes one set of data from all sensors, (iii) stores the data together with a time stamp in its non-volatile memory, and (iv) returns back to sleep mode. In this way, energy consumption is strongly reduced in autonomous measurement mode and the runtime of the energy storage can be optimized. The duration of the sleep mode is user-defined, which allows the adjustment of the acquisition rate to the conditions in the process under investigation in the range between 60^{-1} Hz and 10 Hz.

For analogue interfacing of the pressure and temperature sensor to the microcontroller, two front-end circuits, which are depicted in Fig. 2b and 2c, were designed. The pressure measurement circuit consists of a piezoresistive bridge sensor driven by a constant current

source. The absolute pressure is derived from the measured output voltage of the low power instrumentation amplifier V_p according to the linear regression equation

$$p = k_1 \cdot V_p - k_2 . \tag{1}$$

The parameters, $k_1 = 70.29\ \text{kPa}\cdot\text{V}^{-1}$ and $k_2 = 3.71\ \text{kPa}$, were derived from a calibration procedure in the range of 100…200 kPa. Since the hydrostatic pressure gives an estimate of the vertical position of the capsule in the liquid column, the capsule's immersion depth can be calculated. The immersion depth h is calculated following Pascal's law

$$h = \frac{p - p_0}{\rho \cdot g} , \tag{2}$$

where p is the absolute pressure derived from V_p in (1), p_0 is the actual ambient pressure at the liquid surface, ρ is the liquid density and $g = 9.81\ \text{m}\cdot\text{s}^{-1}$ is the gravitational acceleration. An uncertainty of $u_p = \pm 20.5$ kPa was obtained for the pressure measurement in the temperature range from 10 °C to 70 °C. This results in an uncertainty of $u_h = \pm 20.9$ cm for the measurement of the immersion depth. Typical depths of fermentation reactors are from 5 to 10 m. Thus, the calculated uncertainty is lower than ±4.2%, which is an acceptable tolerance to deliver a rough estimate of the vertical sensor particle position.

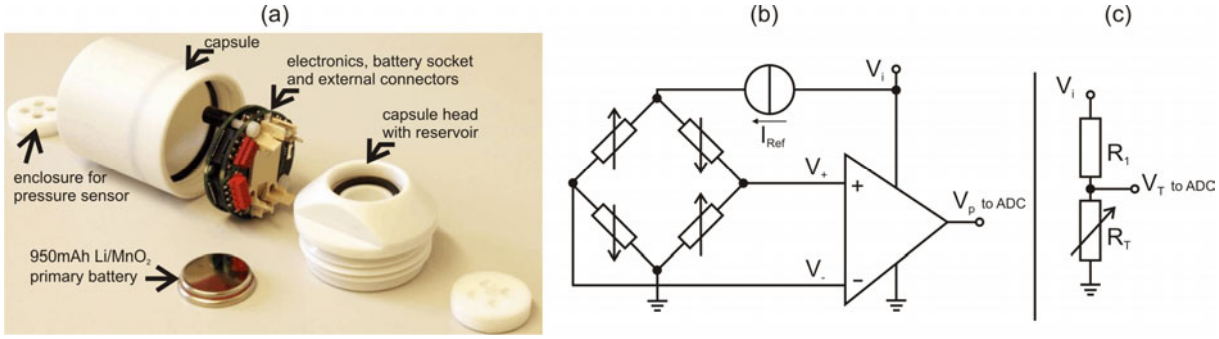

Fig. 2 Left: Photograph of the prototype with the open capsule and all components (a). Right: Schematics of the front end circuits for measurement of the (b) hydrostatic pressure and (c) ambient temperature

The temperature measurement circuit contains a standard NTC thermistor in a high-impedance voltage divider to provide the analogue temperature signal represented by V_T. The resistance value of the thermistor is derived from the measured voltage V_T at the voltage divider of the temperature measurement circuit (see Fig. 2c) according to

$$R_T = \frac{V_T \cdot R_1}{V_i - V_T} . \tag{3}$$

The characteristics of the thermistor's temperature dependence is described by introduction of the simplified NTC thermistor model from [6]

$$R_T = R_0 \cdot \exp\left(b \left(\frac{1}{T} - \frac{1}{T_0} \right) \right) , \tag{4}$$

where R_0 is the nominal resistance and b is the material characteristic temperature, both at temperature T_0. Based on (3) and (4) the calibration function for the measured ambient temperature is formulated as

$$T = a_0 \cdot \left[a_1 + \ln\left(\frac{V_T \cdot a_2}{a_3 - V_T} \right) \right]^{-1} . \tag{5}$$

Parameters $a_0 = 4402.79$ K, $a_1 = 16.52$, $a_2 = 15.07$ und $a_3 = 3.27$ V were obtained from a calibration procedure in a liquid bath temperature calibrator that was operated in the range from 10 to 70 °C. An acceptable uncertainty value of $u_T = \pm 0.51$ K was obtained. Both voltages V_p and V_T are digitized by the internal 10 Bit ADC of the microcontroller. A linear MEMS 3D-inertial sensor is used for the measurement of the capsule's orientation and acceleration. This sensor resides on the analogue PCB. It is a digitally accessible device with a 12-bit resolution.

3. Measurement Results

3.1. Laboratory Flow Experiment

A first flow experiment was conducted, where a single sensor particle was suspended in a stirred reactor model (see Fig. 3a). A central stirring unit with a three-bladed impeller, which has a diameter of 50 cm, is installed in the vessel. The rotational speed is adjustable from 0 to 90 min^{-1}. Furthermore, the vessel has an inlet and an outlet to simulate substrate feed in real reactors. In this way, realistic hydrodynamic conditions could be emulated.

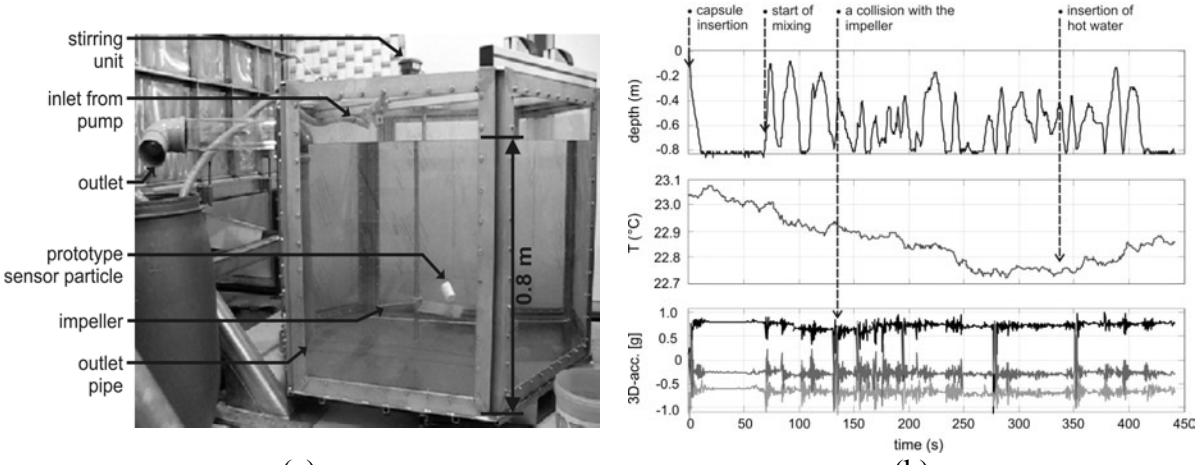

(a) (b)

Fig. 3: Photograph of the stirred reactor model with the sensor particle close to the agitating impeller (a). Diagram of the acquired data series of immersion depth, temperature and 3D-acceleration measured by the sensor particle during the experiment in the reactor model (b)

After adjusting the buoyancy the sensor particle was set to autonomous measurement mode and released into the vessel. During the experiment the sensor particle moved with the flow in the reactor where it was logging the three sensor parameters at an acquisition rate of 2 Hz. The sensor particle was recovered from the process after 15 min and the saved data were downloaded. Fig. 4b depicts a selected range of the measured data series of the experiment. After the release of the sensor particle into the filled reactor vessel it slid down to the bottom of the vessel very slowly over the first 12 s. From the temperature curve it is obvious that the capsule cooled down to the temperature level of the surrounding liquid of $T \approx 22.6$ °C. Then

after 70 s the stirring unit was switched on with 45 min^{-1}. Subsequently, the sensor particle was accelerated by the developing flow caused by the agitation of the impeller. Fast motion and collisions with the rotating impeller can be observed from the 3D-acceleration data, which can be used for motion scheme extraction. To simulate slight temperature gradients in the liquid, 40 L of hot tap water ($T \approx 50$ °C) were inserted at t = 340 s. The resulting local temperature change was captured by the sensor particle, when it passed through the warmer fluid layers in the reactor.

3.2. Swarm Application in Fermentation Reactor

The performance of the sensor particles was further evaluated in a fermentation reactor environment. A swarm of seven capsules was deployed in a 1000 L vessel of a stirred model fermenter depicted in Fig. 5a. A highly viscous aqueous solution of straw was used with a dry mass concentration of about 5.5%, density $\rho \approx 950$ kg·m^{-3}, viscosity $\mu \approx 250$ mPa s at a shear rate of 10 s^{-1} and constant ambient temperature $T \approx 19$ °C. The central three-blade impeller stirrer with a diameter of 0.324 m was adjusted at a rotation speed of 4.4 s^{-1}. Thus, the capsules faced a maximum rotational speed of 4.5 m·s^{-1}. After one hour of operation, the impeller was shifted from 200 mm above vessel ground to 324 mm along the mixer's shaft to simulate varying mixing conditions. The sensor swarm was recovered after two hours of residence in the process environment.

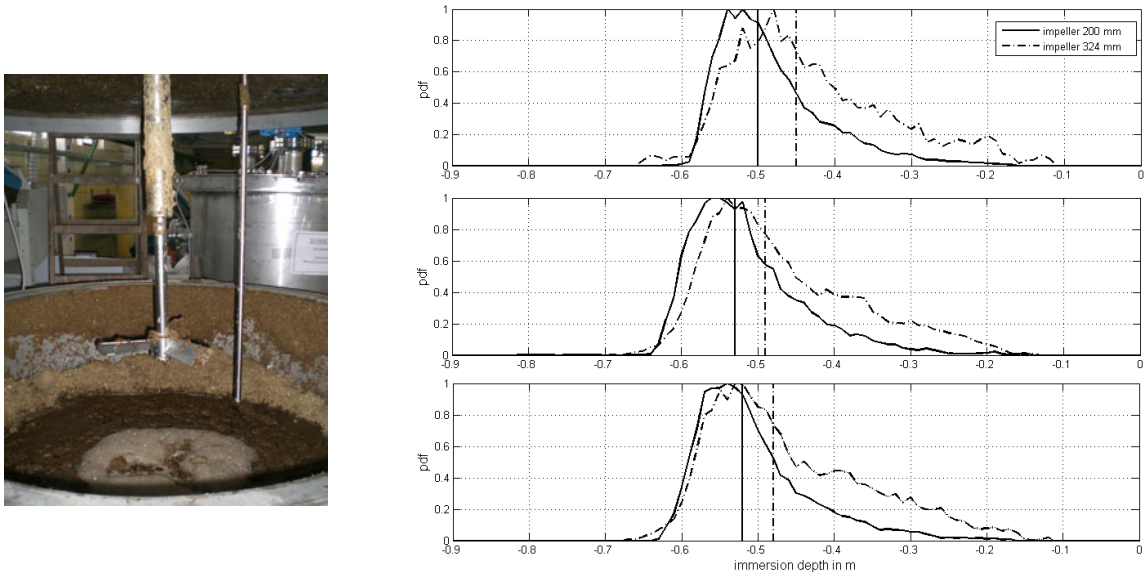

(a) (b)

Fig. 4: Photograph of the opened 1000L fermenter (a) and graphs of the vertical immersion profiles (b). Data are shown as probability density functions of the measured immersion depths of three selected sensor particles and for the both impeller positions. Vertical lines are assigned to the centre of area locations

All acquired data from the seven particles were analyzed and they properly represent the conditions in the vessel. As mentioned above, the process temperature was kept constant at 19 °C which was captured by the swarm correctly. Temporal evolution of the vertical flow component can be observed from the capsule's immersion depth which is calculated from the measured pressure. A probabilistic approach was applied to analyze the acquired data to extract spatial parameter profiles. Fig. 5b depicts the extracted probability functions of the immersion profiles of three selected sensor particles. The immersion profiles were extracted for both impeller positions. To obtain vertical temperature profiles of the reactor the measured

temperature has to be assigned to the corresponding immersion depth of the sensor particle. Since the reactor was operated without a heating unit at that time, which resulted in a constant temperature evolution, visualization of a vertical temperature profile is superfluous here. Further information is contained in the immersion profiles. Asymmetry of the profiles gives evidence that the sensor particles did hardly enter the region between the reactor bottom at depth of -0.9 m and the impeller at -0.7 m. This indicates a locally insufficient mixing or even a dead zone. Only after lifting the impeller to the position at -0.58 m did the sensor particles enter the region below the impeller more frequently. However, this region was insufficiently mixed. Moreover, the impeller position adjustment can be observed from the shift of the centres of area of the probability functions which has a value of approx. 5 cm.

4. Conclusion

A prototype of autonomous sensor particles has been designed and tested. Each sensor particle allows data logging of three different on-board sensor signals, namely temperature, pressure and 3D-acceleration, in a pre-configured autonomous measurement mode. Further parameters may also be logged, such as pH, ORP, pO_2, pCO_2, electrical conductivity and relative permittivity by the inclusion of other sensing elements into the sensor particle. Experimental validation of the sensor swarm proceeded under real flow conditions and also in fermentation reactor environments. The acquired data represent the internal conditions of the reactor such as temperature, pressure, flow dynamics and distribution of dead zones. Furthermore, spatial parameter profiles can be extracted from the data recorded by the sensor swarm. Based on the positive experimental results the sensor swarm may now be used for long term operation in a real reactor vessel such as a biogas fermenter, to investigate the internal reactor conditions and thus evaluate the efficiency of heating and mixing regimes.

References

[1] M. Antoniou, M.C. Boon, P.N. Green, P.R. Green, and T.A. York, “Wireless Sensor Networks for Industrial Processes,” IEEE Sensors Applications Symposium, New Orleans, LA, USA, February 17-19, 2009.

[2] I.F. Akyildiz, W. Su, Y. Sankarasubramaniam, E. Cayirci, “Wireless sensor networks: a survey,” Computer Networks, vol. 38, pp. 393–422, 2002.

[3] S. Thiele, S. Schöne, F. Voigt, M. J. Da Silva, U. Hampel, „Design of a Neutrally Buoyant Self-Powered Multi-Parameter Sensor for Data Logging in Flow Applications,“ IEEE Sensors Conference, 25-28 Oct. 2009.

[4] S. Thiele, M.J. Da Silva, and U. Hampel, „Autonomous sensor particle for parameter tracking in large vessels,“ Meas. Sci. Technol., vol. 21 (8), 2010, DOI: 10.1088/0957-0233/21/8/085201

[5] M.T. Penella, M. Gasulla, “Runtime Extension of Autonomous Sensors Using Battery-Capacitor Storage,” IEEE International Conference on Sensor Technologies and Applications, pp. 325–330, 14-20 Oct. 2007.

[6] J. Fraden, Handbook of modern sensors: physics, designs, and applications, 3rd ed., Springer, New York, Berlin, Heidelberg, 2004.

Acknowledgement

The project described here is supported by Studienstiftung des Deutschen Volkes e.V. We further acknowledge the Fraunhofer IKTS and LEHMANN Maschinenbau GmbH for their cooperation and support during the fermentation reactor experiments at ”Applikationszentrum Bio-Energie Pöhl”.

A POPULATION BALANCE APPROACH CONSIDERING HEAT AND MASS TRANSFER - EXPERIMENTS AND CFD SIMULATIONS

Eckhard Krepper, Matthias Beyer, Martin Schmidtke, and Dirk Lucas

1. Introduction

Bubble condensation in sub-cooled water is a complex process, to which various phenomena contribute. Since the condensation rate depends on the interfacial area density, bubble size distribution changes caused by breakup and coalescence play a crucial role.

Experiments on steam bubble condensation in vertical co-current steam/water flows have been carried out in an 8 m long vertical DN200 pipe at the TOPFLOW facility [9]. Steam is injected into the pipe and the development of the bubbly flow is measured at different distances to the injection using a pair of wire mesh sensors. By varying the steam nozzle diameter the initial bubble size can be influenced. Larger bubbles come along with a lower interfacial area density and therefore condensate slower. Steam pressures between 1-6.5 MPa and sub-cooling temperatures from 2 to 17 K were applied. Due to the pressure drop along the pipe, the saturation temperature falls towards the upper pipe end. This affects the sub-cooling temperature and can even cause re-evaporation in the upper part of the test section. The experimental configurations are simulated with the CFD code CFX using an extended MUSIG approach, which includes the bubble shrinking or growth due to condensation or re-evaporation. The development of the vapour phase along the pipe with respect to vapour void fractions and bubble sizes is qualitatively well reproduced in the simulations. For a better quantitative reproduction, reliable models for the heat transfer at high Reynolds number as well as for bubble breakup and coalescence are needed.

Many activities were done in the last years to improve the modelling of adiabatic bubbly flows in the frame of CFD. In this case models for momentum transfer between the phases are most important. Usually they are expressed as so-called bubble forces. Experimental investigations showed that these bubble forces strongly depend on the bubble size. To simulate different behaviour of small and large bubbles more than one momentum equation is required [5]. For this reason recently the so-called Inhomogeneous-MUSIG (MUltiple SIze Group) model was implemented into the ANSYS-CFX code [6]. It allows the consideration of a number of bubble classes independently for the mass balance. For a proper modelling of bubble coalescence and breakup a large number of bubble groups are required. For the momentum balance only very few classes can be considered due to the high computational effort. Criteria for the classification can be derived from the dependency of the bubble forces on the bubble size, e.g. the change of the sign of the lift force. In the presently implemented version of the Inhomogeneous MUSIG model only transfers between the bubble classes due to bubble coalescence and breakup can be modelled. In case of flows with phase transfer additional transfers between the single classes and the liquid and transfers between bubble classes caused by growth or shrinking of bubbles have to be considered. The equations for the extension of the MUSIG models are described by [7] and [8]. They were recently implemented into the CFX code.

2. Setup of experimental condensation tests K16

Experiments are done using the TOPFLOW facility of the Helmholtz-Zentrum Dresden-Rossendorf. The facility allows producing up to 1.4 kg/s saturated steam at the maximum

operational pressure of 7 MPa by a 4 MW electrical steam generator [9]. For the test and validation of the model extensions tests from the Series K16 at 20 bar were selected (see Table 1).

Table 1: Parameters of the selected tests

Test	J_L [m/s]	J_G [m/s]	T_{sub} [K]	D_{Nozzle} [mm]
118_dt6_1	1.067	0.219	6.0	1
118_dt6_4	1.067	0.219	6.0	4
140_dt3.2_1	1.067	0.534	3.2	1

3. CFD simulation of the K16 tests

3.1. General setup

For the simulation using the code CFX-12.1 the standard framework of Euler/Eulerian two phase flow was adopted. The implemented water/steam tables according to IAPWS IF97 were applied.

The drag force according to Grace [3] was used. The turbulent dispersion force according to Burns [2] and the wall force model of Antal [1] were applied. For the lift force the correlation of Tomiyama [10] with its bubble size dependent lift force coefficient was used. Whereas for air/water a sign change of the lift coefficient at $d_B \approx 6$ mm could be observed, this critical diameter for vapour/water is shifted towards smaller values. For 2 MPa a critical diameter of $d_B \approx 4.5$ mm was found.

In all investigated cases the inhomogeneous MUSIG model including mass transfer was applied. A logarithmic bubble size distribution was used, which enables with a limited number of size classes to span over a quite large bubble size region and a sufficient fine resolution of the smaller bubble sizes. In all tests two velocity groups were simulated, one group lower and one larger than the critical diameter of changing the lift force sign.

Earlier investigations of steam/water tests at saturation conditions had shown, that applying the same models with the same model parameters for bubble fragmentation like for air/water the calculated bubble fragmentation rate exceeds the measured values. Therefore as a first step during these calculations bubble fragmentation and coalescence were neglected. Only the change of gas fraction and bubble size distribution by mass transfer (condensation respective evaporation) was considered.

A 2D cylinder symmetric geometry was used to reduce the computational effort. The experimental results at level A (0.221 m distance from steam injection) were used as inlet condition of the simulation. These concerns the cross sectional averaged bubble size distribution, the radial vapour volume fraction profile and the radial vapour velocity profile. For the level A a constant velocity difference between water and vapour was adjusted so that the specified superficial velocities are met. Inlet conditions for the radial profiles of turbulent kinetic energy and turbulent dissipations were set. These profiles were determined performing a previous single phase calculation. At the outlet a pressure boundary condition was set so that the absolute pressure corresponds to the experimental specifications to simulate the realistic saturation temperatures.

3.2. The bubble-liquid heat transfer coefficient

During the simulations the vapour was assumed to be at saturation conditions, whereas for the liquid phase the energy equation was solved. In general correlations for the heat transfer model between vapour bubbles and liquid have the following form:

$$Nu = 2 + c \cdot \mathrm{Re}^{\alpha}\ \mathrm{Pr}^{0.3} \tag{1}$$

Three different correlations have been investigated here: a) Ranz-Marshall [10] correlation (c=0.6, α=0.2) is only recommended for small Reynolds number (Re<780). Hughmark [4] suggests for larger Reynolds number c=0.27 and α=0.62, whereas Tomiyama [11] proposes c=0.15 and α=0.8 for all Re.

In Fig. 1 the cross sectional averaged vapour void fractions in dependency of the tube height z are shown. The graphs of the measured as well as the simulated values for this condensation dominated test case are approximately straight lines in the semi logarithmic plot. This means that the steam void fraction decreases approximately exponentially with the height.

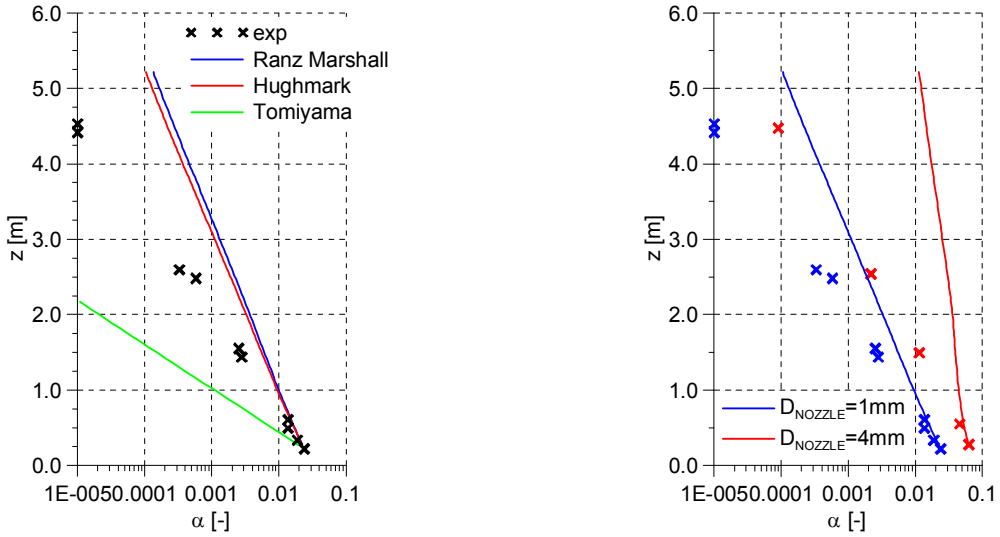

a) Influence of the heat transfer model, (Nozzle diameter: D_{Nozzle}=1mm)

b) Influence of the initial bubble size distribution. (D_{Nozzle}=1 versus 4mm)

Fig. 1: Cross sectional averaged vapour void fractions for tests 118_dt6 (T_{sub}=6K)

Fig. 1a shows a sensitive influence of the applied heat transfer model on the calculated vapour volume fraction. A slight overestimation of the vapour void fraction for the Ranz Marshall correlation and a strong underestimation for the Tomiyama correlation was calculated for test case 118_dt6_1. The best agreement was found for the correlation according to Hughmark. In the following simulations this correlation was used.

3.3. Influence of increasing the initial bubble size distribution

Fig. 2 and 3 show the cross sectional averaged bubble size distribution and the radial vapour profiles for the tests 118_dt6_1 and 118_dt6_4. The vapour is injected from the side (at R=D/2=0.098 m). In both tests the vapour is remaining near the wall (see Fig. 2b and 3b).

Caused by the higher interfacial area for smaller bubble sizes the condensation rate for the 1 mm nozzle size test is higher than for the 4 mm tests. Consequently the steam void fraction is lower (see Fig. 1b for the cross sectional averaged values). Whereas the bubble size distribution in the test 118_dt6_1 is calculated with reasonable agreement to measurements, the size distribution for the 4 mm case is overestimated with respect to bubble sizes and vapour void fraction (see Fig. 3, level H, z=1.495 m). Consequently for this test the cross sectional averaged vapour fraction is calculated too large. For this test bubble fragmentation might play a role.

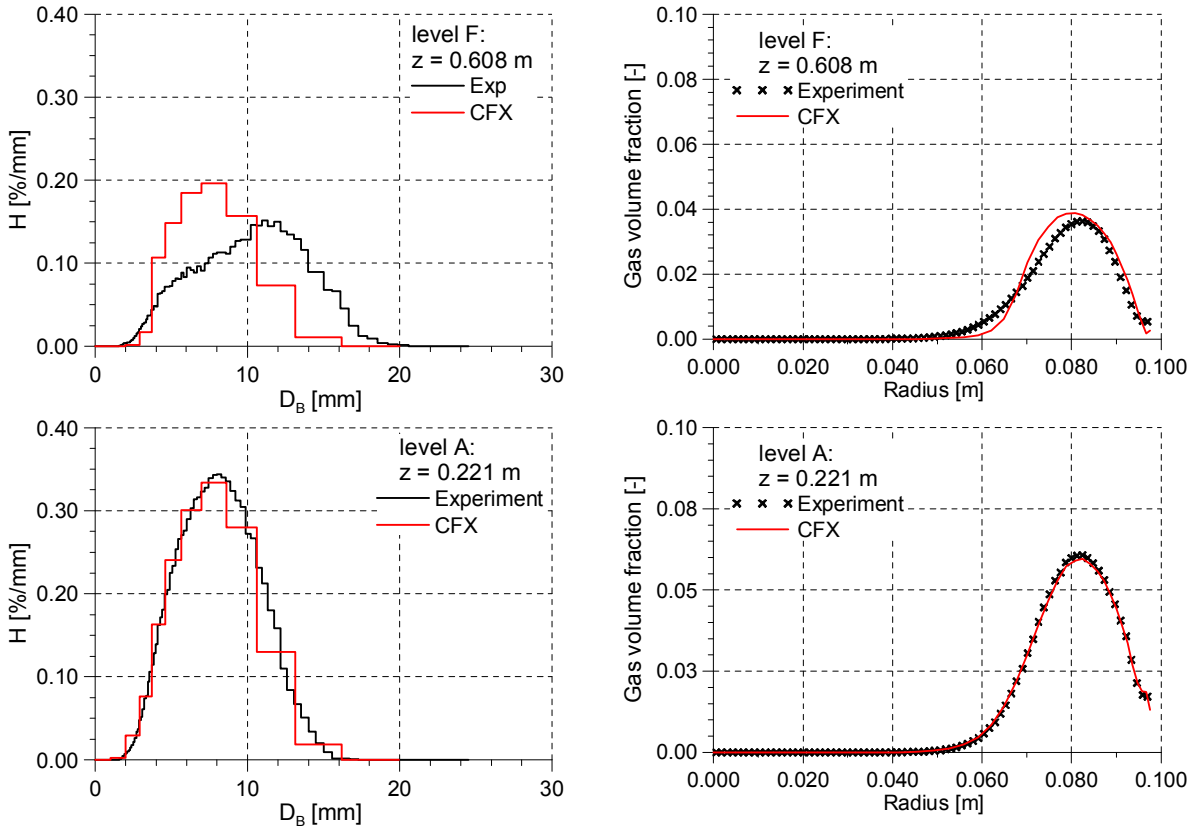

a) Bubble size distribution b) radial vapour void profile

Fig. 2: Development of the vapour void at different distances z from the steam injection Test 118_dt6_1 (T_{sub} = 6K, D_{Nozzle} = 1mm)

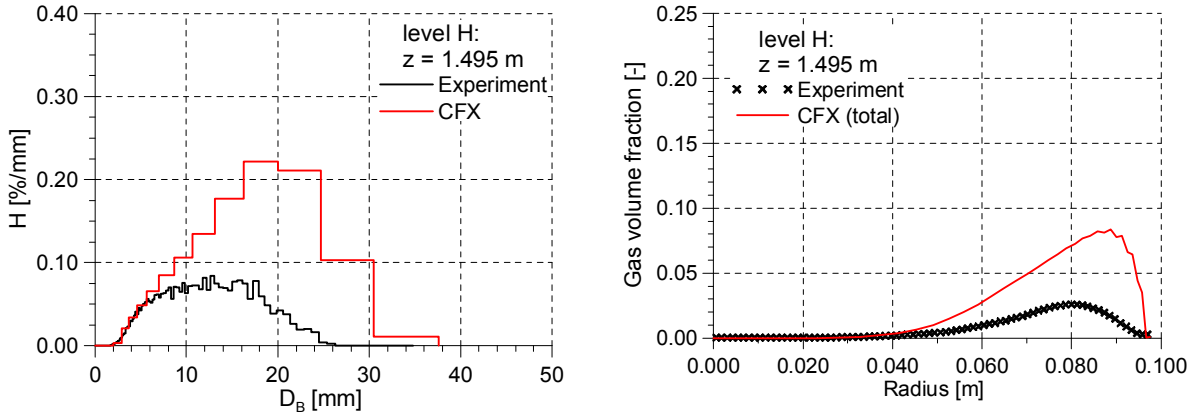

a) Bubble size distribution b) radial vapour void profile

Fig. 3: Development of the vapour void at different distances z from the steam injection Test 118_dt6_4 (T_{sub} = 6K, D_{Nozzle} = 4mm)

3.4. Simulation of a test with re-evaporation

During some tests re-evaporation with the increasing height was observed (see Fig. 4a). This was the case when the inlet temperature was very close to the saturation temperature. With increasing height the hydrostatic pressure decreases and the saturation temperature falls below the liquid temperature (see Fig. 4b). In these cases the exact values of the inlet conditions have a very sensitive influence on the further development of the flow. Furthermore the errors of the temperature measurements are in the order of magnitude of the sub-cooling temperature. The test specification for sub-cooling was related to z=0, whereas in the simulation the inlet condition at level A has to be set. The sensitive influence of the inlet sub-cooling temperature set at level A was investigated (see Fig. 4a for the cross sectional averaged vapour void fraction and Fig. 4b for the cross sectional averaged liquid temperature). Depending on the inlet temperature also in the calculations re-evaporation could be observed.

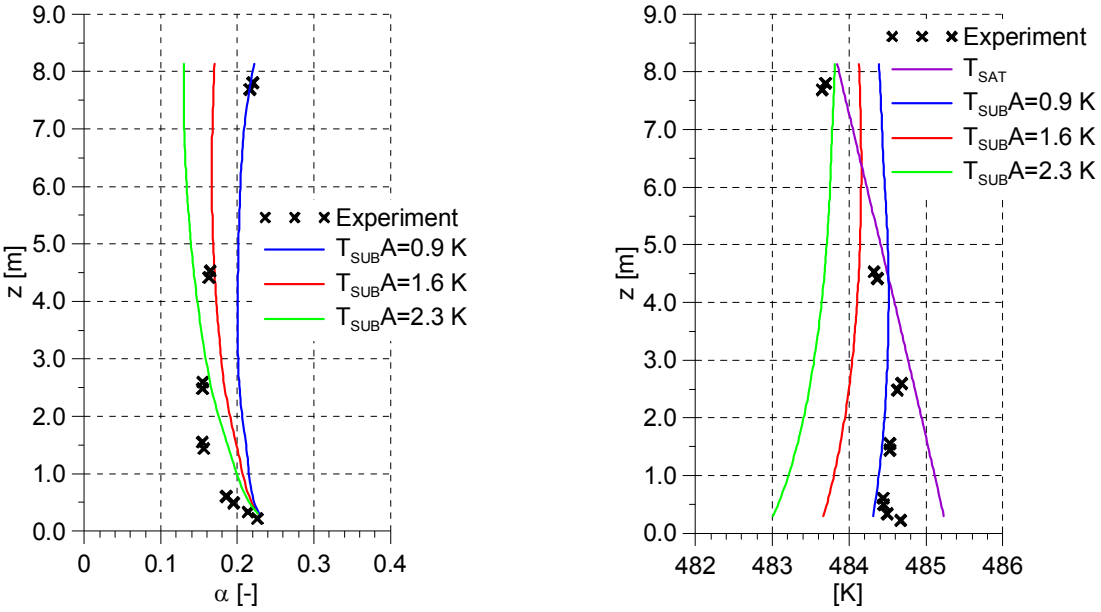

a) Cross sectional averaged vapour void fraction

b) Cross sectional averaged liquid temperature

Fig. 4: Symbols: Experiment: Test 140_dt3.2_1, Lines: Calculations for various T_{sub}

4. Conclusions

The correct operation of the model could be shown. Earlier and also the actual investigations show for vapour/water flow an overestimation of bubble fragmentation applying the same models like for air/water flow. To limit the influences in the presented simulation, as a first step, vapour bubble fragmentation and coalescence were neglected. The influence of the heat transfer model between bubbles and liquid was investigated. The best agreement for the cross sectional averaged vapour void fraction compared to the measurements was found applying the heat transfer correlation proposed by Hughmark. The simulations were extended to tests with larger initial bubble sizes produced with larger injection nozzles. Here the Hughmark model underestimates the condensation and the bubble shrinking. In this case bubble fragmentation may play a role, because it increases the interfacial area and thereby the

condensation. Bubble fragmentation and coalescence will be considered in the future work. Simultaneously attention has to be directed on influence of bubbles on liquid turbulence.

In some tests cases with inlet liquid temperatures close to saturation, after some condensation close to the inlet, further downstream a re-evaporation can be observed. This phenomenon is caused by the drop of saturation temperature due to the decreasing hydrostatic pressure along the pipe height. The simulation of these processes depends on the setting of the inlet temperature very sensitively. Further investigations are necessary.

Acknowledgements

This work is carried out in the frame of a current research project funded by the German Federal Ministry of Economics and Technology, project numbers 150 1328 and 150 1329. The authors like to thank all members of the TOPFLOW team who contributed to the successful performance of these experiments.

References

[1] Antal, S.; Lahey, R. & Flaherty, J., 1991. Analysis of phase distribution in fully developed laminar bubbly two-phase flow, International Journal of Multiphase Flow, 17, 635

[2] Burns, A. D., Frank, T., Hamill, I., Shi, J.-M., 2004. The Favre Averaged Drag Model for Turbulent Dispersion in Eulerian Multi-Phase Flows, 5th International Conference on Multiphase Flow, ICMF'04, Yokohama, Japan, May 30–June 4, 2004, Paper No. 392.

[3] Clift, R., Grace, J.R., Weber, M.E., 1978. Bubble Drops and Particles, Academic Press New York

[4] Hughmark, G. A., 1967. Mass and Heat Transfer from Rigid Spheres, AlChE Journal, 13, 1219

[5] Krepper, E., Lucas, D., Prasser, H.-M., 2005. On the modelling of bubbly flow in vertical pipes, Nuclear Engineering and Design, 235, 597-611

[6] Krepper, E., Lucas, D., Frank, T., Prasser, H.-M., Zwart, P., 2008. The inhomogeneous MUSIG model for the simulation of polydispersed flows, Nuclear Engineering and Design, 238, 1690-1702

[7] Lucas, D., Prasser, H.-M., 2007. Steam bubble condensation in sub-cooled water in case of co-current vertical pipe flow, Nuclear Engineering and Design, 237, 497-508

[8] Lucas, D., Beyer, M., Frank, T., Zwart, P., Burns, A., 2009. Condensation of Steam Bubbles Injected into Sub-Cooled Water, The 13th International Topical Meeting on Nuclear Reactor Thermal Hydraulics (NURETH-13), Paper N13P1097

[9] Prasser, H.-M., Beyer, M., Carl, H., Manera, A., Pietruske, H., Schütz, P., Weiß, F.-P., 2006. The multipurpose thermal-hydraulic test facility TOPFLOW: an overview on experimental capabilities, instrumentation and results, Kerntechnik, 71, 163-173

[10] Ranz, W.E., Marshall, W.R., 1952. Evaporation from drops, part I, part II, Chemical engineering progress Vol. 48 No. 3, pp. 141

[11] Tomiyama, A., 1998. Struggle with computational bubble dynamics, 3rd Int. Conf. on Multiphase Flow, ICMF'98, Lyon, France

EFFECT OF NEUTRON IRRADIATION ON MICROSTRUCTURE AND STRENGTH OF FE-BASED MODEL ALLOYS

Frank Bergner, Mercedes Hernández-Mayoral[1], Estelle Meslin[2], and Andreas Ulbricht

1. Introduction

The application of experimental techniques to the microstructural characterization of neutron-irradiated ferritic model alloys has contributed essentially to the mechanistic understanding of irradiation embrittlement of reactor pressure vessel (RPV) steels [1]. In this context, European projects were initiated [2,3] to bring together the knowledge gained in Europe and abroad from the various fields involved in the multi-scale phenomenon of radiation effects on the mechanical performance of RPV steels. The experimental approach adopted was to investigate Fe-base materials of increasing complexity irradiated in a test reactor. Among the experimental techniques sensitive to irradiation-induced microstructural changes at the nm-scale, atom probe tomography (APT) [4], small-angle neutron scattering (SANS) [5], transmission electron microscopy (TEM) [6] and positron annihilation spectroscopy (PAS) [7] play a particular role. It turned out that, because of the complexity of the problem as well as particular strengths and weaknesses of the individual techniques, there is no single method capable of solving all the related issues [8]. Therefore the work reported here is focussed on the combination of APT, SANS and TEM. Once the irradiation-induced microstructural changes have been well characterized, the dominant features have to be identified and correlated with the irradiation-induced property changes such as hardening and embrittlement. As the time is not yet ripe for a realistic ab-initio prediction of mechanical properties, empirical correlations are in the focus here. Finally, additional insight can be gained by means of post-irradiation annealing treatments of the model alloys under investigation. First results on the characterization of the microstructure after isothermal annealing will also be presented.

2. Experimental

The model alloys are pure Fe, Fe-0.1Cu, Fe-0.3Cu, Fe-1.2Mn-0.7Ni, Fe-1.2Mn-0.7Ni-0.1Cu (wt%) of commercial purity and a 16MND5-type RPV steel of low Cu level of 0.065 wt%. The materials were provided by SCK·CEN Mol (Belgium) in the as-irradiated condition. Irradiation temperature was 300°C, neutron flux was 0.95×10^{18} $m^{-2}s^{-1}$ (E>1MeV), levels of neutron exposure were 0.026 dpa, 0.051 dpa, 0.10 dpa and 0.19 dpa (NRT). Further details and mechanical properties have been reported in [9].

APT is known to be a very efficient tool for the chemical analysis of solute-enriched clusters. Their characteristics – number density, size and composition – as well as matrix composition are accurately determined in the volume accessible. Analyses were performed at a set-up developped at the University of Rouen (France) [4]. To avoid the preferential evaporation of copper, the experiments were carried out at a cryogenic temperature of 50 K and with an electrical pulse fraction of 20% of the standing voltage. All the experiments were performed with a pulse rate limited to 0.03 atom/pulse to reduce the risk of failure of the needle-shape sample. The analyzed volume was typically 15 x 15 x 100 nm^3 for each sample.

[1] CIEMAT Madrid, Spain
[2] CEA Saclay, France

The SANS experiments were performed under coordination of SCK·CEN at the SANS instrument of the SINQ facility of PSI and the PAXE instrument of the Orphee research reactor at LLB Saclay [5]. SANS is capable of characterizing the size distribution of nm-sized irradiation-induced defect-solute clusters in ferritic alloys. This is done by measuring the scattering cross-section in a saturation magnetic field applied to the sample, separating nuclear and magnetic contributions, subtracting the scattering cross-section for an unirradiated control sample and calculating the size distribution by solving an inverse problem [5]. The lower detection limit is about 0.5 nm in cluster radius. An advantage is the averaging capability resulting from a probed volume of some 10 mm^3 and from a number of scattering events of the order of 10^6. In addition, an indicator of the average cluster composition is given by the ratio of magnetic and nuclear scattering.

TEM investigations were performed at CIEMAT Madrid (Spain) [6] using a JEOL type microscope model JEM-2010 operating at 200 keV. This technique is able to detect clusters of point defects (vacancies or interstitials) induced by irradiation at sizes larger than about 1.5 nm. Information from the interstitial component of the radiation damage not detected with other microstructural characterization techniques in such a direct way can be obtained. Diffraction contrast methods were employed for imaging defect microstructures. Counting of defects was performed on TEM images recorded under reflections of type g = (1, 1, 0) where the best contrast was obtained.

3. Results and discussion

The number density and mean size of irradiation-induced solute clusters, scatterers and dislocation loops estimated by means of APT, SANS and TEM, respectively, are presented in Fig. 1 and 2.

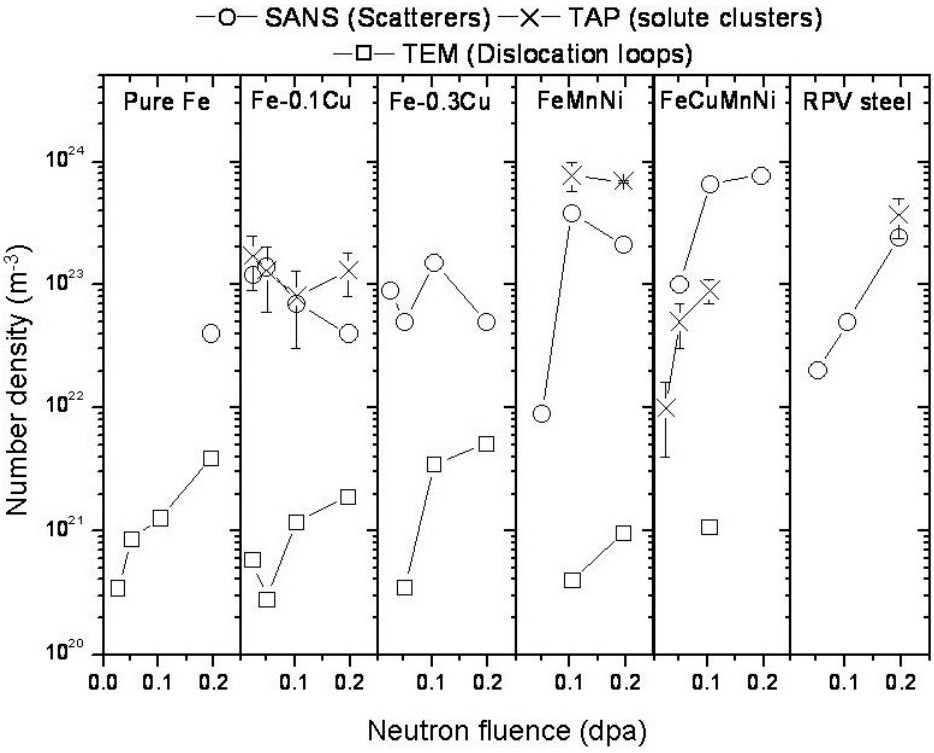

Fig. 1: Number density of irradiation-induced scatterers, solute clusters and dislocation loops estimated from results obtained bySANS (non-magnetic scatterers assumed), APT and TEM, respectively, applied to the same set of materials [8]

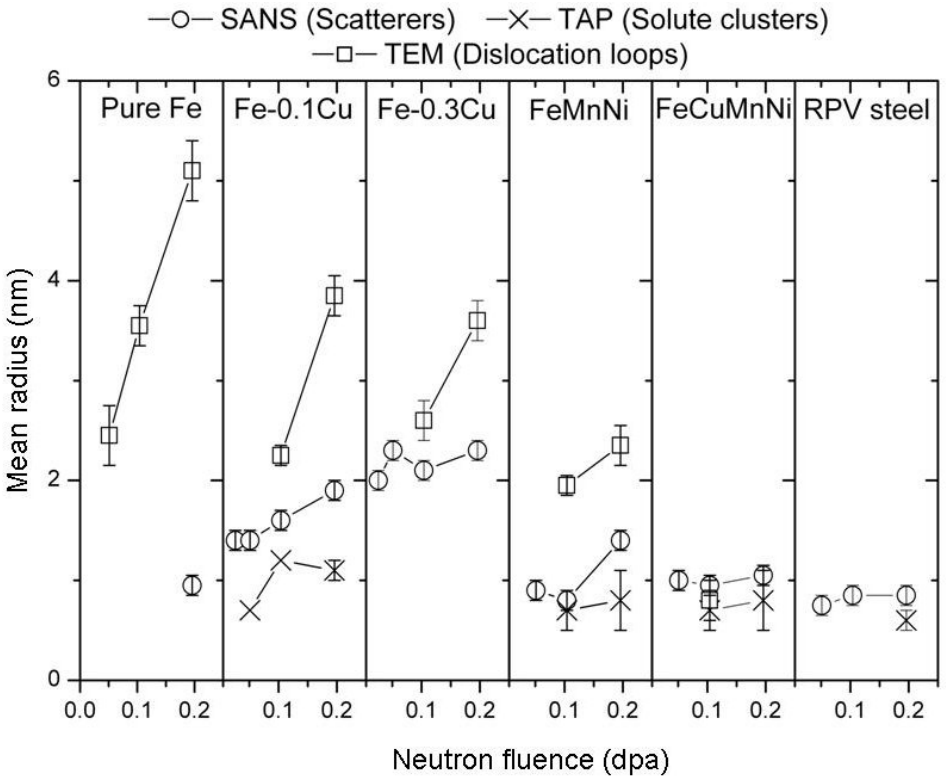

Fig. 2: Size of irradiation-induced scatterers, solute clusters and dislocation loops [8]

The number densities and sizes estimated by means of APT and SANS are generally of the same order of magnitude and exhibit similar trends. It is therefore reasonable to assume that both methods basically detect the same objects. The slightly larger mean size found by SANS may be due to small objects missing in the SANS analysis because of the resolution limit. The composition of the solute clusters estimated by means of APT can be compared with the ratio of magnetic and nuclear scattering derived from SANS data. Significant deviations observed in some cases may be due to differences in the probed volumes and due to uncertainties of the APT analysis with respect to the fraction of Fe atoms and vacancies in the clusters [8]. However, there is agreement that mixed Cu-vacancy clusters are dominant in the binary Fe-Cu alloys and Mn-Ni-enriched clusters are the dominant in FeMnNi. The Cu-vacancy clusters exhibit a core-shell structure with vacancies concentrated in the core and vacancy fractions evolving with increasing fluence in a non-monotonic manner [5]. In the FeMnNi alloy, Mn appears first and the Ni fraction increases with fluence [4,5,8].

The objects detected by TEM were unambiguously identified as dislocation loops [6]. The planar extension of the loops is generally larger and the number density smaller than for the solute clusters. No dislocation loops were observed in the RPV steel [6].

It is well known that the irradiation-induced features characterized in Fig. 1 and 2 are obstacles for dislocation glide and therefore basically responsible for irradiation hardening. The above findings indicate that a two-feature hardening model with solute clusters and dislocation loops as main obstacles should be applicable. In the empirical analysis presented here, the solute clusters are deduced from the SANS analysis instead of the APT analysis simply because the volume probed by means of SANS is many orders of magnitude larger. The correlation between cluster concentration and hardening is expressed in Fig. 3 in terms of cluster volume fraction and irradiation-induced yield stress increase.

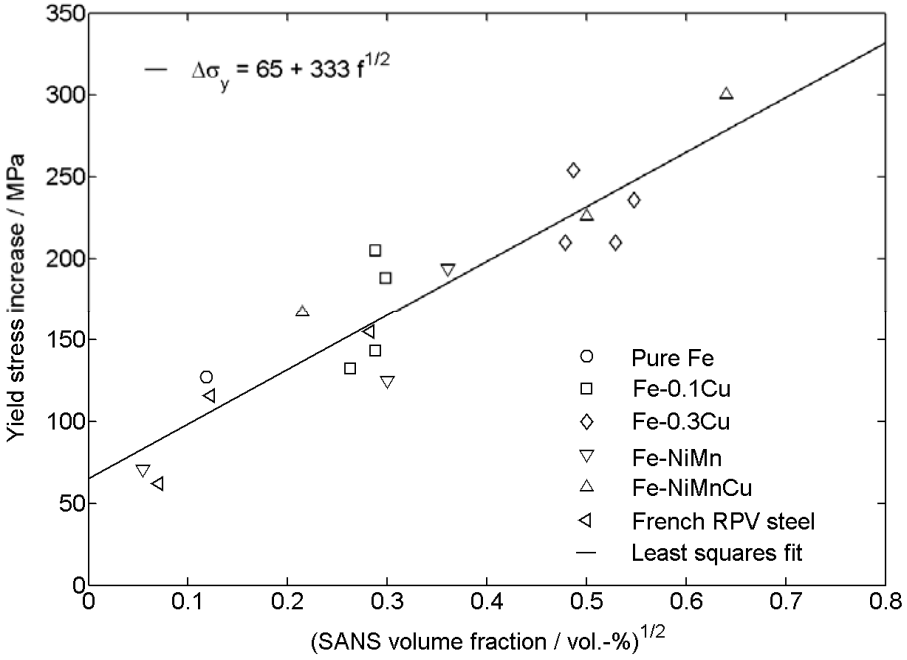

Fig. 3: Scatterplot of yield stress increase and square root of volume fraction [5]

There is a fairly strong correlation in spite of the diversity of the alloy compositions. It is therefore reasonable to assume (though not a strict proof) that the clusters observed by SANS (and APT) are in fact responsible for an increase of the yield stress. However, the scatter of the individual data and the intersection of the regression line indicate that there is a second contribution to irradiation hardening, which is not correlated with the SANS volume fraction. This component can be identified as the above-mentioned hardening contribution caused by dislocation loops [5]. In fact, SANS is rather insensitive to planar dislocation loops. Moreover, Fig. 1 shows that there is indeed no strong correlation between number densities of solute clusters and loops.

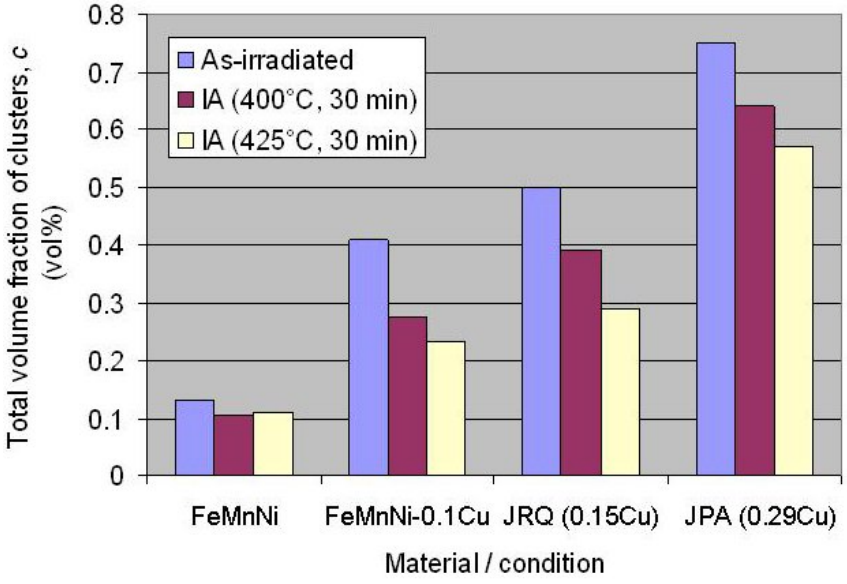

Fig. 4: Effect of post-irradiation annealing on volume fraction of scatterers

It is well known that a post-irradiation annealing treatment gives rise to a (partial or full) recovery of the irradiation-induced hardening features and a related improvement of the mechanical properties. The interest in the annealing behaviour is twofold. First, large-scale annealing treatments have been performed for RPVs of now operating or decommissioned nuclear power plants and the amount of recovery needed (needs) to be specified. Secondly, the annealing kinetics gain additional insight into the detailed nature of the defects. The change of cluster volume fraction with temperature for isochronal annealing at stepwise increasing temperature is presented in Fig. 4 for two model alloys and two RPV steels. The investigation is currently extended towards higher temperatures.

4. Conclusions

Type, concentration and size of the dominant irradiation-induced features, i.e. solute clusters and dislocation loops, were specified by means of APT, SANS and TEM applied to neutron-irradiated Fe-based model alloys. The volume fraction of solute clusters derived from SANS is strongly correlated with irradiation hardening. Dislocation loops do also contribute to hardening in the investigated alloys with the possible exception of the RPV steel.

References

[1] T. Toyama, Y. Nagai, Z. Tang, M. Hasegawa, A. Almazouzi, E. van Walle, R. Gérard, Acta Mater. 55 (2007) 6852.

[2] J.-P. Massoud, S. Bugat, B. Marini, D. Lidbury, S. Van Dyck, J. Nucl. Mater. 406 (2010) 2.

[3] S. Leclercq, D. Lidbury, S. Van Dyck, D. Moinereau, A. Alamo, A. Al Mazouzi, J. Nucl. Mater. 406 (2010) 193.

[4] E. Meslin, B. Radiguet, P. Pareige, A. Barbu, J. Nucl. Mater. 399 (2010) 137.

[5] F. Bergner, M. Lambrecht, A. Ulbricht, A. Almazouzi, J. Nucl. Mater. 399 (2010) 129.

[6] M. Hernández-Mayoral, D. Gómez-Briceño, J. Nucl. Mater. 399 (2010) 146.

[7] M. Lambrecht, A. Almazouzi, J. Nucl. Mater. 385 (2009) 334.

[8] E. Meslin, M. Lambrecht, M. Hernández-Mayoral, F. Bergner, L. Malerba, P. Pareige, B. Radiguet, A. Barbu, D. Gómez-Briceño, A. Ulbricht, A. Almazouzi, J. Nucl. Mater. 406 (2010) 73.

[9] M. Lambrecht, L. Malerba, A. Almazouzi, J. Nucl. Mater. 378 (2008) 282–290.

Acknowledgements

This work was partly supported by the EC within the Integrated Projects PERFECT under Contract No. F6O-CT-2003-508840 and PERFORM-60 under Grant Agreement No. FP7-232612. SANS data were made available for further analysis by A. Almazouzi.

SANS INVESTIGATION OF NEUTRON-IRRADIATED BINARY IRON-CHROMIUM ALLOYS

Cornelia Heintze, Frank Bergner, and Andreas Ulbricht

1. Introduction

Ferritic-martensitic chromium steels and their derivatives such as oxide-dispersion strengthened chromium steels are candidate structural materials for future applications in conventional and nuclear energy applications (including both fission and fusion) and in transmutation systems [1,2]. It is therefore important to know the effect of chromium on the microstructure and properties of this class of materials. However, there are still missing links in a comprehensive understanding of the role of chromium even in the binary Fe-Cr system. For instance, there are uncertainties on the solubility of Cr and Fe in the Fe-rich α-phase and the Cr-rich α'-phase, respectively, and on the mechanism of the α'-phase formation, in particular in irradiated alloys [3,4]. Moreover, the effect of Cr on irradiation hardening, embrittlement and creep is a matter of continuing interest.

Recently, an international effort was undertaken within the European project GETMAT [5] to explore the effect of neutron-irradiation on the microstructure of binary Fe-Cr alloys with Cr-levels ranging from 2.5 to 12.5 at%. Among the methods employed, small-angle neutron scattering (SANS) [6-8], atom probe tomography (APT) [9] and transmission electron microscopy (TEM) [10,11] play an outstanding role. The complete set of SANS results is reported and discussed in this note.

2. Experimental

The material investigated are commercial purity Fe-Cr alloys with nominal Cr levels of 2.5, 5, 9, and 12.5 at% fabricated by SCK·CEN Mol, Belgium. It was obtained by furnace melting of commercial purity Fe and Cr. After casting, the obtained ingots were cold worked under protective atmosphere to fabricate plates of 9 mm in thickness, treated at 1050 °C for 1 h in high vacuum for austenisation and stabilization and tempered at 730 °C for 4 h followed by air cooling. Neutron irradiation was performed in the framework of the MIRE experiment in the reactor BR2 at Mol, Belgium [10]. The irradiation temperature was (300 ± 5) °C. The neutron flux was 9 x 10^{13} n cm^{-2} s^{-1} (E > 1 MeV). The total neutron exposures in terms of displacement per atom were 0.06, 0.6 and 1.5 dpa. The irradiated samples were delivered along with the unirradiated reference samples as coupons of dimensions 7 x 7 x 1 mm^3.

SANS measurements were performed at the SANS-2 facility of GKSS Geesthacht, Germany. The samples were placed in a saturation magnetic field perpendicular to the incident neutron beam direction. A neutron wavelength of 0.58 nm and three sample-detector distances of 1, 4 and 16 m with corresponding beam collimation lengths were used to cover scattering vectors of magnitude, Q, from 0.1 nm^{-1} to 3 nm^{-1}. Scattered neutrons were recorded with an area 3He-detector (50 x 50 cm^2) using 128 x 128 pixel. The SANS data reduction was carried out using the Sandra software package. The azimuthal dependence of scattering was used to separate magnetic and nuclear scattering. In order to calculate the size distribution of scatterers, a dilute two-phase matrix-inclusion microstructure composed of homogeneous spherical scatterers randomly dispersed in an otherwise homogeneous Fe–Cr matrix is assumed except for Fe–12.5 at.%Cr, where a more complex analysis suitable for concentrated systems has to be applied [6].

3. Results and discussion

The magnetic scattering cross sections as functions of the scattering vector, Q, and the reconstructed size distributions of irradiation-induced scatterers are plotted in Fig. 1 to 8 for the four Cr levels and the three neutron fluences investigated.

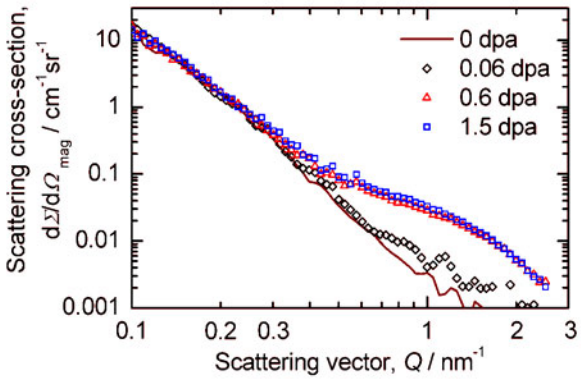

Fig. 1: Magnetic scattering cross sections for Fe-2.5Cr

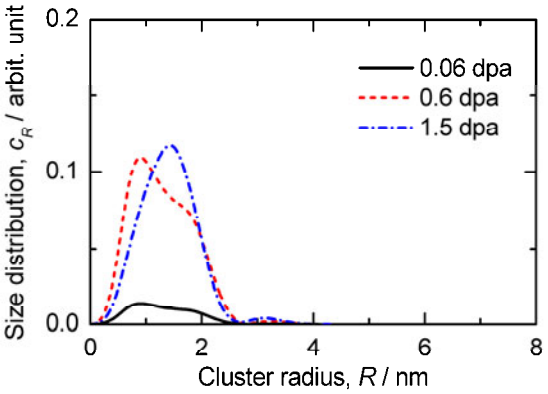

Fig. 2: Reconstructed size distributions of irradiation-induced scatterers in Fe-2.5Cr

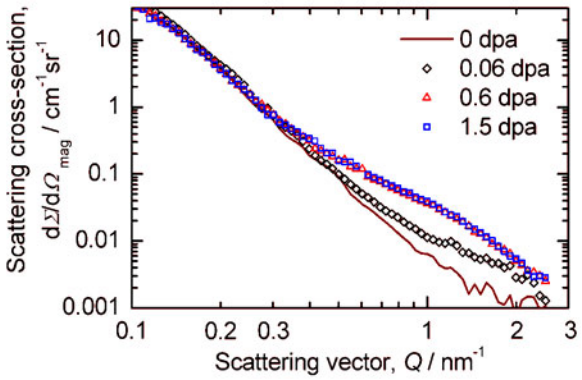

Fig. 3: Magnetic scattering cross sections for Fe-5Cr

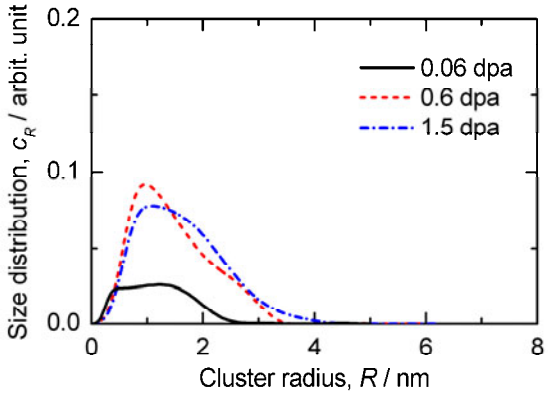

Fig. 4: Reconstructed size distributions of irradiation-induced scatterers in Fe-5Cr

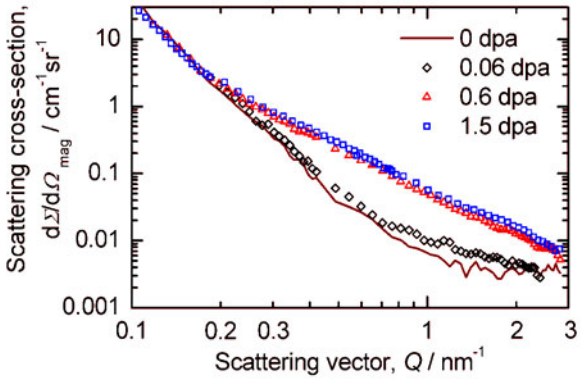

Fig. 5: Magnetic scattering cross sections for Fe-9Cr

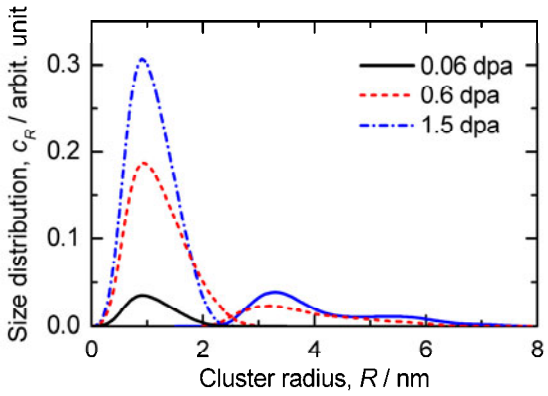

Fig. 6: Reconstructed size distributions of irradiation-induced scatterers in Fe-9Cr

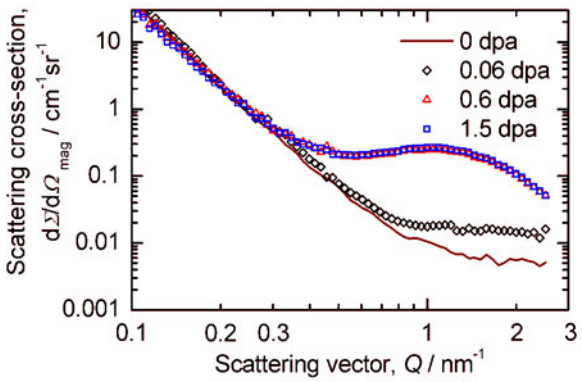

Fig. 7: Magnetic scattering cross sections for Fe-12.5Cr

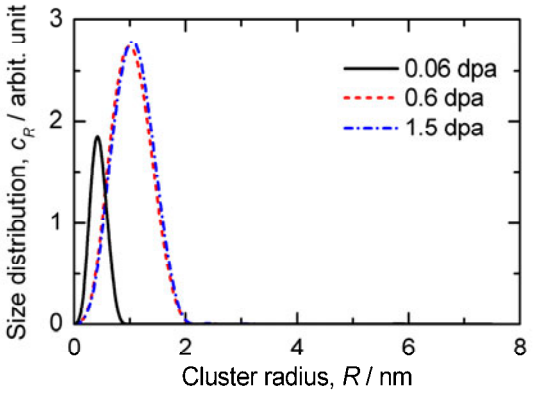

Fig. 8: Reconstructed size distributions of irradiation-induced scatterers in Fe-12.5Cr

The measured average ratio of total (nuclear + magnetic) and nuclear scattering (A-ratio) is plotted in Fig. 9 as function of the alloy Cr content. The levels expected for nanovoids or vacancy clusters, α'-phase particles, and different kinds of Cr-rich carbides are indicated.

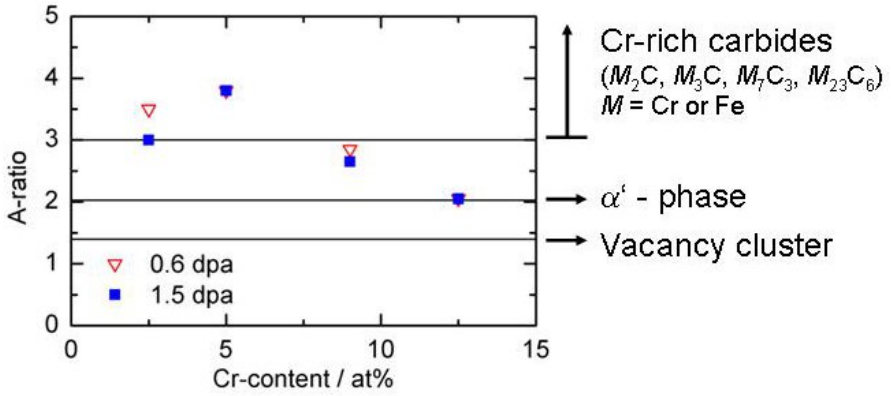

Fig. 9: Measured average A-ratio as function of alloy Cr content. Theoretical A-ratio for candidate scatterers indicated

For any of the Cr contents, nanovoids can be excluded to be the dominant type of scatterers. From the results obtained for Fe-12.5Cr, it is reasonable to assume that the dominant type of scatterers is α'-phase particles. Comparison with the A-ratio calculated for ideal systems indicates that Cr-rich carbides or Cr-C-enriched clusters may explain the experimental results obtained for Fe-2.5Cr and Fe-5Cr. We have checked that the impurity carbon is sufficient for this interpretation [6-8]. However, Ni-Si-enriched clusters reported recently may also play a role [9]. A mixture of Cr-C-enriched clusters and α'-phase particles seems to be present in Fe-9Cr.

Fig. 8 implies for Fe-12.5Cr that both size and volume fraction of α'-phase particles increase at fluences below 0.6 dpa and exhibit a steady state behaviour at fluences in excess of about 0.6 dpa. Based on the assumption that the steady-state value of the volume fraction of α' corresponds to the thermodynamic equilibrium, we have estimated the solubility limit of Cr in Fe at 300°C to be (8.5 ± 0.2) at% [8]. This value is in agreement with the range deduced from a literature review on the occurrence or non-occurrence of ordering/precipitation in Fe-Cr alloys [4].

A similar fluence dependence was observed for Fe-2.5Cr, Fe-5Cr and Fe-9%Cr except that a saturation does not seem to be reached at about 1 dpa in Fe-9Cr. Interestingly, a bimodal size distribution was found for Fe-9Cr. The first and second component can be tentatively interpreted as α'-phase particles and (Cr-C-enriched) dislocation loops. The results of ongoing activities on both modeling and complementary microstructural investigations such as APT and TEM are required to explore the observations in detail.

4. Conclusions

SANS results are reported for commercial purity binary Fe-Cr (2.5 to 12.5 at% Cr) alloys neutron-irradiated at 300°C up to 0.06, 0.6 and 1.5 dpa. The SANS results obtained for neutron-irradiated Fe-12.5Cr indicate Cr-rich α'-phase particles to be the dominant cause of scattering. Saturation of the volume fraction of scatterers was observed to occur at or below 0.6 dpa. Assuming that the saturation level corresponds to the thermodynamic equilibrium, we have estimated a solubility limit of Cr in Fe at 300°C of 8.5at%. The results of complementary microstructural investigations are required to explore the observations in more detail.

References

[1] R.L. Klueh, A.T. NelsonJ. Nucl. Mater. 371 (2007) 37.
[2] M. Gasparotto, R. Andreani, L.V. Boccaccini, A. Cardella, G. Federici, L. Giancarli, G. Le Marois, D. Maisonnier, S. Malang, A. Moeslang, Y. Poitevin, B. van der Schaaf, M. Victoria, Fusion Engng. Des. 66-68 (2003) 129.
[3] L. Malerba, A. Caro, J. Wallenius, J. Nucl. Mater. 382 (2008) 112.
[4] G. Bonny, D. Terentyev, L. Malerba, Scripta Mater. 59 (2008) 1193.
[5] C. Fazio, A. Alamo, A. Almazouzi, S. De Grandis, D. Gomez-Briceño, J. Henry, L. Malerba, M. Rieth, J. Nucl. Mater. 392 (2009) 316.
[6] F. Bergner, A. Ulbricht, C. Heintze, Scripta Mater. 61 (2009) 1060.
[7] C Heintze, A Ulbricht, F Bergner, H Eckerlebe, J. Phys.: Conf. Ser. 247 (2010) 012035.
[8] C. Heintze, F. Bergner, A. Ulbricht, H. Eckerlebe, J. Nucl. Mater. 409 (2011) 106.
[9] V. Kuksenko, C. Pareige, F. Cuvilly, M. Roussel, P. Pareige, J. Nucl. Mater. (2011), doi: 10.1016/j.jnucmat.2011.05.042.
[10] M. Matijasevic, A. Almazouzi, J. Nucl. Mater. 377 (2008) 147.
[11] M. Hernández-Mayoral, Z. Yao, M. L. Jenkins, M. A. Kirk, Phil. Mag. 88 (2008) 2881.

Acknowledgements

This research has been partly supported by the European Commission within the collaborative project GETMAT under Grant Agreement No. 212175.

FRACTURE MECHANICS CHARACTERISATION OF THE BELTLINE WELDING SEAM OF THE DECOMMISSIONED WWER-440 REACTOR PRESSURE VESSEL OF NUCLEAR POWER PLANT GREIFSWALD UNIT 4

Hans-Werner Viehrig, Eberhard Altstadt, Mario Houska, and Matti Valo[1]

1. Introduction

The Greifswald nuclear reactors represent the first generation of the WWER-440 type (V-230). The reactor pressure vessels (RPV) were designed by OKB Gidropress and manufactured by the Izhora Plant in the former Soviet Union at the end of the sixties and beginning of the seventies of the last century. The neutron irradiation induced embrittlement of these WWER-440 first generation RPV's was not monitored by surveillance programmes, instead being based on trend curves. A more realistic evaluation of the toughness response of RPV material to irradiation is achieved by studying directly RPV wall samples taken from decommissioned Greifswald RPVs. The four units of the Greifswald NPP were closed in 1990 after 11–15 years of operation [1,2]. The operation history, the material conditions and the accumulated neutron fluences of the units 1 to 4 are described elsewhere [1-6]. Trepans were extracted from the pressure vessels of the decommissioned units 1, 2 and 4. This paper presents the test results measured for the trepan of the beltline welding seam SN 0.1.4. of the RPV of Greifswald Unit 4, which was shut down after 11 operating cycles. The key part of the testing is focussed on the determination of the fracture toughness reference temperature T_0 according to ASTM Test Standard E1921-10, and its variation through the welding seam thickness. Metallographic and scanning electron microscopic investigations on the bulk material and the fracture surfaces of the specimens were performed in order to interpret fracture toughness T_0-values.

2. Materials and Specimens

The material investigated was extracted from the decommissioned WWER-440 RPVs of the Greifswald NPP unit 4. The trepan No. 4-6 with a diameter of 119 mm was taken through the whole thickness of the circumferential beltline welding seam SN0.1.4. [3-5]. Table 1 summarizes the accumulated neutron fluences and the critical brittleness temperatures predicted by the Russian code [7] for the investigated material. The accumulated neutron fluence of the weld metal (Table 1) corresponds to one third of the designed fluence for 30 years operation [8].

Table 1: RPV steels and irradiation conditions of the investigated trepans sampled from Greifswald unit 4

unit	RPV-material	code trepan	condition	Φ (E>0.5MeV) in 10^{18} n/cm^2 inner wall*2	outer wall*2	T_{K0} *1 °C	T_k *1 °C
4	10 KhMFT	4-6	irradiated	40.92	8.66	-13	123

*1 estimated values [2]; *2 calculated fluences [1,6]

WWER-440/V-230 RPV welding seams are X-butt multilayer submerged arc welds. They consist of a welding root and cover layers welded with an unalloyed wire Sv-08A and the

[1] VTT Manufacturing Technology, P.O.Box 17042, 02044 VTT, Finland

filler material welded with the alloyed wire Sv-10KhMFT and flux AN-42 [2,5,8]. The chemical composition of the investigated trepan No. 4-6 was measured by optical emission spectrometer Spectrolab-S at different thickness locations [9]. Fig. 1 shows a metallographic section and the through thickness distribution of the P and Cu contents in trepan 4-5, which was extracted from the beltline welding seam SN0.1.4. at slightly different azimuthal location than trepan 4-6. As shown in Fig. 1 the P and Cu contents in the weld root region are clearly lower than those of the filling layers. Unalloyed wire Sv-08A is used for the weld root and base metal material from the welded rings is also mixed with the welding root region.

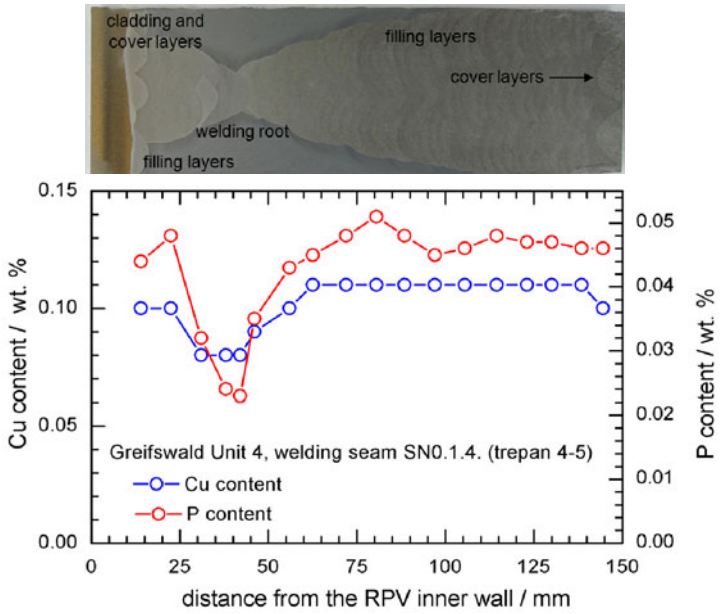

Fig. 1: Metallographic section and P and Cu content through the thickness and of trepan 4-5 extracted from the beltline welding seam SN0.1.4. of the Greifswald Unit 4 RPV [9]

The trepan was cut into 4 discs of 3 mm thickness and 12 discs of 10 mm thickness using a wire travelling electric discharge machine (EDM). From the 3 mm discs 10 pieces of flat tensile and from the 10 mm discs 10 pieces of Charpy-size SE(B) specimens were machined, respectively. The orientation according to ASTM E1823 of the SE(B) specimens is TS (specimen axis along vessel axial direction and crack growth direction across the vessel wall), which is in correspondence with the surveillance specimens in Russian WWER-440/V-213 2nd generation reactors [8]. It is achieved that the neutron loading and structure at the crack tip of the SE(B) specimens from one thickness location are uniform and homogenous, respectively.

The Charpy size SE(B) specimens for fracture toughness testing were pre-cracked (a/W=0.5) and 20% side-grooved.

3. Testing and evaluation

SE(B) specimens machined from one disc form one set of specimens and with them one T_0-value was defined according to ASTM E1921-10. The pre-cracked and side-grooved Charpy-size SE(B) specimens were monotonically loaded until they failed by cleavage instability. Standard Master Curve (MC) reference temperatures T_0 were evaluated with the measured cleavage fracture toughness values, K_{Jc}, by applying the multi-temperature procedure of ASTM E1921-10. Hardness HV10 was measured through the thickness of the welding seam. In addition metallographic investigations and hardness measurements were performed on the

LS and TS plane of selected specimens to characterize the structure in the vicinity of the fatigue crack tip.

4. Results and Discussion

Fig. 2 shows the distribution of the hardness HV10 trough the thickness of the welding seam. The hardness is strongly influenced by the structure of the multilayer welding seam and the decreasing neutron loading towards the outer RPV wall. Close to the cladding and within the welding root region the hardness is defined by the structure of the welding root and the protective layers on the inner surface of the vessel. In general, outside the welding the root area the decreasing neutron fluence results in a decreasing trend in hardness with remarkable scatter.

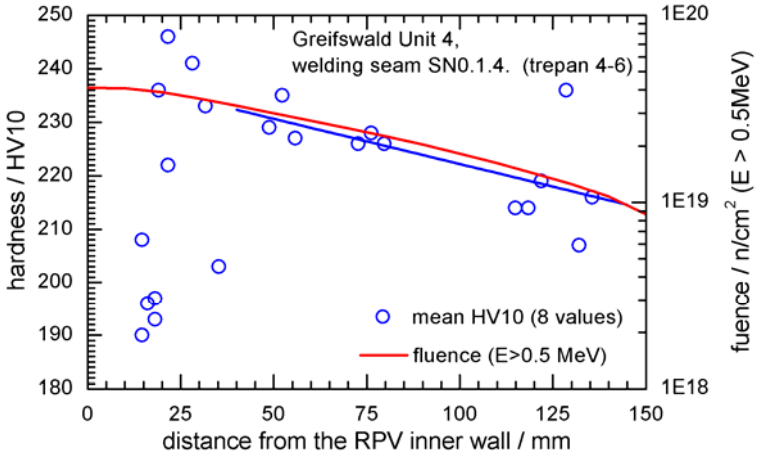

Fig. 2: Hardness HV10 through the thickness of the beltline welding seam SN 0.1.4. of the Greifswald Unit 4 RPV

Fig. 3 shows the through wall variation of the reference temperature T_0 in the beltline multilayer welding seam SN0.1.4 of the Greifswald Unit 4 RPV. As depicted, the T_0–values vary largely across the welding seam. This result differs from the prediction of the Russian code [7], which forecasts a ductile-to-brittle transition temperature (TT) fall of 54 K towards the RPV outer wall, when taking into account the mean P and Cu contents of the filling layers. Beyond the welding root towards the vessel outer surface the mean T_0 is 82,2°C. If the variation of T_0 in this range is considered random variation, its standard deviation is approximately 20°C. Fig. 3 also displays the predicted T_K shift through the thickness of the welding seam, which is based on the Cu and P contents at the specific thickness locations (Fig. 1).

It is obvious that the low P and Cu contents are responsible for the low T_0-values in the weld root region. It can be concluded that the through thickness variation of the T_0results basically from different structures in the weld, which is also supported by the T_0–values measured with reconstituted SE(B) specimens from the 118 mm thickness location. T_0 measured with reconstituted specimens is 81°C and the value measured with full specimens is 117°C (Fig. 3). Crack tips in the reconstituted specimens are at different locations in the weld beat structure than the cracks in the original specimens. Hence, for the same neutron loading a difference in T_0 of 36 K was determined due to variation of the crack tip location in the weld beat structure.

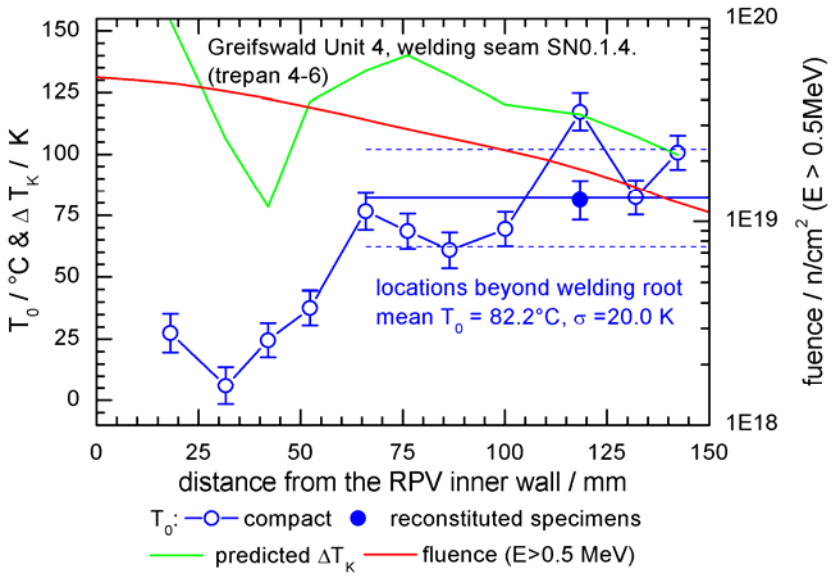

Fig. 3: Reference temperature T_0 through the thickness of the beltline welding seam SN0.1.4. of the Greifswald Unit 4 RPV

5. Conclusions

The test results can be summarised as follows:

- The results represent the material conditions within the multilayer beltline welding seam aged under real operating conditions.
- The hardness HV10 values decrease towards the outer wall of the multilayer beltline welding seam, which is as expected because of decreasing neutron fluence.
- $K_{Jc\text{-}1T}$ values measured with TS-oriented Charpy-size SE(B) specimens prepared from one thickness location in the multilayer welding seam generally follow the MC description rather well but with relatively large scatter.
- There is large variation in the evaluated through-thickness T_0-values of the multilayer welding seams. It is shown that T_0–values measured with the TS-oriented Charpy size SE(B) specimens cut from different thickness locations of the multilayer welding seams strongly depend on the weld structure along the crack tip. The position of crack tip in the multilayer welding seam is crucial.
- Generally, the measured through-thickness T_0–values do not follow the behaviour of the ductile-to-brittle transition temperature (TT) shift predicted by the Russian code [7]. For the present neutron loading of the RPV the predicted decrease of the TT is not visible due to strong variation of toughness caused by the intrinsic weld beat structure and the different filling materials used for weld root and the main weld within the multilayer welding seam.
- The results show that because of the scatter of the evaluated T_0 values, trend curves to forecast the ductile-to-brittle transition temperature shift [7] are not adequate for the investigated WWER-440 welding seam.

References

[1] Konheiser, J., Rindelhardt, U., Viehrig, H.-W., Böhmer, B., Gleisberg, B.: Pressure vessel investigations of the former Greifswald NPP: fluence calculations and Nb based fluence measurements. ICONE14/FEDSM2006 Proceedings, Contribution ICONE 14-89578, 2006M.

[2] Böhmer, B., Böhmert, J., Müller, G., Rindelhardt, U., Utke, H.: Embrittlement studies of the reactor pressure vessel of the Greifswald WWER-440 reactors. Technical Report Task 4: Data Collection; Project Reference: NUCRUS96601 Technical Report, published October 1999, TACIS service DG IA, European Commission, TACIS Information Office, European Commission, Aarlenstraat 88 1/06 Rue d' Arlon, 1040 Brussels, Belgium.
[3] Viehrig, H.-W., Schuhknecht, J., Rindelhardt, U., Weiss, F.-P.: Investigation of the beltline welding seam of the Greifswald WWER-440 unit 1 reactor pressure vessel. Journal of ASTM International 6(2009)5.
[4] Schuhknecht, J., Viehrig, H.-W., Rindelhardt, U.: Investigation of the beltline welding seam and base metal of the Greifswald WWER-440 Unit 1 reactor pressure vessel. Journal of Engineering for Gas Turbines and Power, Transactions of the ASME Vol. 133(2011) 5.
[5] Viehrig, H.-W., Altstadt, E., Houska, M., Valo, M.: Fracture mechanics characterisation of the beltline welding seam of the decommissioned WWER-440 reactor pressure vessels of nuclear power plant Greifswald Unit 4, submitted to Intern. J. Pressure Vessel and Piping, 2011.
[6] Rindelhardt, U., Viehrig, H.-W., Konheiser, J., Schuhknecht, J., Noack, K., Gleisberg, B.: RPV material investigations of the former VVER-440 Greifswald NPP. Nuclear Engineering and Design 239 (2009)9, 1581-1590.
[7] PNAE G-7-008-86: Strength calculation norms for nuclear power plant equipment and piping. Energoatomizad, Moscow, 1989.
[8] IAEA-TECDOC-1442: Guidelines for prediction of irradiation embrittlement of operating WWER-440 reactor pressure vessels. IAEA, Vienna, 2005.
[9] Valo, M.: Pre-characterisation of Greifswald trepan samples. Research Report VTT-R-03746-10, December 2010.

ACKNOWLEDGMENTS

This study was supported by the German Federal Ministry of Economics and Technology, (Reactor Safety Research Project Grant No. 1501331), and by the European Commission through the FP7 project LONGLIFE (contract No. 249360).

CFD-MODELLING OF THE CCFL PHENOMENA IN A MODEL OF A PWR HOT LEG

Deendarlianto, Thomas Höhne, Dirk Lucas

1. Introduction

The detailed three-dimensional (3-D) information on the transient flow behaviour under countercurrent flow limitation (CCFL) in a pressurized water reactor (PWR) hot leg is an important issue in the reactor safety analysis. It relates to a hypothetical scenario of small break Loss of Coolant Accident (LOCA) in a PWR which leads to the reflux-condensing mode. During this scenario, a part of the condensate flows back towards the reactor pressure vessel (RPV) in counter current to the steam. In this mode, a CCFL could occur, affecting the core cooling. Deendarlianto et al. reviewed different applications of CFD codes to simulate the phenomena around the CCFL in a PWR hot leg [1]. They indicated that there is still a lack of knowledge regarding suitable closure models for this application. In some cases empirical correlations originally obtained for one-dimensional codes were used for this multidimensional problem.

Deendarlianto et al. reported in [2] that there are three morphologies during CCFL in a PWR hot leg. Those are air bubbles, stratified flow with a free surface and entrainment of liquid droplets. Separate models, such as interfacial drag and interfacial are density, are necessary for dispersed particles (bubbles and droplet) and continuous phases. According to the above mentioned flow morphologies, separate drag coefficients and interfacial area densities have also to be applied. To solve this problem, Egorov proposed an algebraic interfacial area density model (AIAD) [3]. In this model the 3D effects of the simulated phenomenon and the change of flow morphologies are considered. In extension to this model, Höhne developed a new drag coefficient at the free surface morphology [4]. Next, a blending function was introduced to switches the corresponding morphologies on the basis of the limit of void fraction and their length scales. The aim of the present paper is to simulate the phenomena around the CCFL in a PWR hot leg with newly developed of drag coefficient in the AIAD model to the Euler-Euler problem.

To validate the developed drag coefficient, an experimental series on the CCFL in a rectangular channel of a model of PWR hot leg was carried out at TOPFLOW facility. The experimental apparatus and procedure used in this study were described in the previous papers [2,5]. The test section is composed of a horizontal rectangular channel, a bend that connects it to an upward inclined and expended channel, and a quarter of a circle representing the steam generator inlet chamber. The horizontal part of test section is 2.12 m long and has a rectangular cross-section of 0.05 m × 0.25 m. The height of the rectangular test section (0.25 m) represented the inner pipe diameter of hot leg pipe of a PWR from the German *Konvoi* type at a scale of 1:3.

2. CFD-Modeling

In the present simulation, the flow was treated as a 3-D transient problem. For the solution of the described task, Euler–Euler inhomogeneous mixture model using the commercial CFD code ANSYS CFX 12.0 was used. The calculation model is shown in Fig. 1. In the figure, very carefully developed structured mesh for most of the flow field was adequate, at which

the local refinement on them were carried out. Here a structured mesh consisted of 248,610 hexahedral elements and 281,076 nodes.

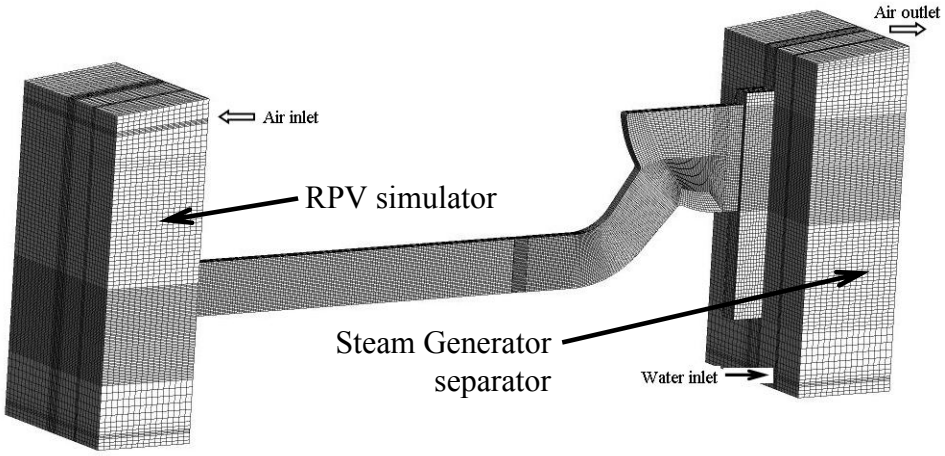

Fig. 1: Calculation meshes

The SST buoyancy turbulence model was used in the simulation. It solves the turbulence/frequency-based model (k–ω) at the wall and the standard k–ω in the bulk flow. Both phases have treated as isothermal and incompressible. The air outlet was modelled with an opening boundary condition. The inner surface of the channel walls has been defined as hydraulically smooth with a non-slip boundary condition applied to both gas and liquid phases. The developed drag coefficient at the free surface within AIAD model, C_D, was implemented into ANSYS CFX via the command language CEL (CFX expression language). The calculations were performed in parallel of 4 processors of HZDR Linux cluster. Typical computation time for each case was about 4 months.

Table 1: Calculation runs

HZDR exp. run	Working fluids	m_G [kg/s]	System pressure [MPa]	Drag Coefficient C_D [-]
30-05	Air-water	0.37 - 0.41	0.30	AIAD
30-09	Air-water	0.18 - 0.27	0.15	AIAD & C_D=0.44
11-01	Steam-water	0.49 - 0.67	1.50	AIAD

Four calculations have been performed of three HZDR experimental run (30-05, 30-09, and 11-01), and they are summarized in Table 1. The injected water mass flow (m_L) for all the calculation series was 0.3 kg/s. The injected gas flow rates were used in current calculation according to experimental injected gas flow rates profiles.

3. Results

In order to examine the validity of new developed drag coefficient, a transient simulation was carried out firstly by using a constant drag coefficient of C_D=0.44 as a default value from ANSYS CFX. The HZDR experimental run of 30-09 was used for this investigation. The results were reported in [6]. The formation of liquid slug and wave crest during CCFL as observed in experiment could not be reproduced by using C_D=0.44.

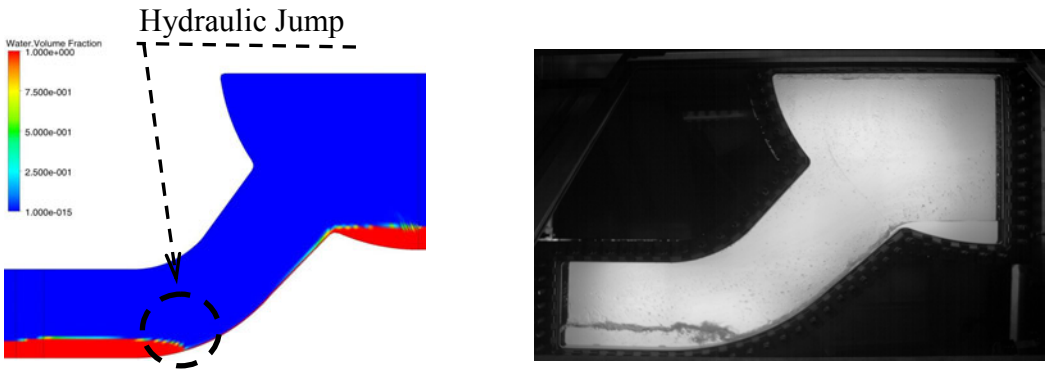

(a) Simulation (b) Experiment

Fig. 2: Flow structure near the elbow before the CCFL (HZDR exp. Run of 30-09, air-water, m_G= 0.181 kg/s)

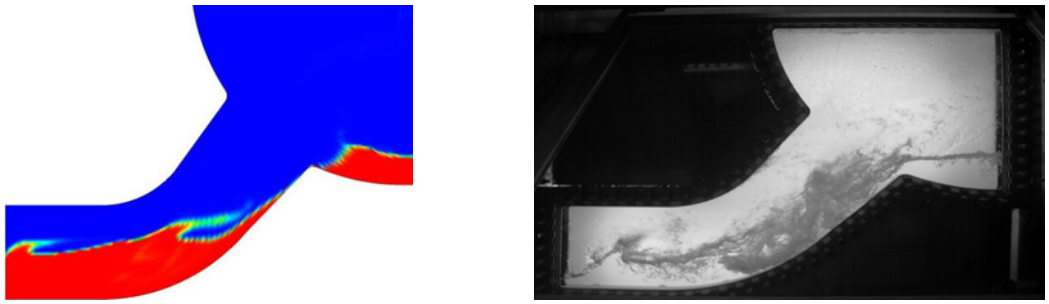

(a) Simulation (b) Experiment

Fig. 3: Flow behaviour near the elbow during the CCFL (HZDR exp. Run of 30-09, air-water, m_G=0.268 kg/s)

For this reason the newly developed drag coefficient in AIAD model was used to simulate the CCFL in a model of PWR hot leg in the following. Fig. 2 and 3 illustrate the examples of flow structure near the elbow in a PWR hot leg before and during CCFL (HZDR exp. Run of 30-09, air-water) respectively. The air mass flow rate were m_G=0.181 kg/s and m_G =0.268 kg/s). In the figures, (a) and (b) correspond respectively to the calculated water volume fraction and the visual observation obtained from the experiment. In comparison between the calculation and experimental observation, it is noticed that the simulation agrees well with the experiment. Before the CCFL, the thin liquid film was found in the bend region, whereas the flow pattern is a supercritical stratified flow. A hydraulic jump as the transition from supercritical to subcritical flow is observed near the bended region. During CCFL, some part of water flows in the same direction with the air, and a big roll wave generated by the merging of small waves due to the interfacial drag is observed near the bended region.

Fig. 4 shows the calculated and experimental results of the rise of water level in the RPV simulator in function of time. Those are plotted against the corresponding experimental data of the injected gas mass flow rate. Close observation of the figure indicated that there are three important regions in counter-current two-phase flow. In the first region, the rise of water level increases with a constant slope independently of the injected gas mass flow rate (stable counter-current flow). In the second region, the slope of the curve of water level in the RPV simulator begins to decrease. The begin of this region is known as the onset of flooding. With further increase of the gas mass flow rate, the rise water level shows a plateau (region 3), and

is known as zero liquid penetration. Next, there is a good agreement between the calculated and experimental data of the rise of water level in RPV simulator.

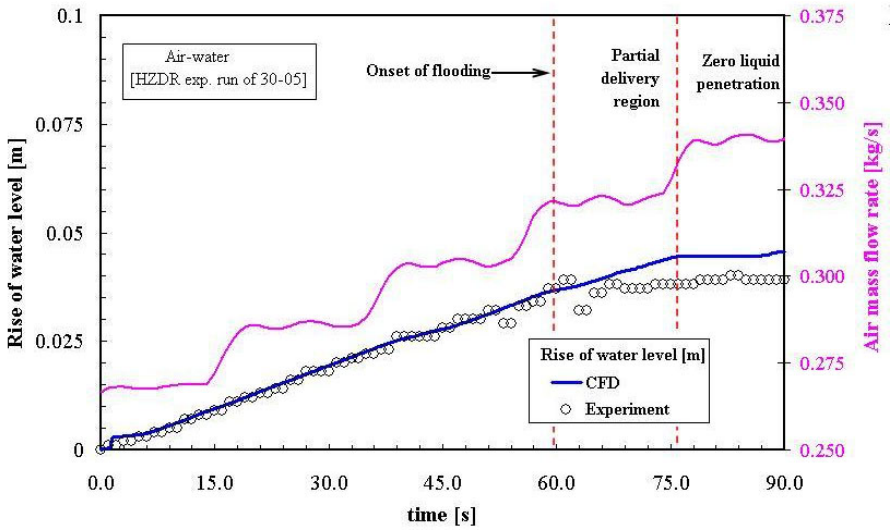

Fig. 4: Example of the calculated the rise of the water level inside RPV channel

The quantitative comparisons between the CFD calculations and experimental data are displayed in terms of the CCFL characteristics and the water level inside the hot leg channels. They are shown in Fig. 5 and 6, respectively. The non-dimensional superficial velocity,

$$J_k^* = J_k \sqrt{\frac{1}{gH} \cdot \frac{\rho_k}{(\rho_L - \rho_G)}}, \qquad (1)$$

known as Wallis parameter is used to describe the CCFL characteristics. Furthermore, an image processing algorithm was developed to capture the gas-liquid interface in the camera frames for the comparison of the water level inside the hot leg channel.

Close inspection of both figures reveal that the calculated results are in a good agreement with the HZDR experimental data. In comparison between the calculated CCFL characteristics of HZDR experimental runs of 30-09 and 11-01 as shown in Fig. 5, it is noticed that the fluid viscosities has a major effect on the CCFL characteristics at high liquid mass flow rate.

Here the flooding curves between both cases increases with $(J_L^*)^{1/2}$. This behavior can be explained by the fact that at this condition the net-flow in the flow path becomes higher. The liquid viscosity which mainly influences the wall and interfacial frictions plays an important role here.

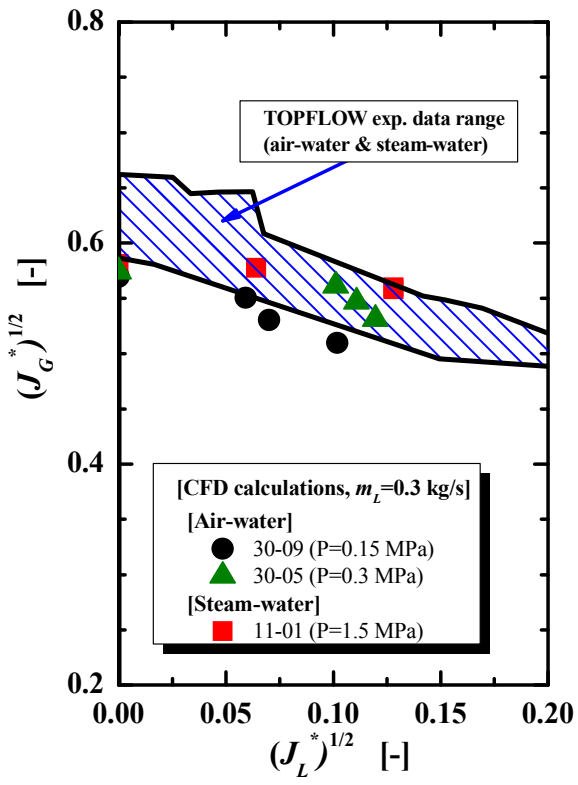

Fig. 5: CCFL characteristics

4. Conclusions

The whole phenomena of CCFL in a PWR hot leg was modelled by applying CFD methods, whereas the new concept of the drag coefficient in the AIAD model was implemented. A full model of a hot leg rectangular channel from TOPFLOW facility represented a 1/3 of the inner pipe diameter of hot leg pipe of a PWR of the German *Konvoi* type was used in the calculation. The results indicated that only AIAD model allows the correct simulation of the relevant CCFL phenomena physically. The developed approach also enables the answering of many practical questions related to this phenomenon. Moreover, further improvement of the model should be carried out to further reduce the calculation time.

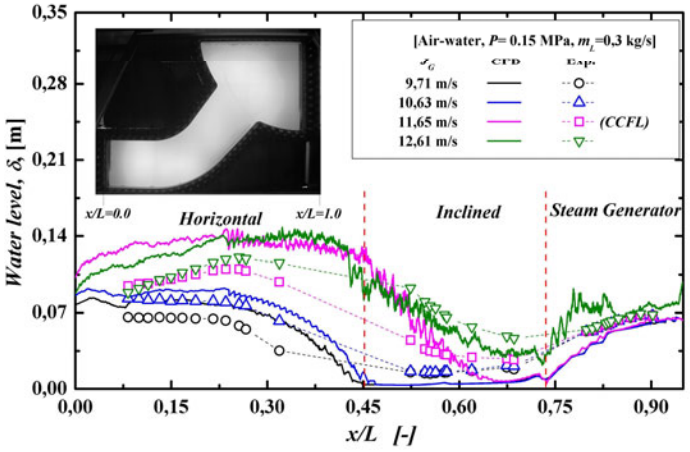

Fig. 6: Water level inside hot leg channel (HZDR Exp. Run of 30-09)

References

[1] Deendarlianto, T. Höhne, D. Lucas, K. Vierow, (2011), Gas-liquid countercurrent two-phase flow in a PWR hot leg: a comprehensive research review. Submitted paper to Nuclear Engineering and Design.

[2] Deendarlianto, C. Vallée, D. Lucas, M. Beyer, H. Pietruske, H. Carl, (2008), Experimental study on the air/water counter-current flow limitation in a model of the hot leg of a pressurized water reactor. Nuclear Engineering and Design, 238 (12), 3389-3402.

[3] Y. Egorov, (2004), Validation of CFD codes with PTS-relevant test cases", 5th Euratom Framework Programme ECORA project.

[4] T. Höhne, (2009), Experiments and numerical simulations of horizontal two-phase flow regimes, Proceeding of the Seventh International Conference on CFD in the Minerals and Process Industries, Melbourne, Australia.

[5] C. Vallée, T. Seidel, D. Lucas, M. Beyer, H.-M. Prasser, H. Pietruske, P. Schütz, H. Carl, (2009), Influence of the fluid properties on co-current two-phase flows in a horizontal channel connected to a riser, Proceedings of the 7th World Conference on Experimental Heat Transfer, Fluid Mechanics and Thermodynamics (ExHFT-7) (pp. 443-452), Krakow, Poland.

[6] Deendarlianto, T. Höhne, D. Lucas, G. A. Montoya, C. Vallée, (2011), CFD studies on the phenomena around the counter-current flow limitations of gas/liquid two-phase flow in a model of PWR hot leg. Submitted paper to Nuclear Engineering and Design.

Acknowledgements

This work is carried out within the frame work of a current research project funded by the German Federal Ministry of Economics and Technology, project number 150 1329. A part of the present research is also supported by the *Alexander von Humboldt Stiftung* in Germany. In addition, the authors would like to thank also the TOPFLOW team for their work on the test facility and the experiments.

THE REACTOR-PHYSICS TREATMENT OF THE DOUBLE HETEROGENEITY OF HTGR FUEL ELEMENTS

Emil Fridman and Bruno Merk

1. Introduction

High Temperature Gas-cooled Reactors (HTGRs) remain an attractive alternative to the conventional Light Water Reactors (LWRs) because they can provide high-grade heat for various industrial processes such as hydrogen production in addition to generating electricity. This unique capability is partially owed to the highly robust tristructural isotropic (TRISO) coated fuel particles concept (Fig. 1) used in HTGRs.

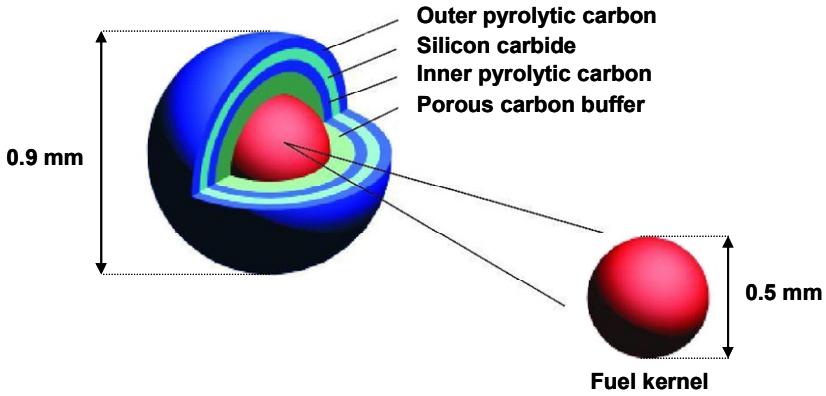

Fig. 1: TRISO coated fuel particle

In block-type HTGRs, the TRISO particles are typically dispersed in graphite fuel elements, which are placed in graphite blocks with cooling channels (Fig. 2). This fuel configuration has a so-called double-heterogeneous structure, which presents a challenge for existing deterministic lattice codes that were originally developed for LWR lattices. A large number of TRISO coated particles which are randomly distributed in the fuel compact introduces an additional complexity into the modeling. Monte Carlo (MC) based codes, which are capable of simulating complex geometries of HTGR fuel elements, are mainly used for the reference calculations. The use of MC codes as production tools for a few-group cross section generation for 3D core simulators is still very limited due to the high computational costs. Thus, it is still a common practice to use 2D deterministic transport codes (e.g. HELIOS [1], CASMO [2], or APOLLO [3]) for a few-group cross section generation.

Recently a new few-group cross section generation methodology for a full core analysis of HTGRs has been proposed [4]. This methodology is based on homogenization approach called Reactivity equivalent Physical Transformation (RPT). The RPT methodology allows combining the high spatial resolution of MC codes with the superior computational speed of deterministic lattice codes. Computational efficiency is essential, since for few-group cross section sets generation about hundreds to thousands branch-off lattice calculations are required. At the first stage, a MC code is used to simulate an HTGR fuel element with explicitly described TRISO particles at the beginning of life (BOL) and at the nominal operational conditions. At the second stage the TRISO particles are homogenized within the fuel compact graphite to get rid of double-heterogeneity problem. A simple volume-weighted homogenization of TRISO particles in the graphite matrix results in the underestimation of

the resonance self-shielding effect. This leads to the incorrect estimation of the neutron flux spectrum, overestimation of absorption rates, and finally to the underprediction of reactivity.

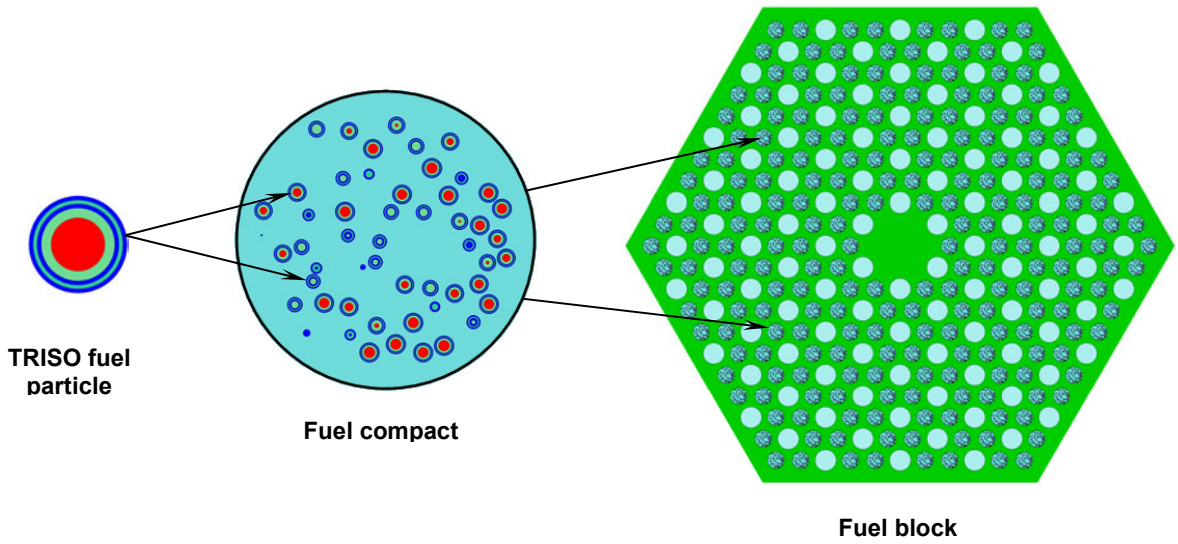

Fig. 2: The double heterogeneity of TRISO fuel particles in fuel compact and compact in the fuel block

However, according to the RPT approach, TRISO particles are homogenized in a smaller central volume rather than in entire fuel compact (Fig. 3b). The volume of the smeared region is adjusted in such way that neutron multiplication factor, k-inf, of the homogenized geometry matches that of the reference 3D heterogeneous one obtained from the MC reference calculations. Since the radius of the smeared zone was determined at the beginning of life (BOL) it is kept constant during depletion calculation. Several papers [5, 6] demonstrated a very good accuracy of the RPT methodology.

2. The modified RPT methodology

The main disadvantage of the 'standard' RPT approach is the fact that originally distributed TRISO particles (Fig. 3a) are smeared together with the compact graphite and constitute one homogeneous material (Fig. 3b). Keeping in mind that the fuel and graphite temperatures may significantly vary during the reactor operation, these temperatures should be decoupled during branch-off calculations for the few-group cross section generation. However, in the majority of lattice codes temperatures are assigned to the regions (e.g. HELIOS code) or to the homogeneous materials (e.g. CASMO code) rather than to particular nuclides like in the MC codes. In order to overcome this disadvantage the RPT methodology has been modified [7] in a way, that only TRISO particles are smeared in the central compact region, while all compact graphite is concentrated in the remained outer compact region (Fig. 3c). This modification allows assigning different temperatures to the fuel as well as to the compact matrix graphite during depletion and branch-off calculations, since each material is now in an extra region. The change in the RPT methodology (separating graphite and fuel) generates a slightly enlarged diameter for the modified RPT region compared to the diameter of the 'standard' RPT region.

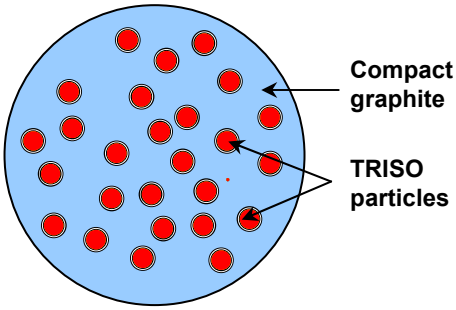

a) Randomly distributed TRISO particles

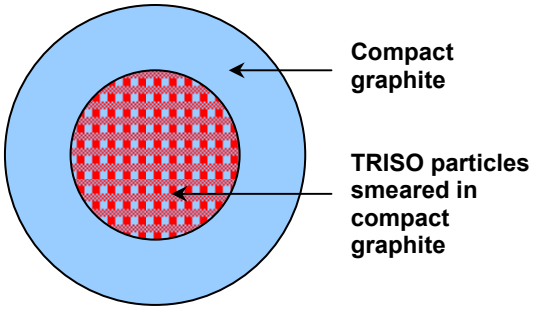

b) Smearing using "standard" RPT

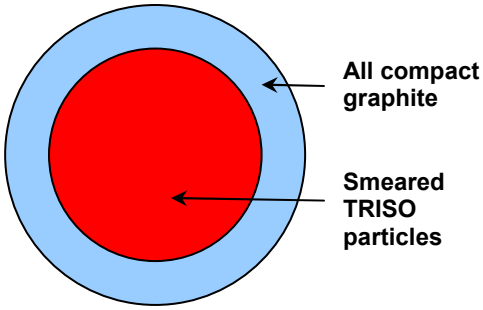

c) Smearing using modified RPT

Fig. 3: RPT methodology

3. Verification of modified RPT methodology

To verify the modified RPT methodology a set of depletion calculations for a prismatic block-type HTGR fuel lattice consisting of fuel and coolant channels was performed. Two models of prismatic fuel assembly were considered: 1) a 3D model with explicitly described TRISO particles; 2) a 2D model, in which TRISO particles are homogenized using the modified RPT approach (Fig. 4). The 3D calculations were performed with the MCNP [8] based depletion code BGCore [9]. 2D calculations were performed with the deterministic lattice code HELIOS 1.9. The results of the 3D BGCore calculations were assumed as a reference for comparison purposes.

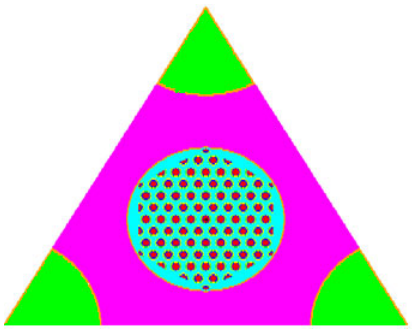

a) TRISO particles in hexagonal lattice

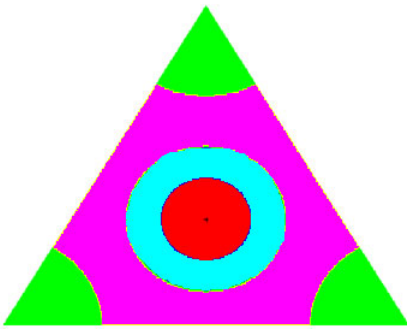

b) TRISO particles smeared using RPT
Red: Smeared TRISO particles
Blue: Compact graphite

Fig. 4: Prismatic fuel lattice models

In the BGCore calculations, MCNP runs were performed with 50,000 neutron histories and 100 active cycles to obtain a standard deviation of k-inf lower than 0.0005. The nuclear data libraries employed by BGCore are based on JEFF-3.1 evaluation while HELIOS utilizes an

internal library with ENDF/B-VI based cross section data. In this study, the HELIOS library with 190 neutron energy groups was used.

Initially, the depletion calculations were performed up to the burnup of 120 MWd/kg with 70 steps assuming the same temperature of 900 K for the fuel and the compact graphite. Then, all transport calculations were restarted at seven specified burnup points with varied fuel temperatures of 600 K and 1200 K to simulate branch-off calculations.

The k-inf as function of burnup and fuel temperature obtained from the 3D BGCore calculation and the HELIOS 1.9 calculation is shown in Fig. 5. The k-inf for the full burnup case (fuel and graphite at 900 K) obtained from the 2D HELIOS calculation agrees well with that of the 3D BGCore run over the whole burnup period. The results for the branch-off calculations at the specified branching points agree well too. The deviation in the burnup calculation is typically lower than 0.3% below 80 MWd/kg. The maximum difference occurs at EOL, where a small systematic error appears. There the difference rises to 0.6%.

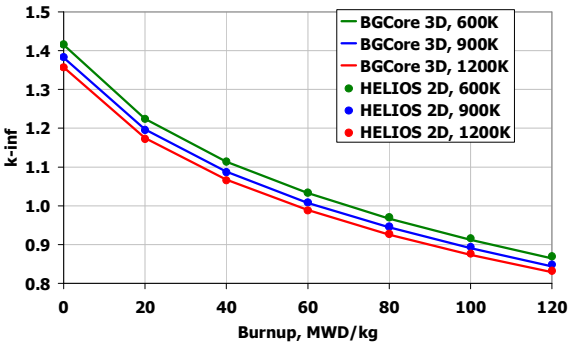

Fig. 5: k-inf as function of burnup: BGCore 3D vs. HELIOS 2D

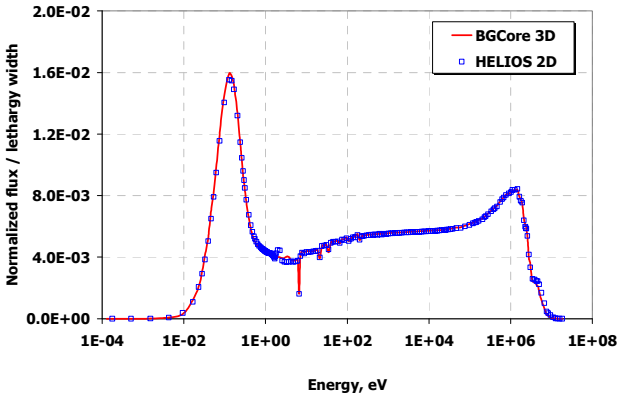

Fig. 6: Normalized flux at BOL: BGCore 3D vs. HELIOS 2D

Fig. 6 compares the neutron spectrum in the fuel region between the 3D BGCore run and that of the 2D HELIOS run. Very good agreement can be observed from the figures including location, height, and width of the thermal and the fast peaks as well as the dimensions of the resonance dips. This indicates that modified RPT homogenization method is capable of accurately reproducing the neutron spectrum of double-heterogeneous systems.

4. Conclusions

The Reactivity equivalent Physical Transformation (RPT) homogenization methodology was proposed for the analysis of HTGR fuel elements in order to get rid of the double-heterogeneity problem, typical for HTGR fuel elements. At the Institute of Safety Research modifications to the RPT method were introduced in order to adopt it for the branch-off calculations.

A preliminary verification study performed on the fuel lattice level with BGCore and HELIOS codes has shown good agreement between the reference solution and the modified RPT method in k-inf as function of burnup and fuel temperature as well as BOL neutron spectra.

Recently, the full core analysis of the reference simplified HTGR core was carried out [10]

with nodal diffusion code DYN3D [11] using macroscopic nodal cross sections provided by HELIOS. The modified RPT approach was applied in order to eliminate the double-heterogeneity of HTGR fuel elements in HELIOS calculations. The results of DYN3D calculations were compared with those obtained from the reference full core MCNP simulation. Good agreement in k-eff and radial power distribution was observed.

The conducted verification studies demonstrate the applicability of the modified RPT approach for deterministic calculations of HTGR lattices. Nevertheless, some additional steps in verification should be done including comparison of burnup dependent fuel isotopic composition, spectral indices, as well as comparison of fuel and moderator temperature reactivity coefficients.

References

[1] R. J. Stammler, HELIOS Methods, Studsvik Scandpower, 2003.

[2] J. Rhodes, M. Edenius, CASMO-4. A Fuel Assembly Burnup Program. User's Manual. Studsvik Scandpower SSP-01/400 Rev. 4, 2004.

[3] R. Sanchez et al., APOLLO II: a user-oriented, portable, modular code for multigroup transport assembly calculations, Nuclear Science and Engineering 100, p. 352, 1988

[4] Y.H. Kim, W. S. Park, Reactivity-Equivalent Physical Transformation for Elimination of Double-Heterogeneity, Transaction of American Nuclear Society, 93, p. 959, 2005.

[5] J. M. Noh, K. S. Kim, Y. Kim, Hyun C. Lee, Development of a computer code system for the analysis of prism and pebble type VHTR cores, Annals of Nuclear Energy 35, 2008, p.1928, 2008.

[6] E. Fridman, E. Shwageraus, HTGR Fuel Element Depletion Benchmark: Stage Three Results, Proc. PHYSOR 2010, Pittsburgh, Pennsylvania, USA, May 8-14, 2010.

[7] E. Fridman, B. Merk, Modification of the Reactivity Equivalent Physical Transformation Method for HTGR Fuel Element Analysis, Proc. HTR 2010, Prague, Czech Republic, October 18-20, 2010.

[8] J. F. Briesmeister Ed., MCNP - A General Monte Carlo N-Particle Code, Version 4C, Los Alamos National Laboratory, LA-13709-M, 2000.

[9] E. Fridman, E. Shwageraus, A. Galperin, Implementation of Multi-Group Cross-Section Methodology in BGCore Monte Carlo-Depletion Code, Proc. PHYSOR 2008, Interlaken, Switzerland, September 14-19, 2008.

[10] E. Fridman, S. Kliem, U. Rohde, Preliminary analysis of HTGR core with DYN3D nodal diffusion code, Proc. HTR 2010, Prague, Czech Republic, October 18-20, 2010.

[11] U. Grundmann, U. Rohde, S. Mittag, DYN3D – three dimensional core model for steady-state and transient analysis of thermal reactors, Proc. PHYSOR 2000, Pittsburgh, Pennsylvania, USA, 2000.

CONTACTLESS FLOW RATE SENSORS FOR LIQUID METAL MEASUREMENTS

Dominique Buchenau, Gunter Gerbeth, and Janis Priede[1]

1. Introduction

Accurate and reliable flow rate measurements are required for various liquid metal systems such as the Na or Lead-flows in fast reactors, the PbBi-flows in transmutation systems, the flows in liquid metal targets or for material processing technologies like melting, refining or casting of metals or alloys. However, velocity measurements in opaque liquid metal flows still represent a challenging task as commercial measuring systems are not available for such melts. In processes involving electrically conducting liquids, the application of an external magnetic field offers efficient opportunities for a contactless flow control and flow handling [1]. Further developments require a better knowledge about the details of the flow, the transport properties of the flow or the technological specifications, respectively.

Commercial flow meters are typically based on the flow-induced electrical voltage, which is measured by electrodes in direct contact to the melt, in a steady magnetic field [2]. For liquid metal flows, a contactless measurement is preferable. We report on the recent development of two types of such flow meters. The first sensor operates by detecting the flow-induced disturbance in the phase distribution of an externally applied AC magnetic field [3, 4, 5, 6]. Such a phase-shift flow meter was developed with an emitting coil at one side of the duct and two sensing coils at the opposite side. The second approach uses a rotatable single cylindrical permanent magnet, which is placed close to the liquid metal duct [7]. The rotation rate of this magnet is proportional to the flow rate. The signal of this sensor is independent on the electrical conductivity of the flowing melt, thus independent on temperature. Both flow rate sensors have been tested at several liquid metal loops: a Na- and a Lead-loop at HZDR, and a PbBi-loop at SCK-CEN Mol (Belgium). In all cases, both sensors show a very good linearity of their signal with the true flow rate in the pipe. For the sodium flow at the NATAN facility of HZDR, the measured flow rates were also compared with measurements of the local velocity profile in the duct performed by ultrasonic Doppler velocimetry.

2. Phase shift flow meter

The phase-shift sensor [3, 4, 5, 6] operates with an alternating magnetic field produced by the emitter coil on one side of the pipe. On the other side two receiver coils are placed (see Fig. 1a, b). The whole set-up is working like an intersected transformer with two secondary coils. We distinguish between the symmetric adjustment ($l^*=0$mm) and the asymmetric adjustment with some shift $l^*\neq 0$mm between the emitter and the receiver coils. The flow in the duct causes a change of the alternating magnetic field. In principle, the amplitude change as well as the phase change can be used for flow rate measurements. In the present implementation, the phase difference between two measuring points is used as measuring quantity.

[1] Applied Mathematics Research Centre, Coventry University, United Kingdom

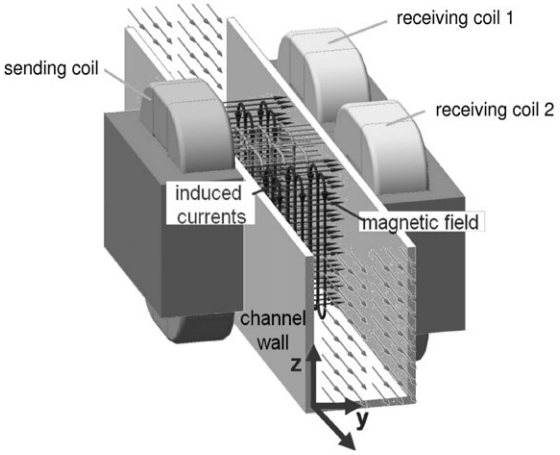

Fig. 1a: Set-up of the phase-shift flow meter

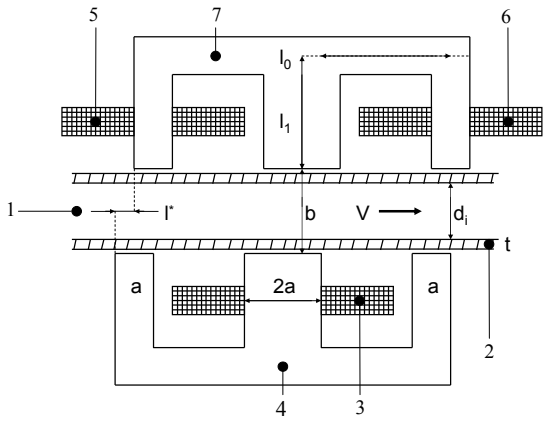

Fig. 1b: Sketch of the phase-shift flow meter in the asymmetric adjustment. 1-duct, 2-duct-wall, 3-emitter coil, 4,7-laminated magnetic iron, 5,6-receiver coils, l-displacement length between emitter and receiver coils*

3. The single Rotating magnet

The second flow rate sensor (see Fig. 2a, b) considered here uses a single cylindrical permanent magnet magnetized perpendicularly to its axis. An almost frictionless bearing allows a free rotation of the magnet. The electromagnetic torque on the magnet caused by the liquid metal flow sets the magnet into rotation. However, the equilibrium rotation rate is determined by a vanishing total electromagnetic torque. The equilibrium rotation rate depends only on the flow rate and the geometry of the system while it is independent of the electromagnetic torque itself. Thus, the rotation rate is not affected neither by the strength of the magnet nor by the conductivity of the liquid metal provided that the friction on the magnet is negligible. For more details of this sensor we refer to [7].

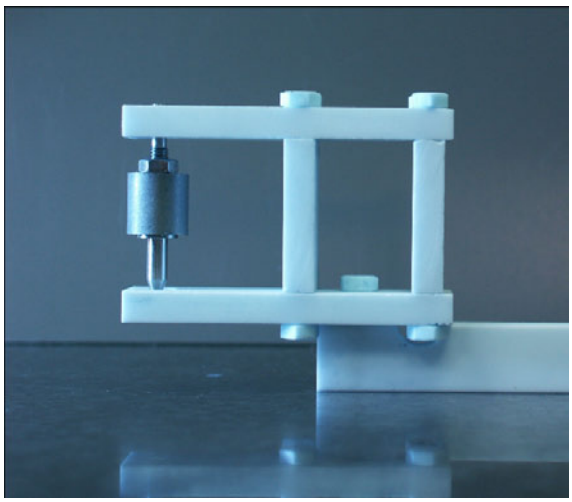

Fig. 2a: Single-magnet rotary flow meter

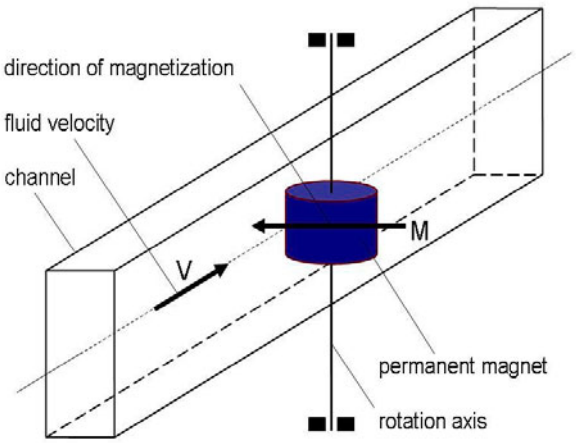

Fig. 2b: Sketch of the single magnet rotary flow meter

4. Results and discussion

4.1. Experiments on the sodium-loop at HZDR

The applied phase-shift sensor, which was used for measurements on the Sodium-loop, operates with a sending coil (500 turns) placed on one side of the channel and two receiving coils (1000 turns each) on the opposite side. This flow meter operates like a split transformer with two secondary coils. The phase shift between the voltages induced in the two receiver coils is measured using a lock-in amplifier with the internal averaging time of 100ms and the accuracy of at least 2%. Receiving and sending coils can be placed either directly against each other or shifted by some displacement l*. Further we refer to these two arrangements as symmetric and asymmetric ones.

The emitter coil is fed by an alternating current in the range of a few hundred mA up to three amperes. Both the sending coil and the receiving coils are furnished with laminated magnetic steel in order to concentrate and conduct the magnetic flux. The coil wires are covered by a double layer of high temperature resistant polyamide (T=260°C). Furthermore, the coils are encased by ceramic material MARCOR which withstands temperatures up to 800°C. This arrangement protects the sending- and receiving coils from the influence of the hot pipe or channel with the liquid melt to be measured.

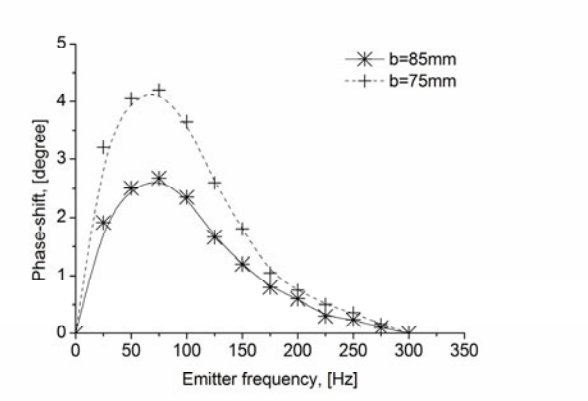

Fig. 3a: Frequency response of the phase-shift flow meter in the symmetric adjustment

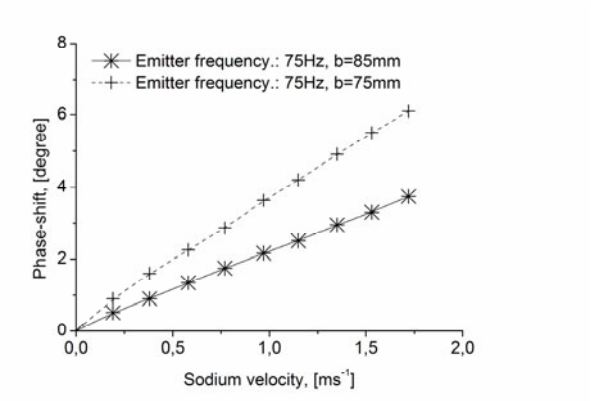

Fig. 3b: Phase-shift in dependence of the averaged velocity of the liquid sodium (symmetric adjustment)

Fig. 3a presents measurements of the frequency response in the symmetric adjustment as a function of the width of the measurement gap for a given flow rate and an input current of 500 mA. The optimal frequency of the phase-shift sensor has to be chosen in such a way that the skin-depth of the emitter field is in the same range as the width of the channel. Comparing both measurements taken at a measurement gap of 85 mm and 75 mm we are able to determine a sensitivity factor K_b=1.6 experimentally. The same sensitivity factor can be found in Fig. 3b, which shows the linear dependence of the measured phase-shift between both sensing coils as a function of the averaged sodium-velocity in the cannel of the vertical test section of the Sodium-loop at HZDR.

Eventually, Fig. 4 shows the measurements with the single-magnet rotary flow meter taken during a measurement campaign on the horizontal test-section of the Sodium-loop at HZDR. The dependence between rotation rate and the averaged sodium-velocity is clearly linear. The

currents induced in the electrically conducting channel walls during rotation of the magnet results in a breaking torque for the rotating magnet. Therefore, beside the effects of remanent magnetism, the extension of the measured line is not passing through the point of origin.

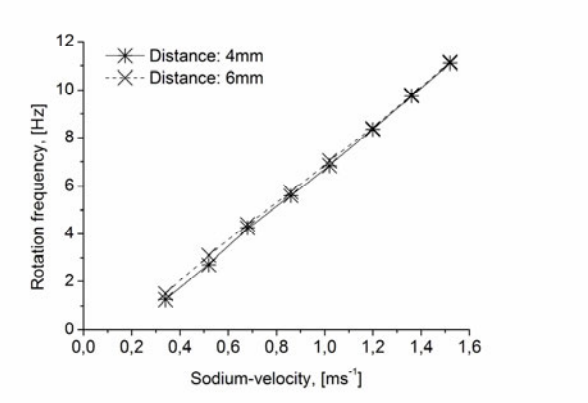

Fig. 4a: Rotation rate in dependence of the averaged sodium-velocity measured on the horizontal test-section of the sodium-loop at HZDR

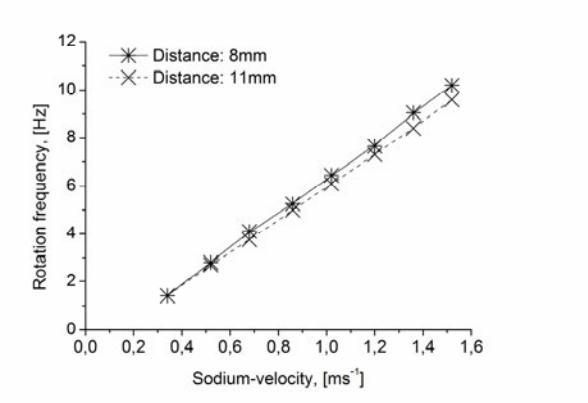

Fig. 4b: Rotation rate in dependence of the averaged sodium-velocity measured on the horizontal test-section of the sodium-loop at HZDR

4.2. Experiments on the WebExpIr at SCK-CEN

The phase-shift flow meter was tested at a LBE pipe flow during a measuring campaign at the WebExpIr-loop of SCK-CEN [8]. The characteristic measurement conditions of the sensor are mainly determined by the properties of the fluid such as the electrical conductivity (σ=0.86x10^6 Sm^{-1} at 170°C, [9]) and the range of the mean velocity of the fluid in the channel (0.7 - 1.6 ms^{-1}). The WebExpIr-loop consists in circular tubes made from stainless steel (σ=1.3x10^6 Sm^{-1}) with an inner diameter of 54.5 mm in the test section where the measurements were conducted. A direct method of calibration was used by comparing the output signals of the developed contactless flow meter and an industrial-proven and commercial constituted vortex-flow meter. A zero adjustment of the flow meter for the case of the liquid metal being at rest was not possible, because the cross section of the pipe was not completely filled in that situation. Therefore, all measurements include an offset in the phase-shift, because especially at the beginning of the measurement the liquid metal level in the pipe and the flow rate increased concurrently.

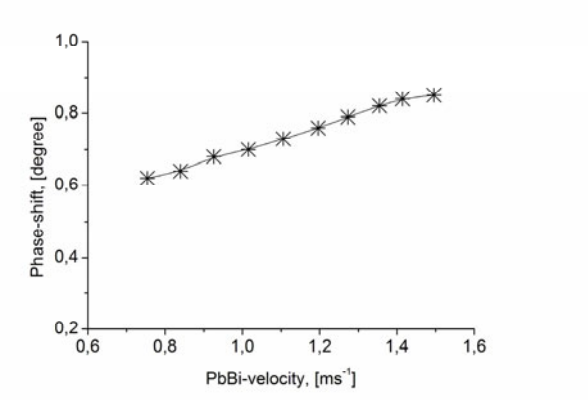

Fig. 5a: Phase-shift in dependence of the averaged LBE-velocity at an emitter frequency of 400Hz

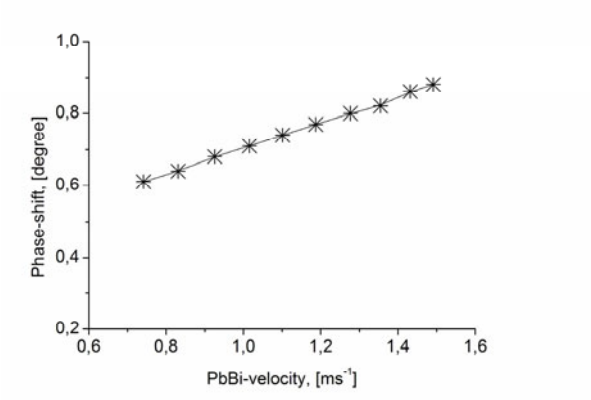

Fig. 5b: Phase-shift in dependence of the averaged LBE-velocity at an emitter frequency of 500Hz

Fig. 5 displays an exemplary measurement obtained with a sensor current of one Ampere (Rms) at 400 Hz and 500 Hz, respectively. The phase-shift increases, as expected, with growing mean velocity of the liquid metal in the pipe. The observed rise of the loop temperature during experiments was never larger than 10°C corresponding to a decrease of the electrical conductivity to $\sigma=0.85 \times 10^6$ Sm^{-1}. The change of electrical conductivity did not cause a phase-shift which exceeds 0.01°. This value is exactly the minimum resolution of the lock-in amplifier. The temperature change caused by the pump has therefore no influence on the measurement results.

4.3. Experiments on lead-loop at HZDR

The electro-mechanical design of the phase-shift sensor which was used for measurements on the Lead-loop is almost identical to the phase-shift sensor applied on the Sodium-loop. Major differences exist in the available measuring gap of the sensor and the winding numbers of the applied inductances. For measurements the emitter coil (500 turns) coil is fed by an alternating current in the range of a few hundred mA. Comparable to the phase-shift sensor which was used for measurements on the Sodium loop the sending coil and the receiving coils (100 turns each) are furnished with laminated magnetic steel in order to concentrate and conduct the magnetic flux. Furthermore the temperature stable housing of the sensor is manufactured by ceramic material MARCOR which withstands temperatures up to 800°C.

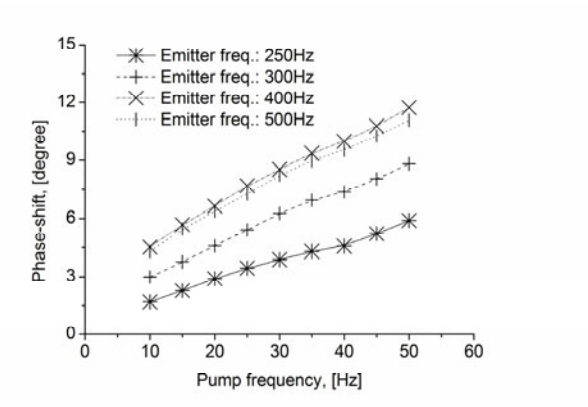

Fig. 6a: Phase-shift in dependence of the averaged lead-velocity for different emitter frequencies in an asymmetric adjustment (l=0.5 mm). Lead temperature: 400°C*

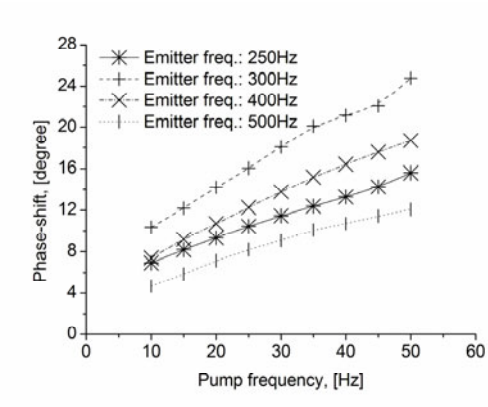

Fig. 6b: Phase-shift in dependence of the averaged lead-velocity for different emitter frequencies in an asymmetric adjustment (l=1.5 mm). Lead temperature: 400°C*

Fig. 6a and b, showing the linear dependence of the measured phase-shift between both sensing coils as a function of the averaged lead-velocity in the test section of the Lead-loop at HZDR. Furthermore it can be seen from both graphs that the optimal frequency of the phase-shift flow meter is clearly dependent from the displacement length l*. An increase of the displacement length leads to a decrease of the optimal frequency, but much more elevated measureable phase-shifts. A reliable calibrated measurement of the averaged velocity of the melt was not available, therefore all measurements are ordered to the adjusted pump frequency.

Fig. 7 shows the measurements with the single-magnet rotary flow meter taken during a measurement campaign on the test-section of the Lead-loop at HZDR. The dependence between rotation rate and the averaged sodium-velocity is according to Fig. 7a and b linear. The currents induced in the electrically conducting channel walls during rotation of the

magnet results in a breaking torque for the rotating magnet. Therefore, beside the effects of remanent magnetism, the extension of the measured line is not passing through the point of origin. A reliable calibrated measurement of the averaged velocity of the melt was not available because of the elevated operation temperature of the loop. Comparative measurements using ultrasonic Doppler Velocimetry were not successful because of difficulties with the wetting between the steel pipe and liquid lead.

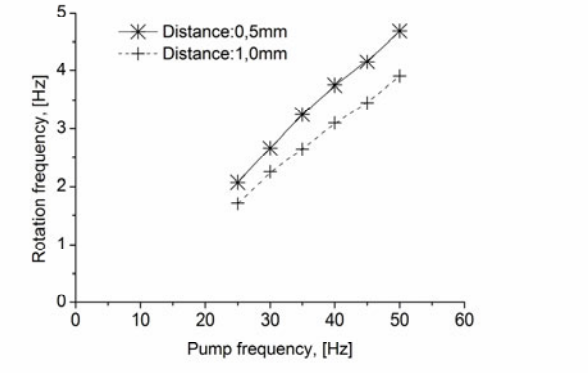

Fig. 7a: Rotation rate in dependence of the averaged lead-velocity measured on the Lead-loop at HZDR. Lead temperature: 400°C

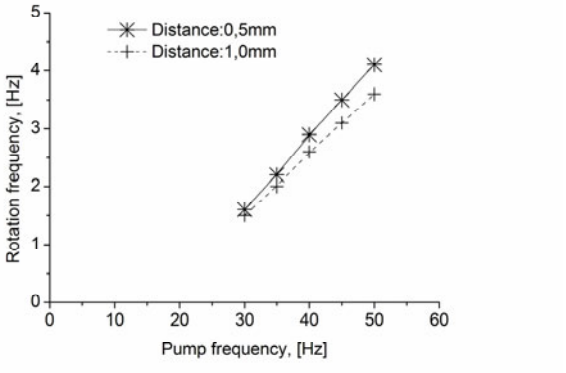

Fig. 7b: Rotation rate in dependence of the averaged lead-velocity measured on the Lead-loop at HZDR. Lead temperature: 500°C

5. Conclusions and prospects

In this paper we reported about some new developments in the field of operational measuring techniques for liquid metal flows. Non-invasive electromagnetic flow meters have been developed at HZDR which enable flow rate measurements at elevated temperatures as required when dealing with liquid sodium, lead or LBE. The flow rate sensors have been successfully tested at different loops, in particular the phase-shift sensor at the WebExpIr facility of SCK-CEN. Both flow meters show a very good linearity of the output signals with the real flow rate in pipes or channels.

The phase-shift sensor is capable of resolving rather low melt velocities, in the present case below 0.1 ms^{-1} both for electrically conducting pipes. The asymmetric adjustment gives larger signals than the symmetric adjustment. A main advantage of the sensor concept consists in its instantaneous reaction on changes of the flow rate.

The main advantage of the single-magnet rotary flow meter consists in its simplicity. The mechanical friction, as well as electrically conducting walls or remanent magnetism reduces the reaction time. Also, the mechanical stability of the bearing is of critical importance for the long-term reliability of the sensor. Likely, further effort on bearings with reduced friction may enlarge this application range.

However, the absolute calibration of the sensors remains, at least partly, as an open issue. In the set-up considered here the phase-shift measurements turned out to be less sensitive to marginal modifications of the measuring parameters compared to the determination of the magnitude response. An important issue not quantified until now is the sensitivity against changes of conductivity of the liquid metal because of the potential occurrence of bubbles,

dissolved gases or oxides. This is of crucial interest for applications in technical systems since the appearance of such kind of inclusions cannot be suppressed there.

References

[1] J. A. Shercliff, "The theory of electromagnetic flow measurement", Cambridge University Press, (1962)

[2] G. Schommartz, "Induktive Strömungsmessung", VEB Verlag Technik Berlin, (1974)

[3] J. Priede, G. Gerbeth, D. Buchenau, S. Eckert, German patent DE 102006018623B4, (2008)

[4] J. Priede, D. Buchenau, G. Gerbeth , 5th Int. Symp. on EPM, Sendai, Proc. 735-740, (2006)

[5] J. Priede, D. Buchenau, G. Gerbeth , "Contactless Electromagnetic Phase-Shift Flowmeter for Liquid Metals", Meas. Sc. Technologie, submitted, (2011)

[6] D. Buchenau, S. Eckert, G. Gerbeth, R. Stieglitz, M. Dierckx, "Measurement technique developments for LBE flows", Journal of Nuclear Materials, submitted, (2011)

[7] J. Priede, D. Buchenau, G. Gerbeth, "Force-free and contactless sensor for electromagnetic flowrate measurements", Magnetohydrodynamics, 45, 451-458, (2009)

[8] D. Buchenau, S. Erlebach, G. Gerbeth, J. Priede, "Development and test of different contactless flowrate sensors for lead measurements", Internal report-VELLA, JRA2, (2009)

[9] Y. Plevachuk, V. Sklyarchuk, S. Eckert, G. Gerbeth, Journal of Nuclear Materials, 376, pp. 363-365, (2008)

CONTACTLESS INDUCTIVE FLOW TOMOGRAPHY IN MODEL EXPERIMENTS FOR CONTINUOUS STEEL CASTING

Thomas Wondrak, Frank Stefani, Thomas Gundrum, Klaus Timmel, Gunter Gerbeth, Anthony J. Peyton[1], Wuliang Yin[1], and Nataša Terzija[1]

1. Introduction

Nowadays, continuous casting is widely used in steel production, and much work has been done on simulating and optimizing this process. The flow structure in the mold plays an important role for the quality of the produced steel. In particular, an inappropriate flow regime can lead to entrapment of oxides, slags or gas bubbles in the steel produced. Open issues of this technology concern the influence of a two phase flow in the submerged entry nozzle (SEN) and the influence of electromagnetic stirrers.

The flow measurement of the liquid steel in the mould is a challenging task due to the high temperature of about 1500°C of the melt. Well established optical methods like Particle Image Velocimetry (PIV) are not applicable due to the opaqueness of the melt. One possibility is to exploit the high conductivity of the melt and to use electromagnetic methods which relay on Faraday induction. Such a measurement technique is the Contactless Inductive Flow Tomography (CIFT) which was proposed for the first time in 2000 [1] and whose experimental feasibility was verified in 2004 at Helmholtz-Zentrum Dresden-Rossendorf (HZDR) [2]. By measuring induced magnetic fields outside the melt, CIFT is able to reconstruct the three-dimensional velocity field in electrically conducting melts. After these promising results this measurement technique was adapted to a model of a continuous caster which is available in our laboratory [3, 4]. Since for thin slab casting the velocity can be assumed to be mainly two-dimensional it is sufficient to apply only one external magnetic field and to measure the induced fields at the narrow faces of the mold.

In collaboration with the University of Manchester in the EU project Magflotom we also used the Mutual Inductance Tomography (MIT) which is a contactless method using electromagnetic fields in order to reconstruct the gas/liquid metal distribution in one cross section in the SEN with a time resolution of 20-40 fps. We will present the results of an experiment with a two phase flow regime and the effects of an electromagnetic stirrer around the submerged entry nozzle on the flow field in the mold.

2. Measurement setup

A cold liquid metal model of a continuous slab caster is the Mini-LIMMCAST facility built up at the HZDR [4]. As liquid metal the eutectic alloy GaInSn is used which is liquid at room temperature. Fig. 1a shows a schematic sketch of the Mini-LIMMCAST facility. A stainless steel cylinder serves as the tundish which contains about 3.5 l of the GaInSn alloy. The melt is discharged through a Plexiglas tube (SEN) with inner diameter of 10 mm into the mold with a rectangular cross section of 140 × 35 mm^2 (also made from Plexiglas). Two nozzle ports with an oval cross section (vertical dimension 18 mm) are situated approximately 80 mm below the free surface in the mold. From the mold the liquid metal flows over a dam into a storage vessel. The vertical position of the dam controls the free surface level in the mold. An electromagnetic pump conveys the melt from the vessel back into the tundish. The

[1] School of Electrical and Electronic Engineering, University of Manchester, Manchester M60 1QD, U.K.

experiments presented here were performed in a discontinuous mode, i.e. after filling the tundish with the melt the stopper rod was lifted to drain the fluid into the mold. During this process the liquid level of both the tundish and the mold were monitored using a laser and an ultrasonic distance sensor, respectively. The liquid flow rate has been derived from the descent of the surface level in the tundish. During the two-phase flow experiments argon gas was injected at the tip of the stopper rod. Gas flow rates were adjusted in a wide range between 50 and 500 cm^3/min and the pressure was measured within the gas feeding system.

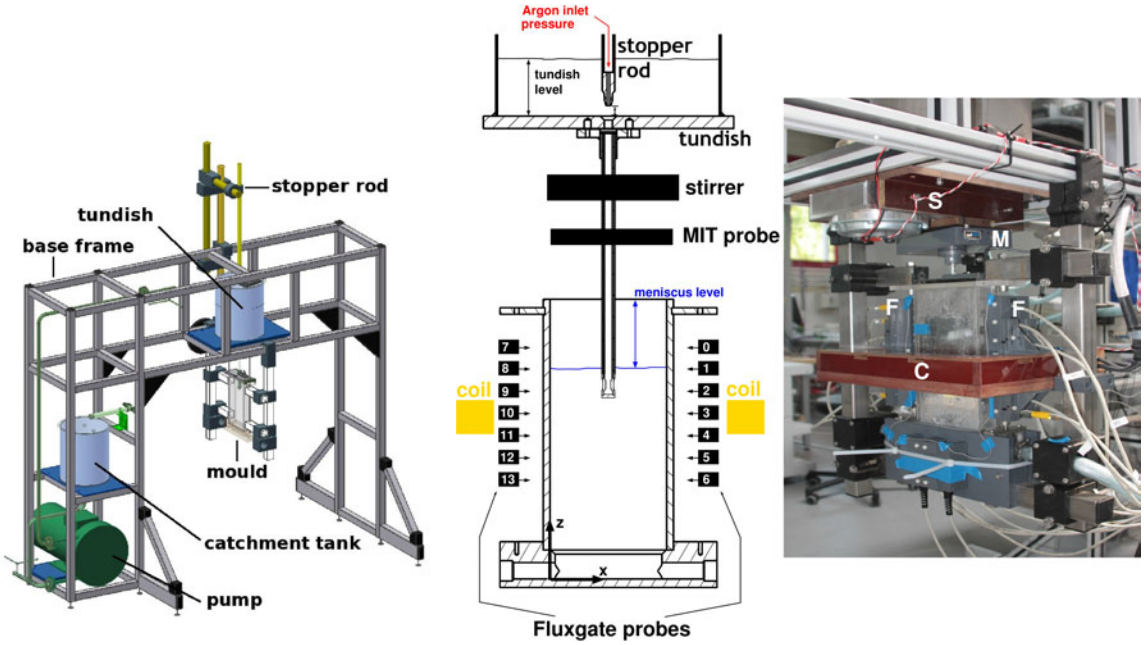

(a) (b)

Fig. 1: Schematic sketch of the Mini-LIMMCAST facility: photograph (a) and a schematic sketch (b) of the instrumentation for the experiments; MIT sensor (M), the rectangular coil (C), the Fluxgate probes (F) and the stirrer (S)

2.1. Contactless Inductive Flow Tomography (CIFT)

The Contactless Inductive Flow Tomography (CIFT) is able to reconstruct a three-dimensional velocity field in highly conducting melts by measuring the flow induced perturbation of applied magnetic fields [1, 2]. For the flow field in the mold of a continuous slab caster it is sufficient to reconstruct only a two-dimensional flow field parallel to the wide faces of the mold, because this is the dominant flow structure in this application [3]. Thus, the applied magnetic field is generated by a rectangular coil mounted around the mold at the height of the jet. This mainly vertical magnetic field generated by the coil minimizes signals from the shape changes of the meniscus as well as from the oscillation of copper walls of the mold. The magnetic field sensors are placed only along the middle of the narrow faces of the mold, because the strongest induced magnetic field is located there [3].

Fig. 1b shows a schematic sketch and a photograph of the instrumentation for CIFT at the mold of Mini-LIMMCAST. The rectangular coil (C) with 16 windings is mounted around the mold at the height of the outlets of the SEN. The coil is fed with 30 A producing a mainly vertical magnetic field of approx. 1 mT in the mold region where the flow field is to be determined. 7 Fluxgate sensors (Foerster) (F) are placed along each narrow side of the mold

and mounted directly at the corpus of the coil in order to avoid variations of the signal due to dislocations between coil and sensor. The actual time resolution of CIFT is 1-2 Hz.

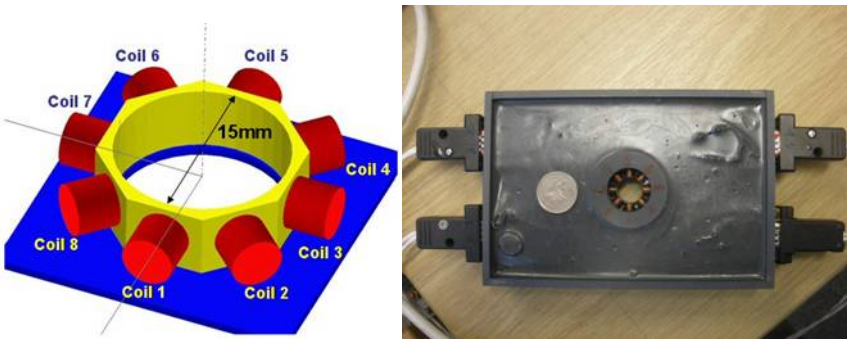

Fig. 2: A schematic sketch and a photograph of the MIT system monitoring the liquid-gas distribution in the SEN

2.2. Mutual Inductance Tomography (MIT)

The Mutual Inductance Tomography (MIT) measures the conductivity distribution in one cross section in the SEN. This is particularly useful in order to distinguish between the liquid metal and air or Argon bubbles in case of the two-phase flow. The technique is based on the principle of Faraday induction. Fig. 2 is a schematic sketch of the MIT sensor. First, an alternating current is applied to the excitation coil (coil 1) producing a primary magnetic field. When this magnetic field interacts with the conductive liquid, eddy currents are induced. The eddy currents create a secondary magnetic field which can be detected by the sensing coils (coil 2-8). As the secondary magnetic field depends on the conductive properties of the material, the measured induced voltages will be also a function of the material conductivity. For one reconstruction of the conductivity distribution, all other coils (coil 2-8) are acting consecutively as excitation coils, too. The present system operates at 40 kHz and has a capture rate of 20-40 frames per second. Fig. 1b shows the position of the MIT sensor at the SEN of the Mini-LIMMCAST facility. More details about the application of MIT to Mini-LIMMCAST can be found in [5].

3. Two phase flow

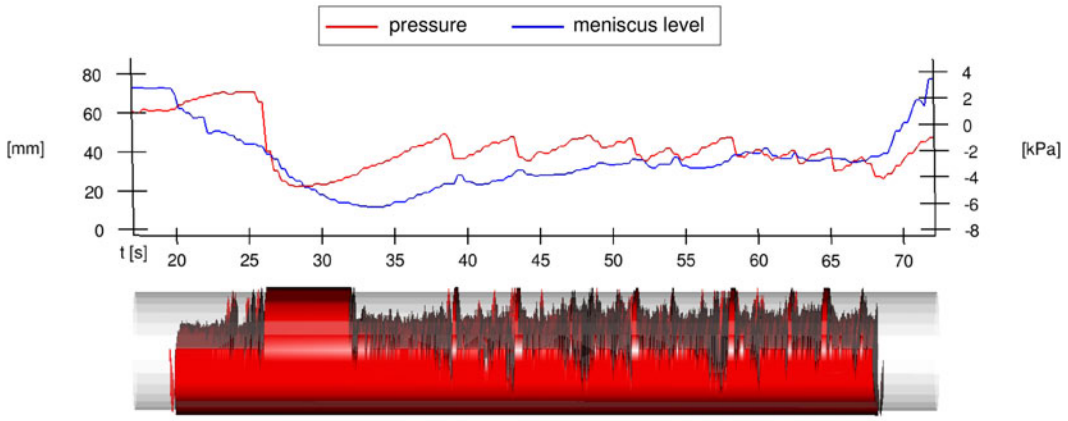

Fig. 3: Reconstructed gas/liquid metal distribution by the MIT sensor for the experiment with 300 cm^3/min Argon flow that shows a number of pressure oscillations

For the investigation of the two phase flow in the SEN and in the mold the MIT system was measuring the gas/fluid fraction in the SEN and CIFT was measuring the flow field in the mold concurrently [6]. As noted in [4], when increasing the gas flow in the SEN, pressure oscillation could be observed. Looking at the reconstructed liquid melt distribution in the SEN, these could be attributed to bubbles of Argon. For a gas flow rate of 300 cm^3/min, Fig. 3 shows the filling of the SEN with liquid metal over time, the pressure in the SEN and the level of the meniscus. It could be clearly seen that after each pressure drop the SEN is completely filled for a short time. Looking at the reconstructed velocity field the double roll pattern is stable over time, but with strong fluctuations of the magnitude of the velocity. Increasing the Argon flow to 500 cm^3/min even changes in the flow structure could be detected. Fig. 4 shows the flow structure in the mold for 4 different instants in time. After starting the experiment, a typically double roll structure is developed in the mold (a). Then, at about $t = 55$ s there is a slight drop in the pressure and the velocity structure changes to a single roll structure at the right side of the mold (b). This regime resumes stable over time, until the position of the liquid metal in the SEN is changing its position (c). At this time, the single roll switches to the left side of the mold. Nearly at the end of the experiment a blob of liquid metal pours down, fully filling the SEN, and generates again a double roll structure in the mold (d).

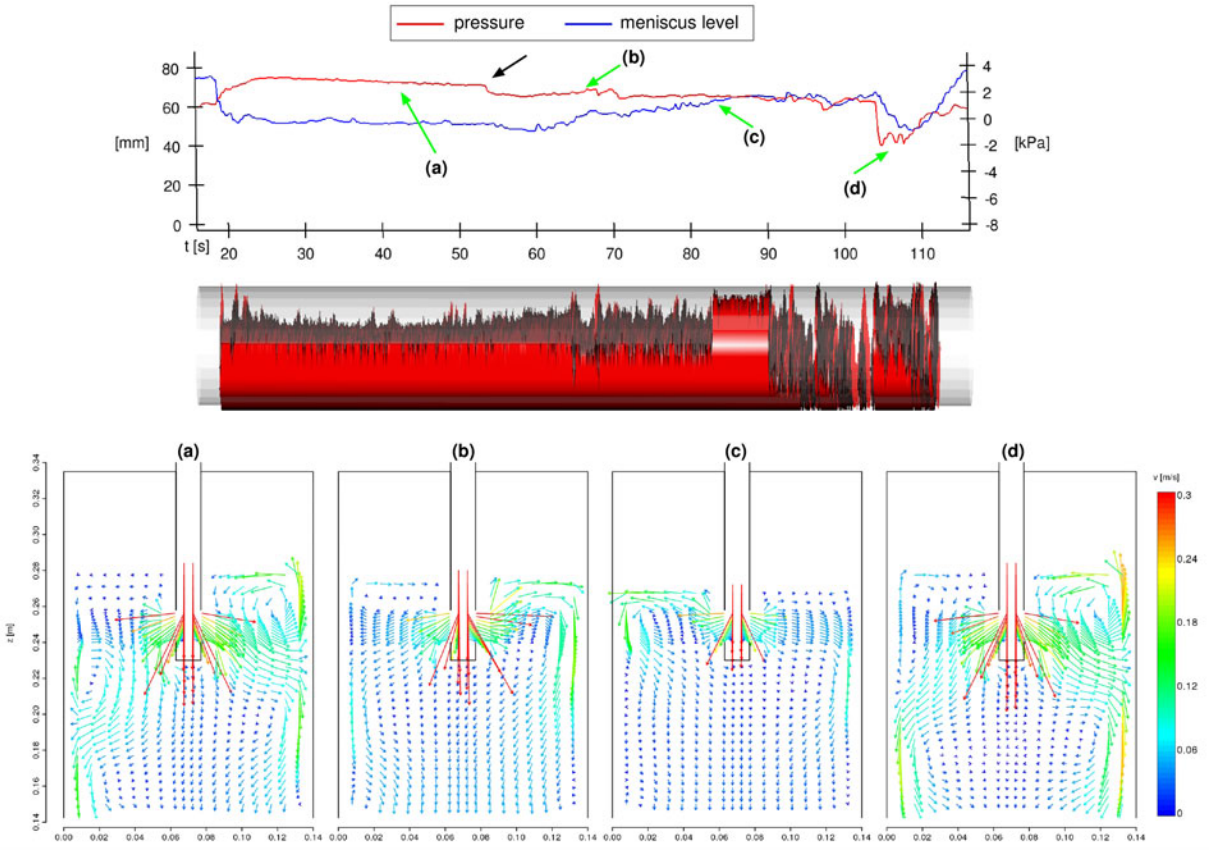

Fig. 4: Reconstructed gas/liquid metal distribution by the MIT sensor for the experiment with 500 cm^3/min Argon flow. Additionally the velocity field reconstructed by CIFT is given for four different instants in time

4. Stirrer around the SEN

The motivation of the investigation of a swirling flow in the SEN is based on the fact that for billet casting typically a single port SEN is used which forms a strong downward flow in the

mold that makes flotation of inclusions and bubbles difficult. By introducing centrifugal forces into the flow field by a swirling flow SEN it is expected to generate a strong upward flow along the wall which should promote inclusions and bubbles going upward to the meniscus. In order to investigate a swirling flow in the SEN at the Mini-LIMMCAST facility the SEN was replaced by a single port SEN with the same inner diameter of 10 mm [7]. A magnetic stirrer consisting of a pair of permanent magnets which are driven by a motor with a maximum rotation frequency of 50 Hz was mounted around the SEN. Fig. 1b shows the position of the stirrer at the Mini-LIMMCAST facility. During the experimental campaign a total of 143 runs with varying stopper rod positions and rotation rates of the stirrer were carried out. In the following we will focus on the experiment for the investigation with a stopper rod position of 13 mm. After reconstructing the velocity field in the mold using our inverse problem solver [3] which was only slightly modified to account for the single-port nozzle geometry, it turned out that at maximum rotation speed of 50 Hz a stronger upward flow along the wall is induced. Fig. 5 shows the complementary *t*- and *z*-dependence of the CIFT-reconstructed *z*-component of the velocity (i.e., $v_z(t,z)$) at $x = 1$ cm. Without any rotation we see a stable vortex at the position of $z = 10$ cm. At maximum rotation, the positive v_z component extends to higher values of *z*, but the price for this is a stronger oscillation.

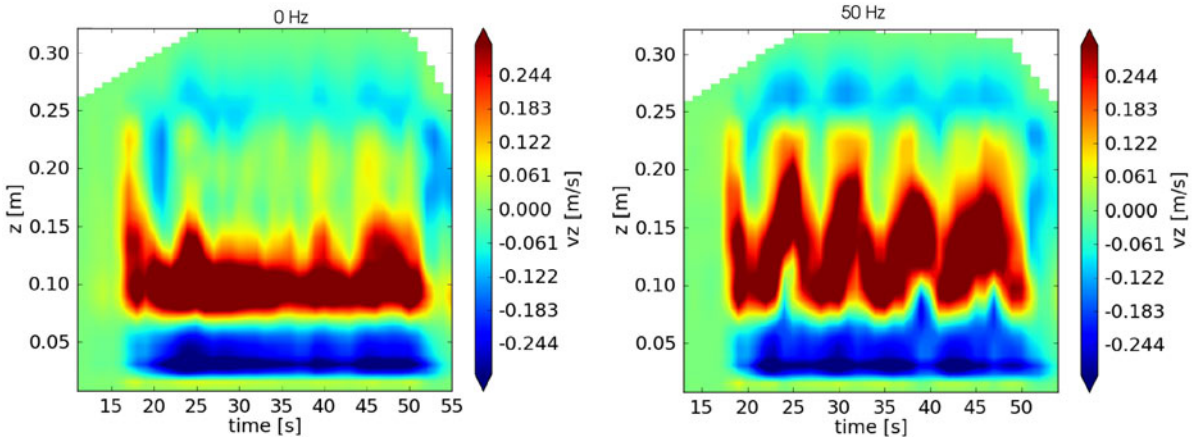

Fig. 5: CIFT-reconstructed $v_z(t,z)$ at $x = 1$ cm for stirring with 0 Hz and 50 Hz.

5. Conclusions

Using 7 sensors on each narrow face of the mould the contactless inductive flow tomography (CIFT) is able to reconstruct the 2-dimensional flow field with a good spatial and temporal resolution. The flow structure in the mould, in particular the position and the intensity of the jet, can be reliably inferred with a time resolution of 1-2 Hz. We have focused on the flat geometry of thin slab casting for which the flow components parallel to the wide face of the mould are the dominant and most interesting ones.

In the two-phase measurement campaign we combined CIFT and MIT simultaneously to examine the liquid metal/gas distribution in the SEN and the resulting flow structure in the mould. With varying argon flow rate, we were able to identify transitions between various flow structures in the SEN and in the mould. At low argon flow rates, we observed relaxation type oscillations of the pressure in the SEN which correspond to the growth of bubbles and their subsequent sudden ejection into the mould. At higher argon flow rates, we see typically an asymmetric, one-sided distribution of the liquid metal in the SEN. Sudden changes of the orientation of this strand can lead to single-port ejections, partly connected with the appearance single-role flow structures in the mould.

In the measurement campaign studying the dependence of the flow in the mold on the swirl intensity in the SEN, CIFT is clearly capable of reproducing the time-dependent left-right asymmetry of the flow in the mold.

Future work will concentrate on the influence of conducting walls, on the effects of the oscillating copper mould in real casting process, on the application of different frequencies to mitigate the non-uniqueness problem of the inversion, and on the use of gradiometric methods in order to make the method better applicable in the rough industrial environment. For a more realistic investigation of the effects of a stirrer one should also think about an enhancement of the CIFT technique, by adding another excitation coil that would help to measure the rotational components of the flow which are hidden in the present set-up of the CIFT-measurement. Another step will be to study the same problem at the much larger LIMMCAST facility working with a continuous flow of SnBi. The installation of the CIFT technique at this larger facility is presently under way.

References

[1] F. Stefani, G. Gerbeth (2000), A contactless method for velocity reconstruction in electrically conducting fluids, Meas. Sci. Techn., 11, 758-765.

[2] F. Stefani, Th. Gundrum, G. Gerbeth (2004), Contactless inductive flow tomography, Phys. Rev., E 70, 056306.

[3] T. Wondrak, V. Galindo, G. Gerbeth, Th. Gundrum, F. Stefani, K. Timmel, (2010), Contactless inductive flow tomography for a model of continuous steel casting, Meas. Sci. Techn., 21, 045402.

[4] K. Timmel, S. Eckert, G. Gerbeth, F. Stefani, T. Wondrak (2010), Experimental modeling of the continuous casting process of steel using low melting point metal alloys – the LIMMCAST program, ISIJ Int., 50, 1134-1141.

[5] N. Terzija, W. Yin, G. Gerbeth, F. Stefani, K. Timmel, T. Wondrak, A. J. Peyton, (2011), Use of electromagnetic induction tomography for monitoring liquid metal/gas flow regimes on a model of an industrial steel caster, Meas. Sci. Technol., 22, 015501.

[6] T. Wondrak, S. Eckert, K. Klotsche, G. Gerbeth, F. Stefani, K. Timmel, A. J. Peyton, W. Yin, N. Terzjia, Combined electromagnetic tomography for determining two-phase flow characteristics in the submerged entry nozzle and in the mould of a continuous-casting model, Metall. Mater. Trans. B, submitted.

[7] T. Wondrak, S. Eckert, V. Galindo, G. Gerbeth, F. Stefani, K. Timmel, A.J. Peyton, W. Yin, Liquid metal experiments with a swirling-flow submerged entry nozzle, Ironmaking and Steelmaking, submitted.

Acknowledgements

This work was supported by European Commission under contract 028679 and by Deutsche Forschungsgemeinschaft in the framework of SFB 609.

Summaries of research activities

Accident Analysis of Nuclear Reactors

The research mainly aims at the enhancement of the predictive capability of computer simulations of accident scenarios in presently operating reactors. This is achieved by improvements of the neutron kinetic and thermal hydraulic methods within the HZDRs reactor dynamics code DYN3D and by coupling of DYN3D on the one hand to thermal hydraulics system codes and to computational fluid dynamics (CFD) simulations and on the other hand to advanced reactor physics codes. The main part of this work is currently performed within the European code platform NURESIM. Moreover, the field of applicability of the reactor dynamics simulations will be extended to innovative reactor concepts aiming at reduced plutonium production or increased plutonium incineration and at the transmutation of minor actinides. New code versions of DYN3D are going to be developed and validated for such designs. Additionally, analytical methods of time-dependent neutron transport theory are developed to basically understand the propagation of neutron pulses in accelerator driven sub-critical systems for transmutation of minor actinides.

S. Kliem,
U. Rohde,
S. Mittag,
F. Schäfer,
S. Baier,
S. Dürigen,
Y. Kozmenkov,
H. Hristov,
Y. Bilodid,
A. Gommlich,
P. Tusheva,
L. Holt

Development, Validation and Application of the Code Complex DYN3D - ATHLET

After accomplishing the coupling of our reactor dynamics code DYN3D with the 3D thermal hydraulic core model FLICA4 (CEA France) within the European code platform NURESIM this code system is now available for national and international users for the conduction of accident analyses. Thereby the role of DYN3D as one of the European reference code for analyses of reactivity initiated accidents was clearly improved. The development of a DYN3D version for gas cooled high temperature reactors is continued. That concerns the further development of the neutron kinetics as well as the thermal hydraulics of DYN3D. The Nuclear Research Institute in Rez (Czech Republic) is a new commercial user of the DYN3D code. In thorium fueled LWR, plutonium which is used as fissile nuclide in the beginning of a fuel cycle, is almost completely burned during the cycle, while only a minimum amount of minor actinides will be generated. Core loading patterns have been developed and corresponding accident analyses have been conducted in order to elaborate the use of such fuel in the near future. A model of the thermal hydraulic test facility INKA (AREVA) modeling the main components of the advanced boiling water reactor KERENA for the system code ATHLET has been developed. This model is able to reproduce experiments for the assessment of the efficiency of passive cooling systems being a part of this reactor.

Supported by
BMWi, BMU, EC, TÜV, E.ON, RWE, VGB

B. Merk,
E. Fridman,
S. Mittag,
A. Ferrari,
J. Konheiser,
V. Glivici-Cotruta,
D. Baldova

Neutron and reactor physics

The positive void reactivity feedback during the boiling of the coolant in sodium cooled fast reactors is one of the disadvantages of this reactor type. Reactor-physical investigations showed that this sodium void effect can be considerably reduced by using a moderation layer on the surface of the fuel pins. The introduction of such a layer does not affect the operational parameters and has only a small influence on the breeding and minor actinide production. Additionally, it could be shown the use of such a moderation layer improves the reactivity effect of the fuel temperature. A corresponding patent application has been submitted. Neutron fluence spectrum calculations of irradiated reactor

pressure vessel material have been performed applying the in-house Monte Carlo code TRAMO. For the validation of the calculation results activity measurements of the elements niobium, nickel and technetium have been performed. For the main part a good agreement could be achieved in spite of the fact that the concentration of niobium in the specimen was very low. The same good results could be obtained for the activity data of technetium and nickel which has been used for the first time for such analyses.

Supported by BMWi and EC

H. Kryk, E. Krepper, A. Grahn, G. Cartland-Glover, W. Hoffmann

Development of CFD models and experimental investigation of corrosion processes in insulation-debris loaded coolant flows

Insulating material (mineral wool) released from pipes and components during a loss-of-coolant accident in an NPP will be transported with the coolant towards the reactor sump. There it may accumulate and give rise to the formation of fibre cakes on the screens which separate the suction chambers of the emergency cooling pumps from the sump. Potential blockage of the screens is of great concern as it leads to the failure of the emergency core cooling system. Within a research project funded by BMWi aimed at the simulation of the behaviour of mineral wool particles in the sump pool flow, models were developed for the transport, sedimentation and re-suspension of insulation material as well as for the transient build-up of the differential pressure at clogged sump screens. The models were implemented into the 3-dimensional flow simulation code ANSYS-CFX. As many components in the reactor containment are made of galvanized steel, one of the project's main topics is dealing with the behaviour of this material towards corrosion in the coolant environment. Recent experiments investigate the effect of coolant composition (boric acid and lithium content), initial fibre cake thickness and water jet characteristics on the corrosion of galvanized samples as well as on the development of the pressure drop over the fibre cake which is subject to deposition of corrosion products. The fibre beds may be clogged mainly by corrosion products of steel as base material. This process is significantly influenced by the coolant composition, the jet type and the positioning of the zinc coated sample. These experiments serve as a basis for the parameterization of an improved model allowing for calculating the long-term development of the pressure drop produced at clogged sump screens. A very small amount of insulation material may penetrate the sump screens and enter the reactor core where it finally accumulates at the spacer grids separating the fuel elements. Elaborate CFD calculations have shown that insulation material preferably deposits on the upper spacer grid plane at the locations of so-called break-through channels. However, at elevated quantities, the insulation material is distributed more evenly across the spacer grid plane. Nevertheless, the pressure difference over the deposited material remains sufficiently small to ensure enough emergency cooling water to enter the reactor core. The results have been used in safety analyses for regulatory purposes.

Supported by BMWi

The work is done in co-operation with the University of Applied Sciences Zittau/Görlitz.

Materials and Components Safety

Reactor construction materials undergo degradation due to fast neutron irradiation. Nano-scaled defects primarily induced by collision cascades caused by the fast neutrons result in a decrease of ductility. The change in the toughness behaviour of reactor pressure vessel materials is investigated in dependence on the irradiation conditions and chemical composition of the steels. For this purpose, material and fracture mechanical parameters of irradiated specimens have to be measured under hot cell conditions. The micro-structural reasons and mechanisms of the neutron embrittlement are studied by small angle neutron scattering and nano indentation experiments supported by nano-scaled modelling. These microstructural methods are also applied to materials which are currently developed for new reactor concepts (GEN-IV reactors).

H.-W. Viehrig, E. Altstadt, M. Houska, M. Thiele, A. Ulbricht, M. Werner,

Fracture mechanics investigation of reactor pressure vessel materials

The neutron irradiation induced ageing of reactor pressure vessel (RPV) materials is explored. The investigation of low Cu steels irradiated to different neutron fluences, revealed a late blooming effect. The irradiation hardening is progressing slowly until reaching a fluence threshold. Beyond this threshold a significant acceleration of the deterioration of the mechanical properties was found.

An extensive research project is being devoted to the post-irradiation examination of the reactor pressure vessels of the decommissioned Greifswald WWER-440 reactors. In the base material of unit 1, which had been re-irradiated after thermal annealing, a high scatter of the fracture toughness (K_{Jc}) values was found. This observation could be explained by a mixture of intergranular and transgranular cleavage fracture. The Master Curve reference temperature T_0 of the weld material of unit 2 (irradiated and annealed) varied over the wall thickness (-38°C at the inner surface and +6°C near the outer surface) to an extent comparable with the results of unit 1 where, however, the mean T_0 was about 40 K higher due to the re-irradiation. The overall low T_0 values measured at the specimens of units 1 and 2 proved the effectiveness of the large scale thermal treatment. Currently the investigation of the core weld of unit 4 is on-going. First results indicate that the fracture toughness along the wall thickness is dominated by differences in the structure of the multi-layer welding seam and by irradiation effects in the same order of magnitude. This is not adequately considered in the currently accepted prediction tools of the Russian standard.

Supported by BMWi

F. Bergner, A. Ulbricht, C. Heintze

Analysis of the irradiation induced micro-structural changes in RPV steels and GEN IV materials

Using ion- and neutron-irradiated binary Fe-Cr alloys and a Cr steel, systematic studies of the effects of the Cr content (up to 12.5%), the fluence (up to 10 dpa) and the temperature (up to 500 °C) were performed. The findings indicate that the irradiation hardening depends on the concentrations of dislocation loops and α' phase particles.

The solubility limit of Cr in Fe (α-Fe–Cr) at low temperatures is a matter of debate. A direct estimation of the solubility limit at 300°C was derived from small-angle neutron scattering (SANS) data obtained for

neutron-irradiated Fe–Cr alloys. The SANS results indicate that the equilibrium concentration of α' was reached via irradiation-enhanced diffusion. The solubility limit was estimated using an iterative approach based on the SANS invariant and the lever rule of phase equilibrium.
In cooperation with IFAM Dresden, a powder metallurgy route based on spark plasma sintering was applied to fabricate oxide dispersion strengthened (ODS) Fe9Cr model materials. These materials along with Eurofer97 and ODS-Eurofer were investigated by means of SANS and TEM. For Fe9Cr–0.6 wt.%Y_2O_3, TEM results indicate a peak radius of the size distribution of Y_2O_3 particles of 4.2 nm with radii ranging up to 15 nm, and a volume fraction of 0.7%, whereas SANS indicates a peak radius of 3.8 nm and a volume fraction of 0.6%. It was found that the non-ODS Fe9Cr and Eurofer97 are suitable reference materials for ODS-Fe9Cr and ODS-Eurofer, respectively, and that the ODS-Fe9Cr variants are suitable model materials for the separated investigation of irradiation - Y_2O_3 particle interaction effects.

Supported by EC

F. Bergner,
U. Birkenheuer,
A. Al-Motasem,
A. Gokhman,
R. Küchler

Modelling of the irradiation induced defects in Fe based alloys

Within the validation of the computer code V3C for the defect simulation by rate theory, it could be shown that in a Fe-0.3%Cu alloy new defects develop up to a neutron dose of 0.02 dpa and that beyond this dose the Ostwald ripening starts to develop. These results are in agreement with SANS measurements. The rate theory model development for Fe-Ni-Cu has been started.
The structure, energetics and thermodynamics of copper–vacancy clusters in bcc-Fe were studied by molecular dynamics modeling using the most recent interatomic potential for Fe–Cu. In the case of mixed clusters a core–shell structure was found where Cu atoms coat the outer surface of vacancy clusters. For small clusters the total binding energy determined in this work shows a good agreement with literature data obtained by first-principle calculations.

Supported by BMWi and EC

Thermal fluid dynamics of multiphase systems

The general aim of the work done in the field of thermal fluid-dynamics is the qualification of Computational Fluid Dynamics (CFD) codes for the simulation of complex two-phase flows with relevance for industrial applications. This qualification process includes the development, test and optimization of closure models for the interaction between the phases, i.e. mass, momentum and heat transfer as well as the validation based on experimental data. For the special case of dispersed bubbly flow, all interfacial transfers strongly depend on the local bubble size distribution. For this reason, the gas phase has to be split into a number of size groups in case of poly-dispersed flows. Transfers between these groups are amongst others determined by bubble coalescence and fragmentation. For stratified flows in horizontal components models for the transfers at the free interface and for the coupling of the turbulence fields are required. Experimental data are required with a high resolution in space and time and are generated by combining large scale experiments at high pressure and temperature at the TOPFLOW facility with innovative two-phase measuring instrumentation including tomography methods. Such measuring techniques are developed in the framework of this project.

E. Krepper,
Y. Liao,
M. Schmidtke,
R. Rzehak,
D. Lucas,
M. Beyer

CFD models for bubbly flows

The Inhomogeneous MUSIG (**MU**ltiple **SI**ze **G**roup) model which was previously developed in cooperation with ANSYS and implemented into the CFD code CFX was validated for the extensions regarding phase transfer. An appropriate experimental data base was established by experi¬ments conduced at the TOPFLOW facility. They include measurements on the condensation of steam injected into upward flow of sub-cooled water in a vertical pipe and experiments on evaporating pipe flow initiated by pressure relief. For some cases of such complex two-phase flows the overall model provides already pretty good results. On the other hand, the limits of the applicability of the implemented models are demonstrated, e.g. in case of the simulations done for the condensation experiments with re-evaporation in the upper part pipe. Further work to expand the area of validity of the individual models for two-phase turbulence, bubble coalescence and breakup, momentum transfer and phase transition is required.

As part of a joint project on boiling processes in pressurized water reactors, the Inhomogeneous MUSIG model was combined with a model for wall boiling. This allows a far more realistic modeling of sub-cooled boiling which may occur e.g. in the core of a pressurized water reactor. To provide experimental data a 3x3 rod bundle was constructed and will be used for measurements by ultra-fast X-ray tomography.

Supported by BMWi and BMBF

T. Höhne,
P. Apanasevich,
Deendarlianto,
Ch. Vallee,
D. Lucas

CFD models for stratified flows

The Algebraic-Interfacial-Area-Density (AIAD) model was successfully used in CFD-simulations on counter-current flow limitation and pressurized thermal shock phenomena. Also in this case the CFD model development and validation bases on new experimental data obtained at the TOPFLOW facility. The counter-current flow limitation was previously investigated in experiments at the hot leg test section. The observed phenomena were well reproduced by the simulations with AIAD model. A good quantitative agreement with the measured flooding curve was obtained. In contrast the standard models of CFX

code failed to predict the onset of flooding correctly. New special data evaluation procedures were developed to extract more detailed data from the high-speed video camera observations applied in the hot leg tests. Thus the time averaged local thickness of the liquid film at the bottom of the hot leg model and its standard deviation were obtained and compared the simulation results. In cooperation with the University of Kobe the database on counter-current flow limitation in hot leg geometries was extended.
The AIAD model was also applied for simulations on experiments of the TOPFLOW-PTS program. One air-water and a steam-water experiment were used as reference, respectively. The simulations were conducted in the frame of the European project NURISP which aims on the establishment of an European code platform for nuclear safety research.

Supported by BMWi and EC

U. Hampel, M. Bieberle, F. Barthel, U. Sprewitz

Ultrafast X-ray tomography

Ultrafast X-ray tomography is used at the TOPFLOW facility to study upward gas-liquid two-phase flow. The tomography scanner ROFEX was qualified for operation on the DN50 titanium pipe test section and extensive measurements were made for upward gas-water flow at different gas and liquid flow rates. Specialized software algorithms had to be developed to analyze phase fraction distributions. Comparison with wire-mesh sensor measurements showed good agreement for many data points but also some deviations for certain measurements. Detailed analysis has to be continued. The methodology of the ultrafast X-ray tomography was further developed in the frame of DFG-funded project "Ultraschnelle Röntgentomographie". Within this project a three-dimensional X-ray tomography with an eight-step target has been performed. This outstanding demonstration showed the capability to image a three-dimensional transient two-phase flow around an obstacle in a pipe with up to 500 volume frames per second.

Supported by BMWi and DFG

T. Barth, E. Krepper

Experimental investigations and modeling of gas-graphite flow

Graphite production in high-temperature gas cooled reactors (HTR) by abrasion is a safety relevant problem because contaminated graphite dust will be released into the confinement in case of a loss-of-coolant accident. Estimation of the graphite dust production and mobilization for such accidents is of continuing interest for design and licensing of HTR reactors. Within the EU project THINS extensive experimental and numerical work is done to study and model the deposition and remobilization of fine particles (dust) in gas channel duct geometries. In the frame of this project an experimental gas-particle loop was setup, which can be operated with air and particles at ambient pressures and temperatures. First experiments were made to study the turbulent gas phase velocity fields with PIV and the transport of different aerosols in the channel with and without obstacles.

Supported by the EU

A. Bieberle, Gregory Cartland-Glover

Experimental investigations and modeling of mixture flows in a wood refiner machine

Energy efficiency of wood refiner machines is essentially coupled to optimization of the mixture flow (steam, water, wood fibers) in the

refiner. Large energy saving potentials are given by optimized flow conditions in the refiner housing and the blow line. HZDR with its expertise in multiphase flow experiments and simulation has performed dedicated experimental analysis and CFD simulation of flow conditions in a model refiner at our cooperation partner Institut für Holztechnologie Dresden. The experiments involved flow measurements with gamma ray tomography and conductivity needle probes. The simulations calculated the flow rates and pressure drops for different housing geometries and fiber outlet geometries. The simulations were validated with the experimental data and gave indications for improved refiner designs, which are now subject to a potential follow-up project.

Supported by BMWi

Magneto-Hydrodynamics

Magnetohydrodynamics investigates the interaction of electrically conducting fluids (liquid metals and semiconductors, electrolytes) with magnetic fields. In various applications, the use of magnetic fields provides a comfortable contact-less possibility to control the transport processes in such melts. Moreover, problems as MHD turbulence, the homogeneous dynamo or the Tayler instability are the subject of intense basic research.

I. Grants,
V. Galindo,
J. Pal,
V. Shatrov,
A. Cramer,
G. Gerbeth

Basics of MHD Flows

The vertical Gradient Freeze (VGF) crystal growth technique works with a stabilizing temperature gradient, i.e. it is cold at the bottom and hot in the upper part of the melt. For an application of a rotating magnetic field (RMF) to control the melt, a better knowledge of the flow stability is needed. Surprisingly, the application of such a thermal stratification leads to a destabilization of the RMF driven flow since it suppresses the secondary meridional flow, thus enhances the primary rotation.

A new experiment for the modelling of Czochralski crystal growth has been installed at the MULTIMAG facility. For rotating crucible and crystal-model it allows to investigate the real silicon flow with the GaInSn melt at much lower temperatures, but in a realistic range of non-dimensional parameters.

The stability of a simple duct flow of quadratic cross-section in a transverse steady magnetic field was analyzed by direct numerical simulations. Without magnetic field this flow is linearly stable for all Reynolds numbers, but due to a non-normal nonlinear transition the flow becomes turbulent above appr. Re = 1077. The magnetic field increases this stability limit and leads to strongly anisotropic flow structures.

supported by DFG

M. Seilmayer,
F. Stefani,
T. Weier,
G. Gerbeth

Tayler Instability and Liquid Metal Battery

The Tayler instability occurs when an electrical current interacts with its own magnetic field giving rise to a flow in the melt above some critical value of the electrical current. This phenomenon has an impact on astrophysical flows, but also very directly to the flow in liquid metal batteries. For the latter the relevance of the Tayler instability has been investigated and related counter measures for a stabilization of the stratified melt layers have been proposed and patented. The solution consists in guiding the electric current on the axis of the cell in opposite direction to the battery current. For the first time, the onset of the Tayler instability has been experimentally obtained in a GaInSn experiment in very good agreement with numerical predictions.

supported by DFG

K. Timmel,
X. Miao,
S. Eckert,
F. Stefani,
Th. Wondrak,
G. Gerbeth

LIMMCAST: Liquid Metal Model of Steel Casting

Systematic experiments on the flow in the mould of a steel casting process have been realized at the model set-up Mini-LIMMCAST. They convincingly revealed the fact that the use of a steady magnetic field, known here also as electromagnetic brake, leads to a significant enhancement of turbulent fluctuations. This is in strong contrast to all previous numerical predictions on the magnetic field action.

The fully contactless inductive flow tomography (CIFT) has been successfully applied to the jet-type mould flow at the steel casting

model. It allows to resolve clogging phenomena in those flows, i.e. non-symmetric behaviours of the jet flows on the two sides of the nozzle outlets.

supported by DFG and BMBF

S. Eckert, Th. Gundrum, F. Stefani, G. Gerbeth

The DRESDYN project

The DRESDYN project belongs to the main future infrastructure projects at HZDR. It will become a European platform for Dynamo-experiments and thermohydraulic studies with liquid metals. After related presentations and defences of the project, it as officially approved and started in 2010. It will comprise a large-scale precession dynamo experiment, MRI and Tayler-Instability experiments, and a pool-type model experiment all operating with liquid sodium. A new X-ray lab for liquid metal flows will also belong to it. The detailed planning of the building and of the large rotating table for the precession experiment has been started. The schedule is to get ready the new building in 2014 and to start first experiments in 2015.

supported by Saxony

Transient Two-Phase Flow Test Facility TOPFLOW

The TOPFLOW (Transient **Tw**O **P**hase **FLOW**) test facility is one of the major research facilities at Helmholtz-Zentrum Dresden – Rossendorf. It is mainly used for the investigation of generic and applied steady state and transient two-phase flow phenomena in either steam-water or air-water mixtures. TOPFLOW has a maximum heating power of 4 MW and allows operation at pressures up to 7 MPa and temperature up to 285°C in pipes and vessel geometries of industrial relevance. It has become the experimental reference facility of the German CFD (Computational Fluid Dynamic) Research Alliance. Currently, there are two major research projects are run at the TOPFLOW facility. One is a BMWi funded project aiming at the development and validation of CFD models for disperse and stratified two-phase flows with heat and mass transfer. Within this project a series of novel two-phase flow experiments are conducted at TOPFLOW in different test sections. Furthermore, an international consortial project dedicated to the investigation of thermal hydraulic phenomena in a pressurised thermal shock scenario (PTS) is run. In the starting phase are a project for boiling heat transfer studies in rod bundles and a project on steam condensation phenomena in inclined pipes.

M. Beyer, T. Seidel, H. Pietruske, P. Schütz, M. Tamme, H. Rußig, K. Linder, S. Weichelt

Two phase flow experiments in the vertical test section DN200 with heat and mass transfer

Investigations of non-adiabatic flows inside the test section "Variable gas injection" were conducted. The experimental series are part of the TOPFLOW-II project funded by BMWi. The condensation of steam injected into sub-cooled water flow was investigated at pressure up to 6.5 MPa and temperature up to 280° C. The steam and water flow rates as well as the sub-cooling were varied too. The extensive experimental matrix includes cases with low sub-cooling for which condensation occurs in the lower part of the pipe, but re-evaporation in the upper part. Such experimental data are of special interest for the CFD model development and validation. In result now a world-wide unique database on the dynamics of the interface in two-phase flows with phase transfer is available. In addition experiments on evaporating were carried out. The evaporation was initiated by pressure relief. Two different scenarios were considered – one with ongoing water circulation during the pressure relief, the other one with stagnant liquid. The experiments are completed. Presently the data are evaluated.

Supported by BMWi

U. Hampel, F. Bartel, U. Sprewitz, M. Beyer, E. Schleicher, P. Schütz, M. Tschofen

Fast X-ray tomography of two-phase flow structures

The tomography scanner ROFEX was qualified for operation on the DN50 titanium pipe test section. Extensive measurements were made for upward gas-water flow at different gas and liquid flow rates. Specialized software algorithms had to be developed to analyze phase fraction distributions.Comparison with wire-mesh sensor measurements showed good agreement for many data points but also some deviations for certain measurements. Detailed analysis has to be continued.

Supported by BMWi

U. Hampel, E. Schleicher, M. Beyer,

TOPFLOW – PTS (thermal hydraulics at pressurized thermal shock)

Pressurized thermal shock may appear if cold water injected into a cold

H. Pietruske, M. Tschofen, M. Tamme, C. Zippe

Supported by CEA, EDF, AREVA NP France, IRSN and PSI

or hot leg of a reactor in an emergency core cooling scenario is insufficiently mixed and leads to large thermal gradients at the pressure vessel wall. The fluid flow dynamics of this scenario are investigated within a consortial project between HZDR, AREVA , EDF, IRSN, CEA, PSI and ETHZ. The experimental facility which resembles a cold-leg geometry of a French nuclear reactor has been setup in the TOPFLOW pressure tank laboratory. First experimental studies were performed on ECC inlet flow conditions and thermal stratification effects with water and air at pressures up to 50 bar.

U. Hampel, F. Barthel, R. Franz

Supported by BMBF

Investigation of boiling processes in rod bundles

Within the BMBF funded project "Siedemodellierung" a 3x3 rod bundle for operation in a refrigerant loop was designed. The project serves the purpose to develop advanced physics-based CFD models for boiling heat transfer on heated surfaces. The facility is a low-pressure loop operated for flow and film boiling and is instrumented with optical camera and a fast X-ray scanner. Rods of the 3x3 bundle with and without spacers can be electrically heated and flow regimes as well as pressure and temperature distributions in the flow can be measured. In this year the test facility was designed, constructed and set-up in the new X-ray laboratory at TOPFLOW.

C. Vallee, U. Hampel, M. Beyer, C. Zippe

Supported by AREVA

Investigation of condensation processes in inclined pipes

Emergency condensers are essential components of passive decay heat removal systems of GEN-III light water reactors. Heat transfer by steam condensation in the single tubes of the condenser bundle is determined by the complex flow conditions and developing film thicknesses at the pipe wall. To study these phenomena an experimental facility was designed, which consists of a single inclined pipe resembling a section of a single emergency core cooling condenser tube of the AREVA KERENA reactor. Steam condensation for steam mass flows up to 1 kg/s and pressures between 5 and 65 bars can be studied. Beside thermal instrumentation an X-ray tomography instrument is foreseen which allows to resolve the flow structure inside the tube. The experimental results will be used by the cooperation partner PSI Switzerland to improve RELAP system codes for modeling emergency condenser systems. The test section has been designed and the TOPFLOW X-ray laboratory prepared for its installation.

Publications

Publications in journals

Atta, A.; Schubert, M.; Nigam, K. D. P.; Roy, S.; Larachi, F.
Co-current descending two-phase flows in inclined packed beds: experiment versus simulations
Canadian Journal of Chemical Engeneering 88(2010)5, 742-750

Azzopardi, B. J.; Abdulkareem, L. A.; Zhao, D.; Thiele, S.; Da Silva, M. J.; Beyer, M.; Hunt, A.
Comparison between electrical capacitance tomography and wire mesh sensor output for air/silicone oil flow in a vertical pipe
Industrial & Engineering Chemistry Research 49(2010), 8805-8811

Bartosiewicz, Y.; Seynhaeve, J.-M.; Vallee, C.; Höhne, T.; Laviéville, J.
Modeling free surface flows relevant to a PTS scenario: comparison between experimental data and three RANS based CFD-codes - Comments on the CFD-experiment integration and best practice guideline
Nuclear Engineering and Design 240(2010), 2375-2381

Bechta, S. V.; Granovsky, V. S.; Khabensky, V. B.; Krushinov, E. V.; Vitol, S. A.; Sulatsky, A. A.; Gusarov, V. V.; Almiashev, V. I.; Lopukh, D. B.; Bottomley, D.; Fischer, M.; Piluso, P.; Miassoedov, A.; Tromm, W.; Altstadt, E.; Fichot, F.; Kymalainen, O.
Interaction between molten corium UO2+x-ZrO2-FeOy and VVER vessel steel
Nuclear Technology 157(2010)4, 210-218

Bergner, F.; Lambrecht, M.; Ulbricht, A.; Almazouzi, A.
Comparative small-angle neutron scattering study of neutron-irradiated Fe, Fe-Cu, Fe-Ni-Mn and Fe-Ni-Mn-Cu
Journal of Nuclear Materials 399(2010), 129-136

Beyer, M.; Lucas, D.; Kussin, J.
Quality check of wire-mesh sensor measurements in a vertical air/water flow
Flow Measurement and Instrumentation 21(2010), 511-520

Bieberle, A.; Schleicher, E.; Hampel, U.
Temperature control design for a high-resolution gamma ray tomography detector
Review of Scientific Instruments 81(2010), 014702

Bieberle, A.; Schubert, M.; Da Silva, M. J.; Hampel, U.
Measurement of liquid distributions in particle packings: use of wire mesh sensor versus transmission tomographic imaging
Industrial & Engineering Chemistry Research 49(2010)19, 9445-9453

Bieberle, M.; Fischer, F.; Schleicher, E.; Koch, D.; Menz, H.-J.; Mayer, H.-G.; Hampel, U.
Ultrafast Cross-Sectional Imaging of Gas-Particle Flow in a Fluidized Bed
AIChE Journal 56(2010)8, 2221-2225

Bieberle, M.; Schleicher, E.; Fischer, F.; Koch, D.; Menz, H.-J.; Mayer, H.-G.; Hampel, U.
Dual-plane ultrafast limited-angle electron beam x-ray tomography
Flow Measurement and Instrumentation 21(2010), 233-239

Bilodid, I.; Mittag, S.
Use of the local Pu-239 concentration as an indicator of burnup spectral history in DYN3D
Annals of Nuclear Energy 37(2010), 1208-1213

Birkenheuer, U.; Ulbricht, A.; Bergner, F.; Gokhman, A.
On the formation of mixed vacancy-copper clusters in neutron-irradiated Fe-Cu alloys
Journal of Physics: Conference Series 247(2010), 012011

Boden, S.; Eckert, S.; Gerbeth, G.
Visualization of freckle formation induced by forced melt convection in solidifying GaIn alloys
Materials Letters 64(2010), 1340-1343

Bomboni, E.; Cerullo, N.; Fridman, E.; Lomonaco, G.; Shwageraus, E.
Comparison among MCNP-based depletion codes applied to burnup calculations of pebble-bed HTR lattices
Nuclear Engineering and Design 240(2010), 918-924

Brzić, D.; Schubert, M.; Häring, H.; Lange, R.; Petkovska, M.
Evaluation of periodic operation of a trickle-bed reactor based on empirical modelling
Chemical Engineering Science (2010)

Cierpka, C.; Weier, T.; Gerbeth, G.
Synchronized force and particle image velocimetry measurements on a NACA 0015 in post stall under control of time periodic electromagnetic forcing
Physics of Fluids 22(2010), 075109

Cramer, A.; Landgraf, S.; Beyer, E.; Gerbeth, G.
Marangoni convection in molten salts - physical modelling toward lower Prandtl numbers
Experiments in Fluids 50(2010)2, 479-490

Cramer, A.; Röder, M.; Pal, J.; Gerbeth, G.
A physical model for electromagnetic control of local temperature gradients in a Czochralski system
Magnetohydrodynamics 46(2010), 317-325

Da Silva, M. J.; Hampel, U.
Kapazitäts-Gittersensor: Prinzip und Anwendung
Technisches Messen 77(2010), 209-214

Da Silva, M. J.; Thiele, S.; Abdulkareem, L.; Azzopardi, B. J.; Hampel, U.
High-resolution gas-oil two-phase flow visualization with a capacitance wire-mesh sensor
Flow Measurement and Instrumentation 21(2010)3, 191-197

Da Silva, M. J.; Thiele, S.; Höhne, T.; Vaibar, R.; Hampel, U.
Experimental studies and CFD calculations for buoyancy driven mixing phenomena
Nuclear Engineering and Design 240(2010)9, 2185-2193

Deendarlianto,.; Ousaka, A.; Indarto,.; Kariyasaki, A.; Lucas, D.; Vierow, K.; Vallee, C.; Hogan, K.
The effects of surface tension on flooding in counter-current two-phase flow in an inclined tube
Experimental Thermal and Fluid Science 34(2010)7, 813-826

Fischer, F.; Hampel, U.
Ultra fast electron beam x-ray computed tomography for two-phase flow measurement
Nuclear Engineering and Design 240(2010)9, 2254-2259

Franke, P.; Heintze, C.; Bergner, F.; Weissgärber, T.
Mechanical properties of spark plasma sintered Fe-Cr compacts strengthened by nanodispersed yttria particles
MP Materials Testing 52(2010), 133-138

Franke, S.; Büttner, L.; Czarske, J.; Räbiger, D.; Eckert, S.
Ultrasound Doppler array system for flow field investigations in liquid metals
Flow Measurement and Instrumentation 21(2010)3, 402-409

Giesecke, A.; Nore, C.; Luddens, F.; Stefani, F.; Leorat, J.; Guermond, J.-L.; Gerbeth, G.
Electromagnetic induction in non-uniform domains
Geophysical and Astrophysical Fluid Dynamics (2010), 505-529

Giesecke, A.; Nore, C.; Plunian, F.; Laguerre, R.; Ribeiro, A.; Stefani, F.; Gerbeth, G.; Leorat, J.; Guermond, J.-L.
Generation of axisymmetric modes in cylindrical kinematic mean-field dynamos of VKS type
Geophysical and Astrophysical Fluid Dynamics 104(2010)2, 249-271

Giesecke, A.; Stefani, F.; Gerbeth, G.
Role of soft-iron impellers on the mode selection in the VKS dynamo experiment
Physical Review Letters 104(2010)4, 044503

Gokhman, A.; Bergner, F.
Cluster dynamics simulation of point defect clusters in neutron irradiated pure iron
Radiation Effects and Defects in Solids 165(2010), 216-226

Grahn, A.; Krepper, E.; Weiß, F.-P.; Alt, S.; Kästner, W.; Kratzsch, A.; Hampel, R.
Implementation of a pressure drop model for the CFD simulation of clogged containment sump strainers
Journal of Engineering for Gas Turbines and Power - Transactions of the ASME 132(2010), 082902

Grants, I.; Gerbeth, G.
Linear and non-linear stability of a thermally stratified magnetically driven rotating flow in a cylinder
Physical Review E 82(2010), 016314

Günther, U.; Kuzhel, S.
PT-symmetry, Cartan decompositions, Lie triple systems and Krein space related Clifford algebras
Journal of Physics A 43(2010), 392002

Günther, U.; Langer, H.; Tretter, C.
On the spectrum of the magnetohydrodynamic mean field α^2-dynamo operator
SIAM Journal on Mathematical Analysis 42(2010), 1413-1447

Heintze, C.
Nanoindentation and transmission electron microscopy of ion-irradiated iron-chromium alloys
atw - International Journal for Nuclear Power 7(2010), 479-481

Heintze, C.; Bergner, F.; Hernández-Mayoral, M.
Ion-irradiation induced damage in FeCr alloys characterized by nanoindentation
Journal of Nuclear Materials (2010)

Hermann, R.; Gerbeth, G.; Priede, J.; Krauze, A.; Behr, G.; Buchner, B.
Convectional controlled crystal-melt interface using two-phase radio-frequency electromagnetic heating
Journal of Materials Science (2010)45, 2228-2232

Höhne, T.
Numerische Strömungsberechnung/Computational Fluid Dynamics
atw - International Journal for Nuclear Power (2010)10, 648-655

Höhne, T.; Vallée, C.
Experiments and numerical simulations of horizontal two phase flow regimes using an interfacial area density model
The Journal of Computational Multiphase Flows 2(2010)3, 131-143

Holzer, L.; Bammert, J.; Rzehak, R.; Zimmermann, W.
Dynamics of a trapped Brownian particle in shear flows
Physical Review E 81(2010), 041124

Johansen, G. A.; Hampel, U.; Hjertaker, B. T.
Flow imaging by high speed transmission tomography
Applied Radiation and Isotopes 68(2010), 518-524

Khripchenko, S.; Khalilov, R.; Kolesnichenko, I.; Denisov, S.; Galindo, V.; Gerbeth, G.
Numerical and experimental modelling of various MHD induction pumps
Magnetohydrodynamics 46(2010)1, 85-97

Kirillov, O.; Stefani, F.
On the relation of standard and helical magnetorotational instability
Astrophysical Journal 712(2010), 52-68

Kliem, S.; Höhne, T.; Rohde, U.; Weiß, F.-P.
Experiments on slug mixing under natural circulation conditions at the ROCOM test facility using high resolution measurement technique and numerical modeling
Nuclear Engineering and Design 240(2010)9, 2271-2280

Koza, J. A.; Mühlenhoff, S.; Zabinski, P.; Nikrityuk, P.; Eckert, K.; Uhlemann, M.; Gebert, A.; Weier, T.; Schultz, L.; Odenbach, S.
Hydrogen evolution under the influence of a magnetic field
Electrochimica Acta 56(2010)6, 2665-2675

Krepper, E.; Beyer, M.
Experimental and numerical investigations of natural circulation phenomena in passive safety systems for decay heat removal in large pools
Nuclear Engineering and Design 240(2010), 3170-3177

Kumar, P.; Ziegler, A.; Grahn, A.; Hee, C. S.; Ziegler, A.
Leaving the structural ivory tower, assisted by interactive 3D PDF
Trends in Biochemical Sciences (2010)

Lambrecht, M.; Meslin, E.; Malerba, L.; Hernández-Mayoral, M.; Bergner, F.; Pareige, A. P.; Radiguet, B.; Almazouzi, A.
On the correlation between irradiation-induced microstructural features and the hardening of reactor pressure vessel steels
Journal of Nuclear Materials 406(2010), 84-89

Liao, Y.; Lucas, D.
A literature review on mechanisms and models for the coalescence process of fluid particles
Chemical Engineering Science 65(2010), 2851-2864

Lucas, D.; Beyer, M.; Kussin, J.; Schütz, P.
Benchmark database on the evolution of two-phase flows in a vertical pipe
Nuclear Engineering and Design 240(2010), 2338-2346

Lucas, D.; Beyer, M.; Szalinski, L.
Experimental investigations on the condensation of steam bubbles injected into sub-cooled water at 1 MPa
Multiphase Science and Technology 22(2010), 33-55

Lucas, D.; Beyer, M.; Szalinski, L.; Schütz, P.
A new database on the evolution of two-phase flows in a large vertical pipe
International Journal of Thermal Sciences 49(2010), 664-674

Matusiak, B.; Da Silva, M. J.; Romanowski, A.; Hampel, U.
Measurement of dynamic liquid distributions in a fixed bed using electrical capacitance tomography and capacitance wire mesh sensor
Industrial & Engineering Chemistry Research 49(2010)5, 2070-2077

Merk, B.; Glivici-Cotruta, V.; Weiß, F. P.
A solution for the Telegrapher's equation with external source: development and first application
Il Nuovo Cimento della Societa Italiana di Fisica B 125(2010)12, 1547-1559

Merk, B.; Weiß, F. P.
A two group analytical approximation solution for an external source problem without separation of space and time
Annals of Nuclear Energy 37(2010), 942-952

Meslin, E.; Lambrecht, M.; Hernández-Mayoral, M.; Bergner, F.; Malerba, L.; Pareige, P.; Radiguet, B.; Barbu, A.; Gomez-Briceno, D.; Ulbricht, A.; Almazouzi, A.
Characterization of neutron-irradiated ferritic model alloys and a RPV steel from combined APT, SANS, TEM and PAS analyses
Journal of Nuclear Materials 406(2010), 73-83

Moiseenko, V.; Noack, K.; Agren, O.
Stellarator-Mirror Based Fusion Driven Fission Reactor
Journal of Fusion Energy 29(2010)1, 65-69

Mutschke, G.; Tschulik, K.; Weier, T.; Uhlemann, M.; Bund, A.; Fröhlich, J.
On the action of magnetic gradient forces in micro-structured copper deposition
Electrochimica Acta 55(2010)28, 9060-9066

Park, J.-S.; Pal, J.; Cramer, A.; Gerbeth, G.
Optimization of induction heating for container-less melt extraction from a metallic sheet
Metallurgical and Materials Transactions B 41(2010), 1074-1083

Perez, V. H.; Azzopardi, B. J.; Kaji, R.; Da Silva, M. J.; Beyer, M.; Hampel, U.
Wisp-like structures in vertical gas-liquid pipe flow revealed by wire mesh sensor studies
International Journal of Multiphase Flow 36(2010)11-12, 908-915

Plevachuk, Yu.; Sklyarchuk, V.; Gerbeth, G.; Eckert, S.
Thermophysical properties of liquid tin-bismuth alloys
International Journal of Materials Research 101(2010), 839-844

Räbiger, D.; Eckert, S.; Gerbeth, G.
Measurements of an unsteady liquid metal flow during spin-up driven by a rotating magnetic field
Experiments in Fluids 48(2010), 233-244

Rohde, M.; Marcel, C. P.; Manera, A.; van der Hagen, Tim H. J. J.; Shiralkar, B.
Investigating the ESBWR stability with experimental and numerical tools: a comparative study
Nuclear Engineering and Design 240(2010)2, 375-384

Rohde, U.
Sektionsberichte Jahrestagung Kerntechnik 2010 - Sektion Reaktorphysik und Berechnungsmethoden
atw - International Journal for Nuclear Power (2010)10, 648-655

Rohde, U.; Höhne, T.; Krepper, E.; Kliem, S.
Application of CFD codes in nuclear reactor safety analysis
Science and Technology of Nuclear Installations 2010(2010), Article ID 198758

Rüdiger, G.; Gellert, M.; Schultz, M.; Hollerbach, R.
Dissipative Taylor-Couette flows under the influence of helical magnetic fields
Physical Review E 82(2010), 016319

Schubert, M.; Hamidipour, M.; Duchesne, C.; Larachi, F.
Hydrodynamics of co-current two-phase flows in slanted porous media - modulation of pulse flow via bed obliquity
AIChE Journal 56(2010)12, 3189-3205

Schubert, M.; Khetan, A.; Da Silva, M. J.; Kryk, H.
Spatially resolved inline measurement of liquid velocity in trickle bed reactors
Chemical Engineering Journal 158(2010)3, 623-632

Schubert, M.; Kryk, H.; Hampel, U.
Slow-mode gas/liquid-induced periodic hydrodynamics in trickling packed beds derived from direct measurement of cross-sectional distributed local capacitances
Chemical Engineering and Processing 49(2010)10, 1107-1121

Schubert, M.; Kryk, H.; Hessel, G.; Friedrich, H.-J.
Residence time measurements in pilot-scale electrolytic cells – Application of laser induced fluorescence
Chemical Engineering Communications 197(2010), 1172-1186

Schuhknecht, J.; Rindelhardt, U.; Viehrig, H.-W.
Study of beltline weld and base metal of WWER-440 first generation reactor pressure vessel
Strength of materials 403(2010)1, 95-104

Shatrov, V.; Gerbeth, G.
Marginal turbulent MHD flow in a square duct
Physics of Fluids 22(2010), 084101

Szalinski, L.; Da Silva, M. J.; Thiele, S.; Beyer, M.; Lucas, D.; Hampel, U.; Hernandez Perez, V.; Abdulkareem, L. A.; Azzopardi, B. J.
Comparative study of gas-oil and gas-water two-phase flow in a vertical pipe
Chemical Engineering Science 65(2010)12, 3836-3848

Talati, M.; Jha, P. K.
Structural phase transition in boron compounds at high pressure
International Journal of Modern Physics B 24(2010)10, 1235-1244

Teschendorff, V.; Glaeser, H.; Kliem, S.
Bedeutung von Experimenten für die Reaktorsicherheit
atw - International Journal for Nuclear Power 55(2010)03, 163-173

Thiele, S.; Da Silva, M. J.; Hampel, U.
Autonomous sensor particle for parameter tracking in large vessels
Measurement Science and Technology 21(2010)8

Timmel, K.; Eckert, S.; Gerbeth, G.
Experimental investigation of the flow in a continuous casting mould under the influence of a transverse DC magnetic field
Metallurgical and Materials Transactions B 42(2010), 68-80

Timmel, K.; Eckert, S.; Gerbeth, G.; Stefani, F.; Wondrak, T.
Experimental modeling of the continuous casting process of steel using low melting point metal alloys - the LIMMCAST program
ISIJ International 50(2010)8, 1134-1141

Timmel, K.; Miao, X.; Eckert, S.; Lucas, D.; Gerbeth, G.
Experimental and numerical modeling of the steel flow in a continuous casting mould under the influence of a transverse DC magnetic field
Magnetohydrodynamics 46(2010), 437-448

Tschulik, K.; Sueptitz, R.; Koza, J.; Uhlemann, M.; Mutschke, G.; Weier, T.; Gebert, A.; Schultz, L.
Studies on the patterning effect of copper deposits in magnetic gradient fields
Electrochimica Acta 56(2010)1, 297-304

Tusheva, P.; Schaefer, F.; Reinke, N.; Altstadt, E.; Rohde, U.; Weiss, F.-P.; Hurtado, A.
Investigation on primary side oriented accident management measures in a station blackout scenario for a VVER-1000 reactor
Kerntechnik (2010)

Ulbricht, A.; Heintze, C.; Bergner, F.; Eckerlebe, H.
SANS investigation of neutron-irradiated Fe-Cr alloys
Journal of Physics: Conference Series 247(2010), 012035

Ulbricht, A.; Heintze, C.; Bergner, F.; Eckerlebe, H.
SANS investigation of a neutron-irradiated Fe-9at%Cr alloy
Journal of Nuclear Materials 407(2010), 29-33

Vallee, C.; Lucas, D.; Beyer, M.; Pietruske, H.; Schütz, P.; Carl, H.
Experimental CFD grade data for stratified two-phase flows
Nuclear Engineering and Design 240(2010), 2347-2356

Voigt, S.; Hoppe, D.
Mass occurrence of penetrative trace fossils in triassic lake deposits (Madygen mossil site, Kyrgyzstan, Central Asia)
Ichnos (2010)

Wondrak, T.; Galindo, V.; Gerbeth, G.; Gundrum, T.; Stefani, F.; Timmel, K.
Contactless inductive flow tomography for a model of continuous steel casting
Measurement Science and Technology 21(2010), 045402

Conference contributions and other oral presentations

Albrecht, T.; Weier, T.; Gerbeth, G.; Metzkes, H.; Stiller, J.
Numerical and experimental investigation of electromagnetic separation control using different wave forms
5th AIAA Flow Control Conference, 28.06.-01.07.2010, Chicago, IL, USA

Al-Motasem, A. T.; Posselt, M.; Bergner, F.
Nucleation of copper-vacancy clusters in bcc-Fe: An atomistic study
Nuclear Materials 2010, An international conference in association with Journal of Nuclear Materials, 04.-07.10.2010, Karlsruhe, Germany

Al-Motasem, A. T.; Posselt, M.; Bergner, F.
Nucleation of Cu-vacancy and Ni-vacancy clusters in bcc-Fe
the 10th International Conference on Computer Simulation of Radiation Effects in Solids, 19.-23.07.2010, Krakow, Poland

Al-Motasem, A. T.; Posselt, M.; Talati, M.; Bergner, F.
Thermodynamics of nanoclusters in bcc-Fe containing copper, nickel and vacancies
The fifth International Conference on Multiscale Materials Modeling (MMM-2010), 04.-08.10.2010, Frieburg, Germany, 04.-08.10.2010, Freiburg, Germany

Altstadt, E.; Bergner, F.; Hein, H.
Irradiation damage and embrittlement in RPV steels under the aspect of long term operation – overview of the FP7 project LONGLIFE
18th International Conference on Nuclear Engineering ICONE18, 17.-21.05.2010, Xian, China

Apanasevich, P.; Lucas, D.; Höhne, T.
Pre-test CFD simulations on TOPFLOW-PTS experiments with ANSYS CFX 12.0
CFD4NRS-3, Workshop on Experimental Validation and Application of CFD and CMFD Codes to Nuclear Reactor Safety Issues. Paper 11.1, 14.-16.09.2010, Washington D.C., USA

Barth, T.; Banowski, M.; Hampel, U.
Experiments on the transport, deposition and resuspension of nuclear aerosols
Doktorandenseminar 2010 im Rahmen des Kompetenzzentrums Ost für Kerntechnik, 16.12.2010, Dresden, Deutschland

Barth, T.; Hampel, U.
Experiments on the transport, deposition and resuspension of nuclear aerosols
International Aerosol Conference – IAC 2010, 29.08.-03.09.2010, Helsinki, Finnland

Bergner, F.; Heintze, C.; Ulbricht, A.
Fluence dependence of small-angle neutron scattering in neutron-irradiated Fe-Cr
17th Workshop on Multiscale Modelling and Basic Experiments of Iron-Chromium Alloys for Nuclear Applications, 03.-04.11.2010, Stockholm, Schweden

Bergner, F.; Ulbricht, A.; Viehrig, H.-W.; Keiderling, U.
SANS investigation of RPV weld material from the decommissioned NPP Greifswald
E-MRS 2010 Spring Meeting, 06.-11.06.2010, Strasbourg, Frankreich

Beyer, M.; Lucas, D.; Szalinski, L.; Pietruske, H.; Schütz, P.; Lindner, K.
Experimentelle Untersuchung polydisperser Dampf/Wasser-Strömungen mit Phasenübergang in einer vertikalen DN200-Teststrecke
Institutsseminar, 09.12.10, FZD, Germany

Beyer, M.; Schleicher, E.; Pietruske, H.; Seidel, T.; Szalinski, L.; Hampel, U.; Weiß, F.-P.
Status of the PTS Experiment at TOPFLOW
Steering Committee Meeting on R&D Cooperation between Forschungszentrum Dresden-Rossendorf and AREVA NP GmbH, 20.09.2010, Dresden, Deutschland

Beyer, M.; Szalinski, L.; Barthel, F.; Lucas, D.; Weiß, F.-P.
Experimentelle Ergebnisse im Rahmen des TOPFLOW-II Projektes
CFD-Forschungsverbund, Entwicklung und Anwendung von Computational Fluid Dynamics (CFD) Programmen für Phänomene im Kühlkreislauf und Sicherheitseinschluss von Leichtwasserreaktoren, 23.09.2010, Grosshartpenning, Deutschland

Bieberle, A.; Hoppe, D.; Hampel, U.
Process diagnostics and non-destructive testing using high-resolution gamma-ray tomography
IEEE International Conference on Imaging Systems and Techniques (IST 2010), 01.-02.07.2010, Thessaloniki, Griechenland

Bieberle, A.; Mäbert, M.; Hampel, U.
Measurement of wood fibre slurry distributions in a laboratory wood refiner using high-resolution gamma-ray tomography
6th World Congress on Industrial Process Tomography, 06.-09.09.2010, Peking, China

Bieberle, A.; Schleicher, E.; Hampel, U.
Hochgenaue Gammastrahlen-Computertomographie für industrielle Anwendungen
Ideas to Market - Dresdner Materialinnovationen für die Praxis & Verleihung "Dresden Barkhausen Award 2009", 15.01.2010, Dresden, Deutschland

Bieberle, M.; Fischer, F.; Hampel, U.
Ultraschnelle Röntgen-Computertomographie für die Untersuchung von Zweiphasenströmungen
Ideas to Market - Dresdner Materialinnovationen für die Praxis & Verleihung "Dresden Barkhausen Award 2009", 15.01.2010, Dresden, Deutschland

Bieberle, M.; Fischer, F.; Hampel, U.
Ultraschnelle Röntgen-Computertomographie für die Untersuchung von Zweiphasenströmungen
Kolloquium des Lehrstuhls für Magnetofluiddynamik, 19.05.2010, Dresden, Deutschland

Bieberle, M.; Fischer, F.; Menz, H.-J.; Mayer, H.-G.; Hampel, U.
Four-dimensional flow imaging by ultrafast X-ray computed tomography
6th World Congress on Industrial Process Tomography, 06.-09.09.2010, Bejing, China

Bieberle, M.; Fischer, F.; Schleicher, E.; Franke, M.; Menz, H.-J.; Mayer, H.-G.; Laurien, E.; Hampel, U.
Ultrafast Multiphase Flow Imaging by Electron Beam X-ray Computed Tomography
7th International Conference on Multiphase Flow, 30.04.-04.06.2010, Tampa, FL, USA

Bilodid, I.
Modeling the spectral history in the depletion of a PWR core.
18th International Conference on Nuclear Engineering (ICONE18), 17.-21.05.2010, Xi'an, China

Bilodid, I.
Modeling the spectral history in the depletion of a PWR core.
18th International Conference on Nuclear Engineering (ICONE18), 17.-21.05.2010, Xi'an, China

Buchenau, D.; Eckert, S.; Gerbeth, G.; Stieglitz, R.; Dierckx, M.
Measurement technique developments for LBE flows
Int. DEMETRA Workshop, 02.-04.03.2010, Berlin, Deutschland

Cartland Glover, G.
Modelling the resuspensions of fibres in the racetrack channel
Fachkolloquium zum BMWi-Vorhaben 150 1363 "Isolationsmaterialbelastete Kühlmittelströmung", 03.03.2010, Dresden, Deutschland

Cartland Glover, G. M.; Krepper, E.; Kryk, H.; Weiss, F. P.; Renger, S.; Seeliger, A.; Zacharias, F.; Kratzsch, A.; Alt, S.; Kästner, W.
Fibre agglomerate transport in a horizontal flow
Benchmarking of CFD Codes for Application to Nuclear Reactor Safety (CFD4NRS-3), 14.-16.09.2010, Bethesda, Maryland, United States of America

Cherubini, M.; Moretti, F.; D'Auria, F.; Ahn, S. H.; Cho, Y. J.; Höhne, T.
Independent assessment of MARS 3D features: use of experimental data and CFD support
8th International Conference on Nuclear Option in Countries with Small and Medium Electrical Grids, 16.-20.05.2010, Dubrovnik, Croatia

Cramer, A.; Pal, J.; Gerbeth, G.
Application of the Ultrasound Doppler Velocimetry in a Czochralski crystal growth model experiment
The 7th International Symposium on Ultrasonic Doppler Methods for Fluid Mechanics and Fluid Engineering, 07.-09.04.2010, Göteborg, Sweden

Cramer, A.; Park, J.-S.; Gerbeth, G.
Optimisation of induction heating for container-less melt extraction from a metallic sheet
Int. Symp. Heating by Electromagnetic Sources, 18.-21.05.2010, Padova, Italia

Cramer, A.; Röder, M.; Pal, J.; Gerbeth, G.
A physical model for electromagnetic control of local temperature gradients in a Czochralski system
International Scientific Colloquium on Modelling for Material Processing, 16.-17.09.2010, Riga, Lettland

Danciu, D.-V.; Zidouni Kendil, F.; Mishra, A.; Schmidtke, M.; Lucas, D.; Hampel, U.
Velocity fields under impinging jets with gas entrainment
7th International Conference on Multiphase Flow ICMF 2010, 30.05.-04.06.2010, Tampa, USA

Deen, D.; Höhne, T.; Lucas, D.; Vallée, C.
CFD modelling to predict the counter-current flow limitations of the air/water counter-current two-phase flow in 1/3rd flat channel model of a hot-leg pressurized water reactor
7th Multiphase Flows Workshop: Simulation, Experiment and Application, 22.-24.06.2010, Forschungszentrum Dresden, Germany

Deendarlianto,-; Höhne, T.; Lucas, D.; Vallée, C.
Numerical simulation of air-water counter-current two-phase flow in a model of the hot-leg of a pressurized water reactor (PWR)
7th International Conference on Multiphase Flow (ICMF 2010), 30.05.-04.06.2010, Tampa, USA

Duerigen, S.; Grundmann, U.; Mittag, S.
A nodal approach to the solution of the multi-group SP_3 equations in trigonal geometry
Jahrestagung Kerntechnik, 04.-06.05.2010, Berlin, Germany

Duerigen, S.; Grundmann, U.; Mittag, S.; Merk, B.; Kliem, S.
A nodal SP3 approach for reactors with hexagonal fuel assemblies
20th Symposium of AER on VVER Reactor Physics and Reactor Safety, 20.-24.09.2010, Hanasaari, Espoo, Finland

Eckert, S.; Gerbeth, G.; Buchenau, D.; Stefani, F.
Instrumentation for liquid metal flows
ESFR Workshop-Education and Training, 15.-19.11.2010, Cadarache, France

Eckert, S.; Gerbeth, G.; Miao, X.; Stefani, F.; Timmel, K.; Wondrak, T.
Investigation of the flow field in a liquid metal continuous casting model
The 6th Japan-France Seminar on Electromagnetic Processing of Materials, 19.-22.05.2010, Hakone, Japan

Eckert, S.; Zhang, C.; Grants, I.; Gerbeth, G.
Quantitative characterization of melt flows in AC magnetic fields
4th Asian Workshop on Electromagnetic Processing of Materials, 03.-06.10.2010, Jeju, South Korea

Fazio, C.; van den Bosch, J.; Martin Muñoz, F. J.; Henry, J.; Roelofs, F.; Turroni, P.; Mansani, L.; Weisenburger, A.; Gorse, D.; Abella, J.; Brissonneau, L.; Dai, Y.; Magielsen, L.; Neuhausen, J.; Vladimirov, P.; Class, A.; Jeanmart, H.; Ciampichetti, A.; Gerbeth, G.; Wetzel, T.; Karbojian, A.; Litfin, K.; Tarantino, M.; Zanini, L.
Development and assessment of structural materials and heavy liquid metal technologies for transmutation systems (DEMETRA): highlights on major results
Technology and components of accelerator-driven systems, 15.-17.03.2010, Karlsruhe, Germany

Ferrari, A.; Beyer, R.; Birgersson, E.; Claussner, J.; Grosse, E.; Hannaske, R.; Junghans, A.; Kögler, T.; Kösterke, I.; Massarczyk, R.; Matic, A.; Schilling, K.-D.; Schramm, G.; Schwengner, R.; Wagner, A.; Weiss, F.-P.
Shielding aspects of the new nELBE photo-neutron source
10th Conference of the Task Force on Shielding Aspects of Accelerators, Targets and Irradiation Facilities, SATIF-10, 02.-04.06.2010, Geneva, Switzerland

Ferrari, A.; Beyer, R.; Birgersson, E.; Claussner, J.; Grosse, E.; Hannaske, R.; Junghans, A.; Kempe, M.; Kögler, T.; Massarczyk, R.; Matic, A.; Schilling, K.-D.; Schramm, G.; Schwengner, R.; Wagner, A.; Weiss, F.-P.; Yakorev, D.
Optimization aspects of the new nELBE photo-neutron source
Measurements and Models of Nuclear Reactions, EFNUDAT Users and Collaboration Workshop, 25.-27.05.2010, Paris, France

Ferrari, A.; Cowan, T.; Margarone, D.; Prokupek, J.; Rus, B.
Shielding assessment for the ELI high intensity laser beamline facility in Czech Republic
10th Conference of the Task Force on Shielding Aspects of Accelerators, Targets and Irradiation Facilities, SATIF-10, 02.-04.06.2010, Geneva, Switzerland

Fischer, F.; Hampel, U.
Study of gas-liquid two-phase flow in pipes with ultrafast electron beam X-ray CT
6th World Congress of Industrial Process Tomography, 06.-09.09.2010, Peking, China

Frank, T.; Lifante, C.; Burns, A.; Krepper, E.; Rzehak, R.
Development and validation of the wall boiling model in ANSYS CFD
8th FZD & ANSYS Short Course and Workshop "Multiphase Flow - Simulation, Experiment and Applications", 22.-24.06.2010, Dresden, Deutschland

Franke, S.; Lieske, H.; Fischer, A.; Büttner, L.; Czarske, J.; Räbiger, D.; Eckert, S.
2d-2c ultrasound Doppler array velocimeter for flow investigations in liquid metals
6th Annual European Rheology Conference (AERC2010), ISUD7, 07.-09.04.2010, Göteborg, Schweden

Fridman, E.
Die Verwendung von Thorium in Druckwasserreaktoren
Kraftwerkstechnischen Kolloquium, 12.-13.10.2010, Dresden, Germany

Fridman, E.; Kliem, S.; Rohde, U.
Preliminary analysis of HTGR core with DYN3D nodal diffusion code
5th International Topical Meeting on High Temperature Reactor Technology, 18.-20.10.2010, Czech Republic, Prague

Fridman, E.; Merk, B.
Modification of the Reactivity Equivalent Physical Transformation Method for HTGR Fuel Element Analysis
5th International Topical Meeting on High Temperature Reactor Technology, 18.-20.10.2010, Prague, Czech Republic

Fridman, E.; Shwageraus, E.
HTGR Fuel Element Depletion Benchmark: Stage Three Results
PHYSOR 2010 – Advances in Reactor Physics to Power the Nuclear Renaissance, 09.-14.05.2010, Pittsburgh, Pennsylvania, USA

Galindo, V.; Niemietz, K.; Paetzold, O.; Gerbeth, G.; Stelter, M.
VGF - type buoyant flow under a Travelling Magnetic Field - Numerical and experimental modelling
7. Workshop Angewandte Simulation in der Kristallzüchtung, 23.-24.11.2010, Burghausen, Deutschalnd

Gerbeth, G.
Strömungsinstabilitäten bei der Kristallzüchtung im TMF
Magnetfelder in der Kristallzüchtung, 09.-10.09.2010, Potsdam, Deutschland

Gerbeth, G.; Eckert, S.; Gundrum, Th.; Stefani, F.
The DRESDYN project at FZD
13th MHD-days, 22.-23.11.2010, Dresden, Germany

Gerbeth, G.; Eckert, S.; Timmel, K.; Miao, X.
Results from the LIMMCAST programme: Modelling the steel flow in the mould with cold liquid metals
The 4th Asian Workshop on EPM, 03.-06.10.2010, Jeju, Korea

Gerbeth, G.; Eckert, S.; Timmel, K.; Miao, X.
Liquid metal modelling of continuous steel casting
TMS Annual meeting "Jim Evans Honorary Symposium", 14.-18.02.2010, Seattle, USA

Giesecke, A.; Stefani, F.; Gerbeth, G.
Reversals and the turbulent alpha-effect in kinematic simulations of natural and experimental dynamos
AGU Fall Meeting 2010, 13.-17.12.2010, San Francisco, USA

Giesecke, A.; Stefani, F.; Gerbeth, G.
High permeability material and dynamo action
MHDDAYS 2010, 22.-23.11.2010, Dresden, Germany

Giesecke, A.; Stefani, F.; Gerbeth, G.
Electromagnetic induction in non-uniform domains
Workshop on Numerical Simulations of MHD flows, 18.-20.10.2010, Karlsruhe, Deutschland

Giesecke, A.; Stefani, F.; Gerbeth, G.
Dynamo action in heterogenous domains
The 8th AIMS Conference on Dynamical Systems, Differential Equations and Applications, 25.-28.05.2010, Dresden, Deutschland

Giesecke, A.; Stefani, F.; Gerbeth, G.
Numerical Simulations of the von Karman Sodium dynamo
Seminar Magnetofluiddynamik TU Dresden, 27.01.2010, Dresden, Deutschland

Gokhman, A. R.; Bergner, F.; Küchler, R.
Rate theory and SANS study of phase separation in a neutron irradiated Fe-12.5at%Cr model alloy
XIV.th Research Workshop Nucleation Theory and Applications, 10.-17.04.2010, Dubna, Russia

Gokhman, A.; Ulbricht, A.; Birkenheuer, U.; Bergner, F.
Cluster dynamics study of neutron irradiation induced defects in Fe-12.5at%Cr alloy
Solid-Solid Phase Transformations in Inorganic Materials, 06.-10.06.2010, Avignon, France

Gomez Torres, A.; Sanchez Espinosa, V.; Kliem, S.; Gommlich, A.; Rohde, U.
Integration of DYN3D inside the NURESIM Platform
17th Pacific Basin Nuclear Conference, 24.-30.10.2010, Cancun, Mexico

Gommlich, A.; Kliem, S.; Rohde, U.; Gomez, A.; Sanchez, V.
Coupling of the neutron-kinetic core model DYN3D with the thermal hydraulic code FLICA-4 within the NURESIM platform
Jahrestagung Kerntechnik 2010, 04.-06.05.2010, Berlin, Deutschland

Grahn, A.
Druckabfall an verstopften Ansaugsieben, Stand der Modellierung
Fachkolloquium zum BMWi-Vorhaben 150 1363 "Isolationsmaterialbelastete Kühlmittelströmung", 03.03.2010, Dresden, Deutschland

Grants, I.; Gerbeth, G.
Suppression of temperature fluctuations by rotating magnetic field in a large scale Rayleigh-Benard cell
Modelling for Material Processing, 16.-17.09.2010, Riga, Lettland

Gundrum, T.; Hüller, J.; Stefani, F.; Gerbeth, G.; Galindo, V.; Herrmannsdörfer, T.; Arnold, F.; Putzke, C.
Alfven wave experiments with liquid rubidium
Science in High Magnetic Fields, 05.-11.09.2010, Ameland, Niederlande

Gundrum, T.; Kretzschmar, N.; Leege, K.-W.; Stefani, F.; Timmel, K.; Wondrak, T.; Gerbeth, G.; Herbrand, F.
Modellexperimente mit Flüssigmetallen
5. Technologietag Prozessautomation, 06.05.2010, Chemnitz, Deutschland

Günther, U.
Exceptional points: Mathematical aspects and Krein space related physics (I + II)
The physics of exceptional points., 02.-05.11.2010, Stellenbosch, South Africa

Günther, U.
Krein spaces and PT quantum mechanics
seminar of the Computational Physics Group, Institute of Theoretical Physics, TU Dresden, 26.11.2010, Dresden, Deutschland

Günther, U.
Three models of Krein-space-related physics: PT-symmetric Quantum Mechanics, Squire equation and the MHD α^2-dynamo
weekly seminar of the Krein space group, 05.05.2010, Ilmenau, Deutschland

Günther, U.
PTQM related Cartan and Clifford structures
Analytic and algebraic methods VI, 10.-11.05.2010, Prague, Czech Republic

Günther, U.; Kuzhel, S.
PT symmetry, Cartan decompositions, Lie triple systems and Krein space related Clifford algebras
21st International Workshop on Operator Theory and its Applications, 12.-16.07.2010, Berlin, Deutschland

Günther, U.; Kuzhel, S.
PTQM related involution structures
Pseudo-Hermitian Hamiltonians in Quantum Physics IX, 21.-24.06.2010, Hangzhou, China

Günther, U.; Samsonov, B.; Rotter, I.; Graefe, E.-M.; Korsch, H.-J.; Niederle, A.
Two models of PT Quantum Mechanics and their behavior in the vicinity of spectral singularities
Many-Body Open Quantum Systems: From Atomic Nuclei to Quantum Dots, 22.-26.02.2010, Trento, Italy

Hampel, U.
Thermal fluid dynamics research at Forschungszentrum Dresden-Rossendorf - sensors, systems and applications
Meeting on the application of multiphase flow measurement techniques in reactor engineering, 28.09.2010, Eindhoven, The Netherlands

Hampel, U.
Thermal fluid dynamics research and multiphase flow measurement and imaging techniques at FZD
Multiphase flow and microbubbles in oil and gas production: Son of DIPSS "Ideas Factory", 27.09.2010, Sheffield, UK

Hampel, U.
Schlagende Herzen und rasante Strömungen - Schnelle bildgebende Messverfahren in Technik und Medizin
Dresdner Seniorenakademie, 09.09.2010, Dresden, Germany

Hampel, U.
Measurement techniques and experimental investigations for multiphase flows
Multiphase Flows - Simulation, Experiment and Application, 22.-24.06.2010, Dresden, Germany

Hampel, U.; Lucas, D.; Vallée, C.; Höhne, T.; Beyer, M.; Fischer, F.; Weiß, F.-P.
Bildgebende Messverfahren und CFD-Simulation für die Energieverfahrenstechnik
42. Kraftwerkstechnisches Kolloquium, 12.-13.10.2010, Dresden, Germany

Heintze, C.
Nanoindentation and transmission electron microscopy of ion-irradiated iron-chromium alloys
Jahrestagung Kerntechnik 2010, 04.-06.05.2010, Berlin, Deutschland

Heintze, C.; Altstadt, E.; Bergner, F.; Hernández Mayoral, M.; Xie, M.; Birkenheuer, U.
Hardening and microstructure of neutron- and ion-irradiated Fe-Cr alloys
OECD Nuclear Energy Agency International Workshop on Structural Materials for Innovative Nuclear Systems (SMINS-2), 31.08.-03.09.2010, Daejeon, Republic of Korea

Heintze, C.; Bergner, F.; Koegler, R.; Lindau, R.
The influence of helium and ODS on the irradiation-induced hardening of Eurofer97 at 300°C
CIMTEC 2010, 5th Forum on New Materials, 13.-18.06.2010, Montecatini Terme, Italia

Heintze, C.; Bergner, F.; Ulbricht, A.; Weißgärber, T.
Microstructure and properties of Fe-Cr and ODS-Fe-Cr model alloys
E-MRS 2010 Spring Meeting, 06.-11.06.2010, Strasbourg, Frankreich

Hermann, R.; Calin, M.; Uhlemann, M.; Wendrock, H.; Gerbeth, G.; Büchner, B.; Eckert, J.
Magnetic field controlled single crystal growth and characterisation of Titanium alloys exposed for biocompatibility
The 16th International Conference on Crystal Growth (ICCG-16), 08.-13.08.2010, Beijing, China

Hoffmann, W.; Kryk, H.
Ergebnisse der Batchversuche und Experimente an der KorrVA zur Korrosion von verzinkten Stahlproben und dem Verhalten der Korrosionsprodukte
Fachkolloquium zum BMWi-Vorhaben 150 1363 „Isolationsmaterialbelastete Kühlmittelströmung“, 03.03.2010, Dresden, Deutschland

Hoffmann, W.; Kryk, H.; Weiß, F.-P.
Corrosion chemistry of galvanized steel in boric acid media
EUROCORR 2010, 13.-17.09.2010, Moscow, Russia

Hoffmann, W.; Kryk, H.; Weiß, F.-P.
Investigation of the corrosion chemistry of hot-dip galvanized steel at LOCA condition
Jahrestagung Kerntechnik 2010, 04.-06.05.2010, Berlin, Deutschland

Höhne, T.
Scale resolved simulations of the OECD/NEA−Vattenfall T-junction benchmark
CFD4NRS-3, 14.-16.09.2010, Washington, USA

Höhne, T.
Simulation der Einströmung des heißseitig eingespeisten Notkühlwassers in den Kern mit Faserablagerungen
Fachkolloquium zum BMWi-Vorhaben 150 1363 "Isolationsmaterialbelastete Kühlmittelströmung", 03.03.2010, Forschungszentrum Dresden-Rossendorf, Deutschland

Höhne, T.
Extention of the AIAD model - The free surface drag model
CFD-network meeting, 21.-22.07.2010, Jülich, Deutschland

Höhne, T.
CFD: Mixing process is it an art of science?
CFD Validation Training, Malaysia, KLCC, KL, 10.-12.07.2010, Kualar Lumpur, Malaysia

Höhne, T.
CFD: Validation of Multiphase flow
CFD Validation Training, Malaysia, KLCC, KL, 10.-12.07.2010, Kualar Lumpur, Malaysia

Höhne, T.
CFD: European experience of 15 years
CFD Validation Training, Malaysia, KLCC, KL, 10.-12.07.2010, Kualar Lumpur, Malaysia

Höhne, T.
CFD: In Nuclear Reactor Safety
CFD Validation Training, Malaysia, KLCC, KL, 10.-12.07.2010, Kualar Lumpur, Malaysia

Höhne, T.
Validation Training with ANSYS CFX
CFD Validation Training, Malaysia, KLCC, KL, 10.-12.07.2010, Kualar Lumpur, Malaysia

Höhne, T.; Grahn, A.; Kliem, S.; Rohde, U.; Weiss, F.-P.
Numerical simulation of the insulation material transport in a PWR core under loss of coolant conditions
18th International Conference on Nuclear Engineering, 17.-21.05.2010, Xi'an, China

Höhne, T.; Grahn, A.; Kliem, S.; Weiss, F. P.
CFD Simulation zum Eintrag von Mineralwolle in den Reaktorkern
Aktuelle Themen der Reaktorsicherheitsforschung in Deutschland-Fachtagung der KTG-Fachgruppen, 07.-08.10.2010, Forschungszentrum Dresden-Rossendorf, Deutschland

Höhne, T.; Grahn, A.; Kliem, S.; Weiß, F. P.
CFD simulation of fibre material transport in a PWR core under loss of coolant conditions
Jahrestagung Kerntechnik 2010, 04.-06.05.2010, Berlin, Deutschland

Höhne, T.; Vallee, C.
Experiments and numerical simulations of horizontal two-phase flow regimes using an interfacial area density model
ANSYS Conference & 28. CADFEM Users´ Meeting 2010, 03.-05.11.2010, Aachen, Deutschland

Imhof, H.; Tost, K.; Thiele, S.; Hampel, U.; Steinbach, J.
Characterization of discharge during depressurization of foaming systems using conductivity wire-mesh sensors
19th International Congress of Chemical and Process Engineering CHISA 2010, 28.08.-01.09.2010, Prague, Czech Republic

Kliem, S.
AER Working Group D on VVER Safety Analysis – report of the 2010 meeting
20th Symposium of AER on VVER Reactor Physics and Reactor Safety, 20.-24.09.2010, Espoo, Finnland

Kliem, S.; Gommlich, A.; Grahn, A.; Rohde, U.; Schütze, J.; Frank, T.; Gomez, A.; Sanchez, V.
Development of Multi-Physics Code Systems based on the Reactor Dynamics Code DYN3D
Fachtag der KTG: "Aktuelle Themen der Reaktorsicherheitsforschung in Deutschland", 07.-08.10.2010, Dresden, Deutschland

Kliem, S.; Grahn, A.; Rohde, U.; Schütze, J.; Frank, T.
Coupling of the CFD code ANSYS CFX with the 3D neutron kinetic core model DYN3D
20th Symposium of AER on VVER Reactor Physics and Reactor Safety, 20.-24.09.2010, Espoo, Finnland

Kliem, S.; Rohde, U.; Schütze, J.; Frank, T.
Prototype coupling of the CFD code ANSYS CFX with the 3D neutron kinetic core model DYN3D
Jahrestagung Kerntechnik 2010, 04.-06.05.2010, Berlin, Deutschland

Kliem, S.; Rohde, U.; Schütze, J.; Frank, T.
Prototype coupling of the CFD software ANSYS CFX with the 3D neutron kinetic core model DYN3D
PHYSOR-2010, 09.-14.05.2010, Pittsburgh, USA

Konheiser, J.
Vorschlag für ein Aktivierungsbenchmark an WWER-440 Reaktordruckbehältern
10. AAA Usergroup Meeting, 06.12.2010, Garching bei München, Deutschland

Krepper, E.
CFD Modellierung von Siedevorgängen in Brennelementbündeln eines Druckwasserreaktors
Festakt zum 15-jährigen Bestehen des IPM, 19.11.2010, Zittau, Deutschland

Krepper, E.
Modelling, Simulation and Experiments to Boiling in Pressurized Water Reactors in the framework of the R&D program "Energie 2020+"
Sitzung des CFD-Verbundes, 21.-22.07.2010, Jülich, Deutschland

Krepper, E.; Grahn, A.; Cartland-Glover, G.; Weiss, F.-P.; Alt, S.; Kratzsch, A.; Renger, S.; Kästner, W.
CFD-Analyses on the behaviour of mineral wool in the reactor sump
Aktuelle Themen der Reaktorsicherheitsforschung in Deutschland Fachtagung der KTG-Fachgruppen, 07.-08.10.2010, Rossendorf, Deutschland

Krepper, E.; Lucas, D.; Schmidtke, M.
Modelling of turbulence in bubbly flows
7th International Conference on Multiphase Flow, ICMF 2010, 30.05.-04.06.2010, Tampa, USA

Krepper, E.; Rzehak, R.
CFD modelling of boiling in rod bundles
8th FZD & ANSYS Short Course and Workshop "Multiphase Flow - Simulation, Experiment and Applications", 22.-24.06.2010, Dresden, Deutschland

Krepper, E.; Scheuerer, G.
Interfacial heat and mass tansfer models
8th FZD & ANSYS Short Course and Workshop "Multiphase Flow - Simulation, Experiment and Applications", 22.-24.06.2010, Dresden, Deutschland

Krepper, E.; Schmidtke, M.; Lucas, D.; Beyer, M.
Steam bubble condensation in polydispersed flow experiments and CFD simulations
Int. Conf. "Nuclear Energy for New Europe", 06.-09.09.2010, Portoz, Slovenien

Krepper, E.; Schmidtke, M.; Lucas, D.; Beyer, M.; Lifante, C.
Steam bubble condensation in polydispersed flow - Experiments and CFD simulations
7th International Conference on Multiphase Flow, ICMF 2010, 30.05.-04.06.2010, Tampa, USA

Krepper, E.; Weiss, F.-P.; Alt, S.; Kratzsch, A.; Renger, S.; Kästner, W.
Some nuclear reactor safety related aspects of plunging jets
18th International Conference on Nuclear Engineering, ICONE18, 17.-21.05.2010, Xi'an, China

Kryk, H.; Hoffmann, W.; Härting, H.-U.
Versuchsanlagen für die Untersuchung von Korrosionsprozessen
Fachkolloquium zum BMWi-Vorhaben 150 1363 „Isolationsmaterialbelastete Kühlmittelströmung", 03.03.2010, Rossendorf, Deutschland

Kryk, H.; Hoffmann, W.; Waas, U.
Einfluss von Korrosionsprozessen auf den Differenzdruck über die Sumpfansaugsiebe von Notkühlsystemen
KTG-Fachtagung „Aktuelle Themen der Reaktorsicherheitsforschung in Deutschland", 07.-08.10.2010, Dresden, Deutschland

Labois, M.; Panyasantisuk, J.; Lakehal, D.; Höhne, T.; Kliem, S.
On the prediction of boron dilution using the CMFD code TRANSAT: the ROCOM test case
CFD4NRS-3, 14.-16.09.2010, Washington, USA

Liao, Y.; Lucas, D.
Development and validation of models for bubble coalescence and breakup
3rd Milestone-Workshop, CFD-Network on Nuclear Reactor Safety Research, 23.09.2010, Grosshartpenning (bei Holzkirchen), Germany

Liao, Y.; Lucas, D.; Krepper, E.
Influence of two-phase turbulence models on the bubble coalescence and breakup behavior in bubbly pipe flow
The 8th International Topical Meeting on Nuclear Thermal-Hydraulics, Operation and Safety (NUTHOS-8), 10.-14.10.2010, Shanghai, China

Liao, Y.; Lucas, D.; Krepper, E.
Validation of a generalized model for bubble coalescence and breakup in MUSIG approach
Jahrestagung Kerntechnik 2010, 04.-06.05.2010, Berlin, Germany

Lifante, C.; Frank, T.; Burns, A. D.; Lucas, D.; Krepper, E.
Prediction of polydisperse steam bubble condensation in sub-cooled water using the Inhomogeneous MUSIG model
CFD4NRS-3, Workshop on Experimental Validation and Application of CFD and CMFD Codes to Nuclear Reactor Safety Issues, 14.-16.09.2010, Washington D.C., USA

Lifante, C.; Frank, T.; Burns, A. D.; Lucas, D.; Krepper, E.
Prediction of polydisperse steam bubble condensation in sub-cooled water using the Inhomogeneous MUSIG model
7th International Conference on Multiphase Flow, ICMF 2010, 30.05.-04.06.2010, Tampa, FL, USA

Lopez, Jose M.; Danciu, Dana V.; Da Silva, Marco J.; Hampel, U.; Mohan, R.
Experiments on air entrainment due to free falling- and wall-jets
ASME 2010 Fluids Engineering Summer Meeting FEDSM2010, 01.-05.08.2010, Montreal, Canada

Lopez, Jose M.; Danciu, Dana V.; Da Silva, Marco J.; Hampel, U.; Mohan, R.
Experimental study of gas entrainment by liquid falling film around a stationary Taylor bubble in vertical downward flow
2010 ECTC Proceedings ASME Early Career Technical Conference, 25.-27.03.2010, Tulsa, USA

Lucas, D.
Experimental observations related to the lateral lift force in poly-dispersed bubbly flows
48th European Two Phase Flow Group Meeting, 27.-30.06.2010, London, United Kingdom

Lucas, D.; Beyer, M.; Schmidtke, M.; Zhang, D.; Krepper, E.; Höhne, T.; Deendarlianto, F. Barthel; Seidel, T.; Vallée, C.; Schleicher, E.; Zippe, C.; Weiß, F.-P.
TOPFLOW-II - Aktueller Stand, wichtige Ergebnisse und Pläne zur Weiterführung der Arbeiten
3. Meilenstein-Workshop des CFD-Forschungsverbunds "Entwicklung und Anwendung von Computational Fluid Dynamics (CFD) Programmen für Phänomene im Kühlkreislauf und Sicherheitseinschluss von Leichtwasserreaktoren", 23.09.2010, Großhartpenning, Deutschland

Lucas, D.; Beyer, M.; Szalinski, L.
A new CFD-grade database on condensation in poly-dispersed bubbly flows
Workshop on Multiphase Flows - Simulation, Experiment and Application, 22.-24.06.2010, Dresden, Deutschland

Lucas, D.; Beyer, M.; Szalinski, L.
CFD-grade databases on two-phase upwards vertical pipe flows
ANS 2010 Winter Meeting, 07.-11.11.2010, Las vegas, U.S.A.

Lucas, D.; Beyer, M.; Szalinski, L.
Experimental data on steam bubble condensation in poly-disperded upward vertical pipe flow
CFD4NRS-3, International Workshop on Experimental Validation and Application of CFD and CMFD Codes to Nuclear Reactor Safety Issues, 14.-16.09.2010, Washington D.C., USA

Lucas, D.; Krepper, E.
Modeling poly-dispersed flows with the Inhomogeneous MUSIG model
ANS 2010 Winter Meeting, 07.-11.11.2010, Las Vegas, U.S.A.

Lucas, D.; Weiß, F.-P.
Stand und Perspektiven der Kernenergie in Deutschland und „Umgebung“
3. VDI-KTG-Kolloquium "Perspektiven der Kernenergie", 26.10.2010, Dresden, Deutschland

Mäbert, M.; Bieberle, A.; Krug, D.; Hampel, U.
Optimization of the pulp process regarding energy efficiency and fibre pulp quality
7th European Wood-based Panel Symposium, 13.-15.10.10, Hannover, Deutschland

Merk, B.; Glivici-Cotruta, V.; Weiß, F. P.
A solution for the telegrapher’s equation with external source: application to YALINA - SC3A and SC3B
PHYSOR 2010, 09.-14.05.2010, Pittsburgh, USA

Merk, B.; Scholl, S.; Fridman, E.
Analsyis of the spatial isotopic distributions during the burnup of UMOX- and ThMOX-fuels on unit cell basis
PHYSOR 2010, 09.-14.05.2010, Pittsburgh, USA

Miao, X.; Lucas, D.; Gerbeth, G.
Numerical simulation of the melt flow in the continuous casting process with respect to gas injection and the impact of a DC magnetic field
Symposium zur Simulation metallurgischer Strömungen an österreichischen und deutschen Universitäten, 17.-18.06.2010, Kirnitzschtal, Germany

Mutschke, G.; Koschichow, D.; Peipmann, R.; Bund, A.; Fröhlich, J.; Weier, T.; Tschulik, K.; Uhlemann, M.
Magnetic field effects in electrochemical reactions
Pacifichem 2010, 15.-20.12.2010, Honolulu, Hawaii, USA

Mutschke, G.; Tschulik, K.; Weier, T.; Uhlemann, M.; Bund, A.; Fröhlich, J.
On the action of magnetic gradient forces in micro-structured copper deposition
61st Annual Meeting of the International Society of Electrochemistry, 26.09.-01.10.2010, Nizza, Frankreich

Nariai, T.; Tomiyama, A.; Vallée, C.; Lucas, D.; Kinoshita, I.; Murase, M.
Counter-current flow limitation in a scale-down model of a PWR hot leg
The 8th International Topical Meeting on Nuclear Thermal-Hydraulics, Operation and Safety (NUTHOS-8), 10.-14.10.2010, Shanghai, China

Niemietz, K.; Galindo, V.; Pätzold, O.; Gerbeth, G.; Stelter, M.
Flow modelling with relevance to Vertical Gradient Freeze crystal growth under the Influence of a travelling magnetic field
The 16th International Conference on Crystal Growth(ICCG-16), 08.-13.08.2010, Beijing, China

Nishida, K.; Soneda, N.; Nomoto, A.; Dohi, K.; Bergner, F.; Viehrig, H.-W.
Atom probe characterization of solute atom clustering in decommissioned Greifswald unit 4 weld metal
MRS Fall Meeting, 29.11.-03.12.2010, Boston, USA

Pal, J.; Cramer, A.; Gerbeth, G.
The sensitivity of the flow driven by a travelling magnetic field to axial alignment
The 7th International Symposium on Ultrasonic Doppler Methods for Fluid Mechanics and Fluid Engineering, 07.-09.04.2010, Göteborg, Sweden

Pal, J.; Cramer, A.; Gerbeth, G.
Electromagnetic control of local temperature gradients in a Czochralski crystal growth model
81st Annual Meeting of the International Association of Applied Mathematics and Mechanics (GAMM), 22.-26.03.2010, Karlsruhe, Deutschland

Park, J.-S.; Pal, J.; Cramer, A.; Gerbeth, G.; Taniguchi, S.
Induction heating for pendent-drop melt extraction from a metallic sheet
The 4th Asian Workshop on EPM, 03.-06.10.2010, Jeju, Korea

Plevachuk, Y.; Sklyarchuk, V.; Hermann, R.; Gerbeth, G.
Thermophysical properties of intermetallic Ti-Al alloys in the liquid state
Liquid and Amorphous Metals Conference (LAM 14), 11.-16.07.2010, Rom, Italy

Plevachuk, Y.; Sklyarchuka, V.; Gerbeth, G.; Eckert, S.
Thermophysical and structure-sensitive properties of low-temperature ternary liquid metal eutectics
XIV Liquid and Amorphous Metals Conference (LAM 14), 11.-16.07.2010, Rom, Italy

Pöpping, U.; Thiele, S.; Bärtling, Y.; Hampel, U.
Multiphase flow measurement techniques in industrial safety analysis
6th Dresden Symposium, "HAZARDS DETECTION AND MANAGEMENT", 20.-24.09.2010, Dresden, Deutschland

Posselt, M.; Al-Motasem, A.; Bergner, F.; Birkenheuer, U.
Atomistic study of copper-vacancy clusters in bcc-Fe
5th Forum on New Materials, 14.-18.06.2010, Montecatini Terme, Italy

Pryadko, E. L.; Reuther, H.; Shevchenko, N.; Markov, A. B.; Kolitsch, A.
Phase Composition of 316L Stainless Steel after Electron-Beam Irradiation Followed by Chromium Ion Implantation
10th Int. Conf. on Modification of Materials with Particle Beams and Plasma Flows, 19.-24.09.2010, Tomsk, Russland

Räbiger, D.; Eckert, S.; Gerbeth, G.
Anwendung zeitmodulierter AC-Magnetfelder zur Strömungskontrolle in metallischen Schmelzen
Symposion zur Simulation metallurgischer Strömungsprozesse an österreichischen und deutschen Universitäten, 16.-19.06.2010, Kirnitzschtal, Deutschland

Räbiger, D.; Leonhardt, M.; Eckert, S.; Gerbeth, G.
Anwendung zeitmodulierter AC-Magnetfelder zum Rühren metallischer Schmelzen während der Erstarrung einer Al-Si-Legierung
Tagung Stranggiessen, 15.-17.11.2010, Neu-Ulm, Deutschland

Räbiger, D.; Zhang, C.; Grants, I.; Eckert, S.; Gerbeth, G.
Investigations of the bulk flow inside a cylindrical liquid metal column generated by diverse AC magnetic fields
6th Annual European Rheology Conference (AERC2010), ISUD7, 07.-09.04.2010, Göteborg, Schweden

Rindelhardt, U.; Fröhler, D.
Betriebserfahrungen mit der 40-MW-Photovoltaik-Anlage Waldpolenz
25. Symposium Photovoltaische Solarenergie, 03.02.-05.03.2010, Staffelstein, Deutschland

Rohde, U.; Baier, S.; Duerigen, S.; Fridman, E.; Merk, B.; Weiss, F.-P.
Development of the coupled 3D neutron kinetics/thermal-hydraulics code DYN3D-HTR for the simulation of transients in block-type HTGR
5th Topical Meeting in High Temperature Reactor Technology, 18.-20.10.2010, Prague, Czech Republic

Rohde, U.; Merk, B.; Baier, S.; Fridman, E.; Dürigen, S.; Kliem, S.; Weiss, F.-P.
Development of a reactor dynamics code for block-type HTR at Forschungszentrum Dresden-Rossendorf
Fachtag der KTG: "Aktuelle Themen der Reaktorsicherheitsforschung in Deutschland", 07.-08.10.2010, Dresden, Deutschland

Rzehak, R.; Krepper, E.
Boiling models for CFD
8th FZD & ANSYS Short Course and Workshop "Multiphase Flow - Simulation, Experiment and Applications", 22.-24.06.2010, Dresden, Deutschland

Schäfer, F.; Tusheva, P.; Weiss, F.-P.
Sicherheitstechnische Fragestellungen im Reaktorbetrieb am Beispiel eines DWR
3. VDI-KTG Kolloquium "Perspektiven der Kernenergie", 26.10.2010, Dresden, Deutschland

Schäfer, T.; Schubert, M.; Kryk, H.; Hampel, U.
Temperaturfeldmessung und Detektion von Hotspots in Schüttungen
ProcessNet-Jahrestagung 2010 und 28. DECHEMA-Jahrestagung der Biotechnologen, 21.-23.09.2010, Aachen, Deutschland

Schmidtke, M.; Krepper, E.; Lucas, D.
Validierung des Inhomogenen MUSIG-Modells mit Phasenübergang
3. Meilenstein Workshop / CFD-Forschungsverbund Entwicklung und Anwendung von Computational Fluid Dynamics (CFD) Programmen für Phänomene im Kühlkreislauf und Sicherheitseinschluss von Leichtwasserreaktoren, 23.09.2010, München-Holzkirschen, Deutschland

Schmidtke, M.; Krepper, E.; Lucas, D.; Beyer, M.
CFD-simulations and experiments on steam condensation in polydisperse bubbly flows
Jahrestagung Kertnechnik 2010, 04.-06.05.2010, Berlin, Deutschland

Springer, R.; Schubert, M.; Hampel, U.
Development of an inline multiphase flow metering sensor
IEEE Sensors 2010 Conference, 01.-04.11.2010, Waikoloa, Hawaii

Stefani, F.
Liquid metal experiments on dynamo action and related magnetic instabilities
International Summer School and Workshop on Self-Organization in Turbulent Plasmas and Fluids, 03.-14.05.2010, Dresden, Germany

Stefani, F.; Gerbeth, G.; Gundrum, T.; Hollerbach, R.; Kirillov, O.; Priede, J.; Rüdiger, G.; Szklarski, J.
Helical magnetorotational instability in theory and experiment
AIMS 8th International Conference, 25.-28.05.2010, Dresden, Germany

Stefani, F.; Wondrak, T.; Gundrum, T.; Gerbeth, G.
Applying the contactless inductive flow tomography to a model of continuous steel casting
GAMM 2010, 22.-26.03.2010, Karlsruhe, Germany

Talati, M.; Posselt, M.; Bonny, G.; Al-Motasem, A. T.; Bergner, F.
Contribution of Lattice Vibrations to the Thermodynamics of Vacancy Clusters in bcc-Fe
The fifth International Conference on Multiscale Materials Modeling (MMM-2010), 04.-08.10.2010, Freiburg, Germany

Timmel, K.; Eckert, S.; Gerbeth, G.
The steady magnetic field impact on the mould flow at the continuous casting process of steel
13th MHD-days, 22.-23.11.2010, Dresden, Deutschland

Timmel, K.; Eckert, S.; Gerbeth, G.
Experimentelle Untersuchung der Flüssigmetallströmung im Stranggussprozess unter Einfluss eines DC – Magnetfeldes
Symposium zur Simulation metallurgischer Strömungen an österreichischen und deutschen Universitäten, 16.-18.06.2010, Kirnitzschtal, Deutschland

Timmel, K.; Eckert, S.; Gerbeth, G.
Ultrasonic flow measurements in a low temperature liquid metal model of the continuous steel casting process
6th Annual European Rheology Conference (AERC2010), ISUD7, 07.-09.04.2010, Göteborg, Schweden

Timmel, K.; Galindo, V.; Miao, X.; Eckert, S.; Gerbeth, G.
Physikalische Modellierung des Stranggussprozesses mit niedrig schmelzenden Legierungen
Symposium Stranggießen, 15.-17.11.2010, Neu-Ulm, Deutschland

Timmel, K.; Miao, X.; Lucas, D.; Eckert, S.; Gerbeth, G.
Experimental and numerical modeling of the steel flow in a continuous casting mould exposed to a transverse DC magnetic field
Workshop "Modelling for Material Processing", 16.-17.09.2010, Riga, Latvia

Tselishcheva, Elena A.; Podowski, Michael Z.; Antal, Steven P.; Post Guillen, D.; Beyer, M.; Lucas, D.
Analysis of developing gas/liquid two-phase flows
7th International Conference on Multiphase Flow, ICMF 2010, 30.05.-04.06.2010, Tampa, USA

Tusheva, P.; Altstadt, E.; Weiss, F.-P.
Investigations on in-vessel melt retention for VVER-1000 reactors
Jahrestagung Kerntechnik 2010, 04.-06.05.2010, Berlin, Germany

Tusheva, P.; Schäfer, F.; Reinke, N.; Weiss, F.-P.
Assessment of early-phase accident management strategies in a station backout scenario for VVER-1000 Reactors
ICONE 18, 17.-21.05.2010, Xi'an, China, 17.-21.05.2010, Xi'an, China

Vallée, C.
Overview of the FZD and of the Institute of Safety Research / Counter-current flow limitation experiments in a model of the hot leg of a PWR
Young scientists seminar, 08.11.2010, Mihama-cho (Fukui), Japan

Vallée, C.; Seidel, T.; Lucas, D.; Tomiyama, A.; Murase, M.
Comparison of countercurrent flow limitation experiments performed in two different models of the hot leg of a PWR with rectangular cross-section
18th International Conference on Nuclear Engineering (ICONE18), 17.-21.05.2010, Xi'an, China

Viehrig, H.-W.
The Master Curve approach an approved fracture mechanics test method for more than one decade
COMAT 2010 RECENT TRENDS IN STRUCTURAL MATERIALS, 25.-26.11.2010, Plzen, Czech Republic

Viehrig, H.-W.; Gillemot, F.; Horvat, M.; Acosta, B.; Debarberis, L.
Irradiation Response of Greifswald Unit 8 RPV Steels
IAEA Specialists' Meeting on Irradiation Embrittlement and Life Management of Reactor Pressure Vessels, 18.-22.10.2010, Znojmo, Czech Republic

Viehrig, H.-W.; Houska, M.
Previous results of the investigation on the decommissioned reactor pressure vessels of the Greifswald NPP
IAEA Specialists' Meeting on Irradiation Embrittlement and Life Management of Reactor Pressure Vessels, 18.-22.10.2010, Znojmo, Czech Republic

Viehrig, H.-W.; Houska, M.; Arora, K. S.; Rindelhardt, U.
What one learns from reactor pressure vessels of decommissioned nuclear power plants.
International Symposium FONTEVRAUD 7: Contribution of Materials Investigations to Improve the Safety And Performance of LWRs, 26.-30.09.2010, Avignon, France

Viehrig, H.-W.; Houska, M.; Arora, K. S.; Rindelhardt, U.
Post Mortem Investigations of Greifswald WWER-440 Reactor Pressure Vessels
11th International Conference "Material Issues in Design, Manufacturing and Operation of Nuclear Power Plants Equipment, 14.-18.06.2010, St. Petersburg, Russia

Viehrig, H.-W.; Zurbuchen, C.; Schindler, H.-J.; Kalkhof, D.
Effects of specimen size, initial crack acuity and test temperature on the master curve reference temperature
18th European Conference on Fracture, 30.08.-03.09.2010, Dresden, Germany

Weiss, F.-P.
Im Kern die Sicherheit
FDP Technologieforum, 27.05.2010, Dresden, Deutschland

Weiss, F.-P.; Schaefer, F.; Kliem, S.; Tusheva, P.
Analysis of Design Basis Accidents
FJOH Summer School 2010, 24.-26.08.2010, Aix-en-Provence, Frankreich

Willschütz, H.-G.; Diercks, F.; Leyer, S.; Krüssenberg, A.-K.; Schäfer, F.; Hristov, H. V.
Experimentelle und analytische Untersuchungen zu passiven Komponenten des KERENA TM Konzeptes im Versuchsstand INKA
42. Kraftwerkstechnisches Kolloquium 2010, 12.-13.10.2010, Congress Center Dresden, Deutschland

Willschütz, H.-G.; Leyer, S.; Krüssenberg, A.-K.; Schäfer, F.
Calculation of the operation mode of the emergency condenser (EC) of the INKA test facility with ATHLET
Annual Meeting on Nuclear Technology (Jahrestagung Kerntechnik), 04.-06.05.2010, Berlin, Deutschland

Wondrak, T.; Stefani, F.; Gerbeth, G.; Gundrum, T.
Contactless inductive flow tomography: principles and applications
5th International Conference: Inverse Problems: Modeling and Simulation, 24.-29.05.2010, Antalya, Türkei

Wondrak, T.; Stefani, F.; Timmel, K.; Galindo, V.; Gundrum, T.; Gerbeth, G.
Contactless inductive flow tomography: principles and application to a model of continuous casting
6th World Congress on Industrial Process Tomography, 06.-9.9.2010, Peking, China

Wondrak, T.; Timmel, K.; Gundrum, T.; Stefani, F.; Gerbeth, G.
Examination of different flow regimes in the mold of a model of continuous casting using the contactless inductive flow tomography
13th MHD-days, 22.-23.11.2010, Forschungszentrum Dresden-Rossendorf, Germany

Contributions to proceedings and other collected editions

Al-Motasem, A. T.; Posselt, M.; Talati, M.; Bergner, F.
Thermodynamics of nanoclusters in bcc-Fe containing copper, nickel and vacancies
The fifth international conference on Multiscale Materials Modeling , Freiburg-Germany, 04.-08.10.2010, Freiburg, Germany
MMM2010 Multiscale Materials Modeling, 978-3-8396-0166-2

Altstadt, E.; Bergner, F.; Hein, H.
Irradiation damage and embrittlement in RPV steels under the aspect of long term operation – overview of the FP7 project LONGLIFE
18th International Conference on Nuclear Engineering ICONE18, 17.-21.05.2010, Xian, China
Proceedings of the 18th International Conference on Nuclear Engineering ICONE18

Apanasevich, P.; Lucas, D.; Höhne, T.
Pre-test CFD simulations on TOPFLOW-PTS experiments with ANSYS CFX 12.0
CFD4NRS-3, Workshop on Experimental Validation and Application of CFD and CMFD Codes to Nuclear Reactor Safety Issues, 14.-16.09.2010, Washington D.C., USA

Bestion, D.; Lucas, D.; Smith, B.; Boucker, M.; Scheuerer, M.; D'Auria, F.; Lakehal, D.; Macek, J.; Tilelj, I.; Hazi, G.; Tanskanen, V.; Ilvonen, M.; Seiler, N.; Boetcher, M.; Anglart, H.; Bartosiewicz, Y.
Two-phase CFD advances in the NURESIM and NURISP projects
18th International Conference on Nuclear Engineering, ICONE18, paper ICONE 18-30205, 17.-21.05.2010, Xi'an, China

Bieberle, A.; Hoppe, D.; Hampel, U.
Process diagnostics and non-destructive testing using high-resolution gamma-ray tomography
IEEE International Conference on Imaging Systems and Techniques (IST 2010), 01.-02.07.2010, Thessaloniki, Griechenland
Process diagnostics and non-destructive testing using high-resolution gamma-ray tomography

Bieberle, A.; Mäbert, M.; Hampel, U.
Measurement of wood fibre slurry distributions in a laboratory wood refiner using high-resolution gamma-ray tomography
6th World Congress on Industrial Process Tomography, 06.-09.09.2010, Peking, China
Measurement of wood fibre slurry distributions in a laboratory wood refiner using high-resolution gamma-ray tomography

Bieberle, M.; Fischer, F.; Menz, H.-J.; Mayer, H.-G.; Hampel, U.
Four-dimensional flow imaging by ultrafast X-ray computed tomography
6th World Congress on Industrial Process Tomography, 06.-09.09.2010, Bejing, China
Proc. of 6th World Congress on Industrial Process Tomography, 457-462

Bieberle, M.; Fischer, F.; Schleicher, E.; Franke, M.; Menz, H.-J.; Mayer, H.-G.; Laurien, E.; Hampel, U.
Ultrafast Multiphase Flow Imaging by Electron Beam X-ray Computed Tomography
7th International Conference on Multiphase Flow, 30.05.-04.06.2010, Tampa, FL, USA
Proceeding of 7th International Conference on Multiphase Flow, 9.3.2

Bilodid, I.
Modeling the spectral history in the depletion of a PWR core.
18th International Conference on Nuclear Engineering (ICONE18), 17.-21.05.2010, Xi'an, China
Proceedings of the 18th International Conference on Nuclear Engineering (ICONE18) May 17-21, 2010 • Xi'an, China

Cartland Glover, G. M.; Krepper, E.; Kryk, H.; Weiss, F. P.; Renger, S.; Seeliger, A.; Zacharias, F.; Kratzsch, A.; Alt, S.; Kästner, W.
Fibre agglomerate transport in a horizontal flow
Benchmarking of CFD Codes for Application to Nuclear Reactor Safety (CFD4NRS-3), 14.-16.09.2010, Bethesda, Maryland, United States of America
Fibre agglomerate transport in a horizontal flow

Cherubini, M.; Moretti, F.; D'Auria, F.; Ahn, S. H.; Cho, Y. J.; Höhne, T.
Independent assessment of MARS 3D features: use of experimental data and CFD support
8th International Conference on Nuclear Option in Countries with Small and Medium Electricity Grids, 16.-20.05.2010, Dubrovnik, Croatia
Proceedings of the 8th International Conference on Nuclear Option in Countries with Small and Medium Electricity Grids Dubrovnik, Croatia, 16-20 May 2010, CD-ROM

Cheung, S. C. P.; Yeoh, G. H.; Tu, J. Y.; Krepper, E.; Lucas, D.
Numerical study of bubbly flows using direct quadrature method of moments
7th International Conference on Multiphase Flow, ICMF, 30.05.-04.06.2010, Tampa, USA

Cramer, A.; Pal, J.; Gerbeth, G.
Application of the Ultrasound Doppler Velocimetry in a Czochralski crystal growth model experiment
The 7th International Symposium on Ultrasonic Doppler Methods for Fluid Mechanics and Fluid Engineering, 07.-09.04.2010, Göteborg, Sweden
Proceedings of the 7th International Symposium on Ultrasonic Doppler Methods for Fluid Mechanics and Fluid Engineering, 978-91-7290-292-3, 57-60

Cramer, A.; Park, J.-S.; Gerbeth, G.
Optimisation of induction heating for container-less melt extraction from a metallic sheet
Int. Symp. on Heating by Electromagnetic Sources, 18.-21.05.2010, Padova, Italia
Int. Symp. on Heating by Electromagnetic Sources Induction, Dielectric and Microwaves, Conduction & Electromagnetic Processing, Padova: SGE Ditoriali, 241-248

Cramer, A.; Röder, M.; Pal, J.; Gerbeth, G.
Elektromagnetische Strömungskontrolle lokaler Temperaturgradienten in einem Modell des Czochralski-Prozesses
Workshop Elektroprozesstechnik, 23.-24.09.2010, Ilmenau - OT Heyda, Deutschland

Cramer, A.; Röder, M.; Pal, J.; Gerbeth, G.
A physical model for electromagnetic control of local temperature gradients in a Czochralski system
International Scientific Colloquium Modelling for Material Processing, 16.-17.09.2010, Rīga, Latvija
Proceedings of the 6th International Scientific Colloquium Modelling for Material Processing, 978-9984-45-223-4, 41-46

Da Silva, M. J.; Fischer, F.; Hampel, U.
Comparison of ultrafast x-ray electron beam tomography and capacitance wire-mesh sensor imaging applied to multiphase flow measurement
6th World Congress On Industrial Process Tomography (WCIPT6), 06.-09.09.2010, Bejing, China
Proceedings of the 6th World Congress On Industrial Process Tomography, 421-429

Da Silva, M. J.; Hampel, U.; Rodriguez, I. H.; H. Rodriguez, O. M.
Visualization and holdup measurement of viscous oil-water dispersed pipe flow by capacitance wire-mesh sensor
6th World Congress On Industrial Process Tomography (WCIPT6), 06.-09.09.2010, Bejing, China
Proceedings of the 6th World Congress On Industrial Process Tomography, 1334-1440

Danciu, D.-V.; Zidouni Kendil, F.; Mishra, A.; Schmidtke, M.; Lucas, D.; Hampel, U.
Velocity fields under impinging jets with gas entrainment
7th International Conference on Multiphase Flow, ICMF 2010, 30.05-04.06.2010, Tampa,USA, 30.05.-04.06.2010, Tampa, USA
International Conference on Multiphase Flow

Deen, D.; Höhne, T.; Lucas, D.; Vallée, C.
CFD modelling to predict the counter-current flow limitations of the air/water counter-current two-phase flow in 1/3rd flat channel model of a hot-leg pressurized water reactor
7th Multiphase Flows Workshop: Simulation, Experiment and Application, 22.-24.06.2010, Forschungszentrum Dresden, Germany
CFD modelling to predict the counter-Current flow limitations of the air/water counter-current two-phase flow in 1/3rd flat channel model of a hot-leg pressurized water reactor

Deendarlianto,-; Höhne, T.; Lucas, D.; Vallée, C.
Numerical simulation of air-water counter-current two-phase flow in a model of the hot-leg of a pressurized water reactor (PWR)
7th International Conference on Multiphase Flow (ICMF 2010), 30.05.-04.06.2010, Tampa, USA
Proceeding of the 7th International Conference on Multiphase Flow

Duerigen, S.; Grundmann, U.; Mittag, S.
A nodal approach to the solution of the multi-group SP_3 equations in trigonal geometry
Jahrestagung Kerntechnik, 04.-06.05.2010, Berlin, Germany

Duerigen, S.; Grundmann, U.; Mittag, S.; Merk, B.; Kliem, S.
A nodal SP3 approach for reactors with hexagonal fuel assemblies
20th Symposium of AER on VVER Reactor Physics and Reactor Safety, 20.-24.09.2010, Hanasaari, Espoo, Finland

Eckert, S.; Gerbeth, G.; Miao, X.; Stefani, F.; Timmel, K.; Wondrak, T.
Investigation of the flow field in a liquid metal continuous casting model
The 6th Japan-France Seminar on Electromagnetic Processing of Materials, 19.-22.05.2010, Hakone, Japan
Electromagnetic Processing of Materials - Development of New Fields and Applications, 1-10

Eckert, S.; Zhang, C.; Grants, I.; Gerbeth, G.
Quantitative characterization of melt flows in AC magnetic fields
4th Asian Workshop on Electromagnetic Processing of Materials, 03.-06.10.2010, Jeju, South Korea, 172-175

Ferrari, A.; Beyer, R.; Birgersson, E.; Claussner, J.; Grosse, E.; Hannaske, R.; Junghans, A.; Kempe, M.; Kögler, T.; Massarczyk, R.; Matic, A.; Schilling, K.-D.; Schramm, G.; Schwengner, R.; Wagner, A.; Weiss, F.-P.; Yakorev, D.
Optimization aspects of the new nELBE photo-neutron source
Measurements and Models of Nuclear Reactions, EFNUDAT Users and Collaboration Workshop, 25.-27.05.2010, Paris, France
Optimization aspects of the new nELBE photo-neutron source, Paris: European Physical Journal, EDP Sciences, 978-2-7598-0585-3 DOI:10.1051/epjconf/20100805002

Franke, S.; Lieske, H.; Fischer, A.; Büttner, L.; Czarske, J.; Räbiger, D.; Eckert, S.
2d-2c ultrasound Doppler array velocimeter for flow investigations in liquid metals
6th Annual European Rheology Conference (AERC2010), ISUD7, 07.-09.04.10, Göteborg, Schweden
Proceedings of the 7th International Symposium on Ultrasonic Doppler Methods for Fluid Mechanics and Fluid Engineering, 89-92

Fridman, E.
Die Verwendung von Thorium in Druckwasserreaktoren
Kraftwerkstechnischen Kolloquium, 12.-13.10.2010, Dresden, Germany
Die Verwendung von Thorium in Druckwasserreaktoren

Fridman, E.; Kliem, S.; Rohde, U.
Preliminary analysis of HTGR core with DYN3D nodal diffusion code
5th International Topical Meeting on High Temperature Reactor Technology, 18.-20.10.2010, Prague, Czech Republic
Preliminary analysis of HTGR core with DYN3D nodal diffusion code

Fridman, E.; Merk, B.
Modification of the Reactivity Equivalent Physical Transformation Method for HTGR Fuel Element Analysis
5th International Topical Meeting on High Temperature Reactor Technology, 18.-20.10.2010, Prague, Czech Republic
Modification of the Reactivity Equivalent Physical Transformation Method for HTGR Fuel Element Analysis

Fridman, E.; Shwageraus, E.
HTGR Fuel Element Depletion Benchmark: Stage Three Results
PHYSOR 2010 – Advances in Reactor Physics to Power the Nuclear Renaissance, 09.-14.05.2010, Pittsburgh, Pennsylvania, USA

Gado, J.; Rohde, U. (Editors)
Nuclear Engineering Handbook - Chapter 1.4: VVER-type reactors of Russian design
D. G. Cacuci, J. Gado, U. Rohde: Handbook of Nuclear Engineering; Vol.IV - Reactors of Generation III and IV, Chapter 20: VVER-Type Reacctors of Russian Design, Heidelberg: Springer, 2010, 978-0-387-98130-7

Gerbeth, G.; Eckert, S.; Timmel, K.; Miao, X.
Results from the LIMMCAST programme: Modelling the steel flow in the mould with cold liquid metals
The 4th Asian Workshop on EPM, 03.-06.10.2010, Jeju, Korea
Results from the LIMMCAST programme: modelling the steel flow in the mould with cold liquid metals, 9-12

Gerbeth, G.; Eckert, S.; Timmel, K.; Miao, X.
Liquid metal modelling of continuous steel casting
TMS Annual meeting, 14.-18.02.2010, Seattle, USA
"Jim Evans Honorary Symposium", 55-62

Giesecke, A.; Stefani, F.; Gerbeth, G.
Reversals and the turbulent alpha-effect in kinematic simulations of natural and experimental dynamos
AGU Fall Meeting 2010, 13.-17.12.2010, San Francisco, USA
Reversals and the turbulent α-effect in simulations of natural and experimental dynamos

Gokhman, A.; Bergner, F.
Study of metastable states of the precipitates in reactor steels under neutron irradiation
S. Rzoska, A. Drozd-Rzoska, V. Mazur: Metastable systems under pressure, Heidelberg, New York: Springer, 2010, 978-90-481--3408-3, 411-418

Gomez Torres, A.; Sanchez Espinosa, V.; Kliem, S.; Gommlich, A.; Rohde, U.
Integration of DYN3D inside the NURESIM Platform
17th Pacific Basin Nuclear Conference, 24.-30.10.2010, Cancun, Mexico
Proc. 17th Pacific Basin Nuclear Conference - CDROM

Gommlich, A.; Kliem, S.; Rohde, U.; Gomez, A.; Sanchez, V.
Coupling of the neutron-kinetic core model DYN3D with the thermal hydraulic code FLICA-4 within the NURESIM platform
Jahrestagung Kerntechnik 2010, 04.-06.05.2010, Berlin, Deutschland
Tagungsband der Jahrestagung Kerntechnik 2010 paper 111, Berlin: INFORUM GmbH

Grants, I.; Gerbeth, G.
Suppression of temperature fluctuations by rotating magnetic field in a large scale Rayleigh-Benard cell
Modelling for Material Processing, 16.-17.09.2010, Riga, Lettland
Suppression of temperature fluctuations by rotating magnetic field in a large scale Rayleigh-Benard cell, pp. 293-298

Hampel, U.
Ultrafast electron beam tomography
Krzysztof Iniewski: Semiconductor Radiation Detection Systems, Boca Raton: CRC Press, Taylor & Francis Group, 2010, 978-1-4398-0385-1, 263-280

Hampel, U.; Lucas, D.; Vallée, C.; Höhne, T.; Beyer, M.; Fischer, F.; Weiß, F.-P.
Bildgebende Messverfahren und CFD-Simulation für die Energieverfahrenstechnik
M. Beckmann, A. Hurtado: Kraftwerkstechnik - Sichere und nachhaltige Energieversorgung - Band 2,, Neuruppin: TK Verlag Karl Thomé-Kozmienski, 2010, 978-3-935317-57-3, 769-786

Heintze, C.; Bergner, F.; Koegler, R.; Lindau, R.
The influence of helium and ODS on the irradiation-induced hardening of Eurofer97 at 300°C
CIMTEC 2010, 5th Forum on New Materials, 13.-18.06.2010, Montecatini Terme, Italia
5th Forum on Materials Part B: Trans Tech Publications Ltd, 124-129

Hoffmann, W.; Kryk, H.
Ergebnisse der Batchversuche und Experimente an der KorrVA zur Korrosion von verzinkten Stahlproben und dem Verhalten der Korrosionsprodukte
Fachkolloquium zum BMWi-Vorhaben 150 1363 „Isolationsmaterialbelastete Kühlmittelströmung“, 03.03.2010, Dresden, Deutschland

Hoffmann, W.; Kryk, H.; Weiß, F.-P.
Corrosion chemistry of galvanized steel in boric acid media
EUROCORR 2010, 13.-17.09.2010, Moscow, Russia
CD-ROM

Hoffmann, W.; Kryk, H.; Weiß, F.-P.
Investigation of the corrosion chemistry of hot-dip galvanized steel at LOCA condition
Jahrestagung Kerntechnik 2010, 04.-06.05.2010, Berlin, Deutschland
CD-ROM

Höhne, T.
CFD: Mixing process is it an art of science?
CFD Validation Training, Malaysia, KLCC, KL, 10.-12.07.2010, Kualar Lumpur, Malaysia
Hand-out

Höhne, T.
CFD: Validation of Multiphase flow
CFD Validation Training, Malaysia, KLCC, KL, 10.-12.07.2010, Kualar Lumpur, Malaysia
Hand-out

Höhne, T.
CFD: European experience of 15 years
CFD Validation Training, Malaysia, KLCC, KL, 10.-12.07.2010, Kualar Lumpur, Malaysia
Hand-out

Höhne, T.
CFD: In Nuclear Reactor Safety
CFD Validation Training, Malaysia, KLCC, KL, 10.-12.07.2010, Kualar Lumpur, Malaysia
Hand-out

Höhne, T.
Validation Training with ANSYS CFX
CFD Validation Training, Malaysia, KLCC, KL, 10.-12.07.2010, Kualar Lumpur, Malaysia
CD-ROM, Hand-out

Höhne, T.
Scale resolved simulations of the OECD/NEA−Vattenfall T-junction benchmark
CFD4NRS-3, 14.-16.09.2010, Washington, USA
CD-ROM

Höhne, T.; Grahn, A.; Kliem, S.; Rohde, U.; Weiss, F.-P.
Numerical simulation of the insulation material transport in a PWR core under loss of coolant conditions
18th International Conference on Nuclear Engineering, 17.-21.05.2010, Xi'an, China

Höhne, T.; Grahn, A.; Kliem, S.; Weiss, F. P.
CFD Simulation zum Eintrag von Mineralwolle in den Reaktorkern
Aktuelle Themen der Reaktorsicherheitsforschung in Deutschland-Fachtagung der KTG-Fachgruppen, 07.-08.10.2010, Forschungszentrum Dresden-Rossendorf, Deutschland
CD-ROM

Höhne, T.; Grahn, A.; Kliem, S.; Weiß, F. P.
CFD simulation of fibre material transport in a PWR core under loss of coolant conditions
Jahrestagung Kerntechnik 2010, 04.-06.05.2010, Berlin, Deutschland
CD-ROM, paper 055

Höhne, T.; Vallee, C.
Experiments and numerical simulations of horizontal two-phase flow regimes using an interfacial area density model
ANSYS Conference & 28. CADFEM Users´ Meeting 2010, 03.-05.11.2010, Aachen, Deutschland
CD-ROM

Imhof, H.; Tost, K.; Thiele, S.; Hampel, U.; Steinbach, J.
Characterization of discharge during depressurization of foaming systems using conductivity wire-mesh sensors
19th International Congress of Chemical and Process Engineering, 28.08.-01.09.2010, Prag, Czech Republic
Characterization of discharge during depressurization of foaming systems using conductivity wire-mesh sensors

Kinoshita, I.; Murase, M.; Utanohara, Y.; Lucas, D.; Vallée, C.; Tomiyama, A.
Countercurrent gas-liquid flow in a hot leg under reflux cooling - numerical calculations for steam-water tests at FZD
Annual meeting of the Atomic Energy Society of Japan, 26.-28.03.2010, Ibaraki, Japan, 237

Kinoshita, I.; Murase, M.; Utanohara, Y.; Lucas, D.; Vallée, C.; Tomiyama, A.
Numerical calculations for steam-water CCFL tests using the 1/3rd scale rectangular channel simulating a PWR hot leg
The 8th International Conference on Nuclear Thermal Hydraulics, Operations and Safety (NUTHOS-8), paper N8P0044, 10.-14.10.2010, Shanghai, China

Kliem, S.
AER Working Group D on VVER Safety Analysis – report of the 2010 meeting
20th Symposium of AER on VVER Reactor Physics and Reactor Safety, 20.-24.09.2010, Espoo, Finnland
Proceedings of the 20th Symposium of AER on VVER Reactor Physics and Reactor Safety, CDROM paper 5.1, Budapest: KFKI AEKI

Kliem, S.; Gommlich, A.; Grahn, A.; Rohde, U.; Schütze, J.; Frank, T.; Gomez, A.; Sanchez, V.
Development of Multi-Physics Code Systems based on the Reactor Dynamics Code DYN3D
Fachtag der KTG: "Aktuelle Themen der Reaktorsicherheitsforschung in Deutschland", 07.-08.10.2010, Dresden, Deutschland
Tagungsband des Fachtages der KTG: "Aktuelle Themen der Reaktorsicherheitsforschung in Deutschland", CDROM: FZ Dresden-Rossendorf

Kliem, S.; Grahn, A.; Rohde, U.; Schütze, J.; Frank, T.
Coupling of the CFD code ANSYS CFX with the 3D neutron kinetic core model DYN3D
20th Symposium of AER on VVER Reactor Physics and Reactor Safety, 20.-24.09.2010, Espoo, Finnland
Proceedings of the 20th Symposium of AER on VVER Reactor Physics and Reactor Safety, CDROM paper 5.5, Budapest: KFKI AEKI

Kliem, S.; Rohde, U.; Schütze, J.; Frank, T.
Prototype coupling of the CFD code ANSYS CFX with the 3D neutron kinetic core model DYN3D
Jahrestagung Kerntechnik 2010, 04.-06.05.2010, Berlin, Deutschland
Tagungsband der Jahrestagung Kerntechnik 2010 paper 104, Berlin: INFORUM GmbH

Kliem, S.; Rohde, U.; Schütze, J.; Frank, T.
Prototype coupling of the CFD software ANSYS CFX with the 3D neutron kinetic core model DYN3D
PHYSOR 2010, 09.-14.05.2010, Pittsburgh, USA
Proceedings of the PHYSOR 2010, La Grange Park, Illinois, USA: ANS, 9780894480799

Kratzsch, A.; Renger, S.; Kaestner, W.; Hampel, R.; Krepper, E.
Influence of an impinging jet on sedimented debris
18th International Conference on Nuclear Engineering, ICONE18, 17.-21.05.2010, Xi'an, China

Krepper, E.; Grahn, A.; Cartland-Glover, G.; Weiss, F.-P.; Alt, S.; Kratzsch, A.; Renger, S.; Kästner, W.
CFD-Analyses on the behaviour of mineral wool in the reactor sump
Fachtagung der KTG-Fachgruppen, 07.-08.10.2010, Rossendorf, Deutschland
Aktuelle Themen der Reaktorsicherheitsforschung in Deutschland

Krepper, E.; Lucas, D.; Schmidtke, M.
Modelling of turbulence in bubbly flows
7th International Conference on Multiphase Flow, ICMF 2010, 30.05.-04.06.2010, Tampa, USA

Krepper, E.; Schmidtke, M.; Lucas, D.; Beyer, M.
Steam bubble condensation in polydispersed flow experiments and CFD simulations
Int. Conf. "Nuclear Energy for New Europe", 06.09.-09.10.2010, Portoz, Slovenien

Krepper, E.; Weiss, F.-P.; Alt, S.; Kratzsch, A.; Renger, S.; Kästner, W.
Some nuclear reactor safety related aspects of plunging jets
18th International Conference on Nuclear Engineering, ICONE18, 17.-21.05.2010, Xi'an, China

Kryk, H.; Hoffmann, W.; Härting, H.-U.
Versuchsanlagen für die Untersuchung von Korrosionsprozessen
Fachkolloquium zum BMWi-Vorhaben 150 1363 „Isolationsmaterialbelastete Kühlmittelströmung, 03.03.2010, Rossendorf, Deutschland

Labois, M.; Panyasantisuk, J.; Lakehal, D.; Höhne, T.; Kliem, S.
On the prediction of boron dilution using the CMFD code TRANSAT: the ROCOM test case
CFD4NRS-3, 14.-16.09.2010, Washington, USA
CD-ROM

Liao, Y.; Lucas, D.; Krepper, E.
Influence of two-phase turbulence models on the bubble coalescence and breakup behavior in bubbly pipe flow
The 8th International Topical Meeting on Nuclear Thermal-Hydraulics, Operation and Safety (NUTHOS-8), 10.-14.10.2010, Shanghai, China

Liao, Y.; Lucas, D.; Krepper, E.
Validation of a generalized model for bubble coalescence and breakup in MUSIG approach
Jahrestagung Kerntechnik 2010, 04.-06.05.2010, Berlin, Germany

Lifante, C.; Frank, T.; Burns, A. D.; Lucas, D.; Krepper, E.
Prediction of polydisperse steam bubble condensation in sub-cooled water using the Inhomogeneous MUSIG model
CFD4NRS-3, Workshop on Experimental Validation and Application of CFD and CMFD Codes to Nuclear Reactor Safety Issues, paper 13.3, 14.-16.09.2010, Washington D.C., USA

Lifante, C.; Frank, T.; Burns, A. D.; Lucas, D.; Krepper, E.
Prediction of polydisperse steam bubble condensation in sub-cooled water using the Inhomogeneous MUSIG model
7th International Conference on Multiphase Flow, ICMF 2010, 30.05.-04.06.2010, Tampa, FL, USA
paper 5.6.4

Lopez, Jose M.; Danciu, Dana V.; Da Silva, Marco J.; Hampel, U.; Mohan, R.
Experiments on air entrainment due to free falling- and wall-jets
ASME 2010 Fluids Engineering Summer Meeting FEDSM 2010, 01.-05.08.2010, Montreal, Canada

Lopez, Jose M.; Danciu, Dana V.; Da Silva, Marco J.; Hampel, U.; Mohan, R.
Experimental study of gas entrainment by liquid falling film around a stationary Taylor bubble in vertical downward flow
2010 ECTC Proceedings ASME Early Career Technical Conference, 25.-27.03.2010, Tulsa, USA

Lopez, Jose M.; Danciu, Dana V.; Da Silva, Marco J.; Hampel, U.; Mohan, R.
Experimental study and flow visualization of gas entrainment in downward flow
7th International Conference on Multiphase Flow,ICMF 2010, 30.05.-04.06.2010, Tampa, Florida, USA

Lucas, D.; Beyer, M.; Szalinski, L.
CFD-grade databases on two-phase upwards vertical pipe flows
ANS 2010 Winter Meeting, 07.-11.11.2010, Las Vegas, U.S.A.
Transactions of the ANS 2010 Winter Meeting

Lucas, D.; Beyer, M.; Szalinski, L.
Experimental data on steam bubble condensation in poly-disperded upward vertical pipe flow
CFD4NRS-3, International Workshop on Experimental Validation and Application of CFD and CMFD Codes to Nuclear Reactor Safety Issues, Paper 13.1, 14.-16.09.2010, Washington D.C., USA

Lucas, D.; Krepper, E.
Modeling poly-dispersed flows with the Inhomogeneous MUSIG model
ANS 2010 Winter Meeting, 07.-11.11.2010, Las Vegas, U.S.A.
Transactions of the ANS 2010 Winter Meeting

M. Murase, M.; Kinoshita, I.; Utanohara, Y.; Lucas, D.; Vallée, C.; Tomiyama, A.
Numerical calculations for air-water tests on CCFL in different-scale models of a PWR hot leg
18th International Conference on Nuclear Engineering (ICONE18), paper ICONE18-29092, 17.-21.05.2010, Xi'an, China
Proceedings of the 18th International Conference on Nuclear Engineering

Merk, B.; Glivici-Cotruta, V.; Weiß, F. P.
A solution for the telegrapher's equation with external source: application to YALINA - SC3A and SC3B
PHYSOR 2010, 09.-14.05.2010, Pittsburgh, USA

Merk, B.; Scholl, S.; Fridman, E.
Analsyis of the spatial isotopic distributions during the burnup of UMOX- and ThMOX-fuels on unit cell basis
PHYSOR 2010, 09.-14.05.2010, Pittsburgh, USA

Murase, M.; Kinoshita, I.; Utanohara, Y.; Lucas, D.; Vallée, C.; Tomiyama, A.
Countercurrent gas-liquid flow in a hot leg under reflux cooling - numerical calculations for air-water tests at FZD
Annual meeting of the Atomic Energy Society of Japan, 26.-28.03.2010, Ibaraki, Japan, 236

Mutschke, G.; Tschulik, K.; Weier, T.; Uhlemann, M.; Bund, A.; Fröhlich, J.
On the action of magnetic gradient forces in micro-structured copper deposition
61st Annual Meeting of the International Society of Electrochemistry, 26.09.-01.10.2010, Nizza, Frankreich

Nariai, T.; Tomiyama, A.; Vallée, C.; Lucas, D.; Kinoshita, I.; Murase, M.
Counter-current flow limitation in a scale-down model of a PWR hot leg
The 8th International Topical Meeting on Nuclear Thermal-Hydraulics, Operation and Safety (NUTHOS-8), 10.-14.10.2010, Shanghai, China, # N8P0109

Pal, J.; Cramer, A.; Gerbeth, G.
The sensitivity of the flow driven by a travelling magnetic field to axial alignment
The 7th International Symposium on Ultrasonic Doppler Methods for Fluid Mechanics and Fluid Engineering, 07.-09.04.2010, Göteborg, Sweden
Proceedings of the 7th International Symposium on Ultrasonic Doppler Methods for Fluid Mechanics and Fluid Engineering, 978-91-7290-292-3, 85-88

Park, J.-S.; Pal, J.; Cramer, A.; Gerbeth, G.; Taniguchi, S.
Induction heating for pendent-drop melt extraction from a metallic sheet
The 4th Asian Workshop on EPM, 03.-06.10.2010, Jeju, Korea
Induction heating for pendent-drop melt extraction from a metallic sheet, pp. 252-256

Pryadko, E. L.; Reuther, H.; Shevchenko, N.; Markov, A. B.; Kolitsch, A.
Phase Composition of 316L Stainless Steel after Electron-Beam Irradiation Followed by Chromium Ion Implantation
10th Int. Conf. on Modification of Materials with Particle Beams and Plasma Flows, 19.-24.09.2010, Tomsk, Russland
Proc. 10th Int. Conf. on Modification of Materials with Particle Beams and Plasma Flows: Publishing House of the IOA SB RAS, 153-155

Räbiger, D.; Leonhardt, M.; Eckert, S.; Gerbeth, G.
Anwendung zeitmodulierter AC-Magnetfelder zum Rühren metallischer Schmelzen während der Erstarrung einer Al-Si-Legierung
Tagung Stranggiessen, 15.-17.11.2010, Neu-Ulm, Deutschland
Stranggießen, Frankfurt: Werkstoff-Informationsgesellschaft mbH, 978-3-88355-384-9, 163-168

Räbiger, D.; Zhang, C.; Grants, I.; Eckert, S.; Gerbeth, G.
Investigations of the bulk flow inside a cylindrical liquid metal column generated by diverse AC magnetic fields
6th Annual European Rheology Conference (AERC2010), ISUD7, 07.-09.04.10, Göteborg, Schweden
Proceedings of the 7th International Symposium on Ultrasonic Doppler Methods for Fluid Mechanics and Fluid Engineering, 81-84

Rindelhardt, U.; Fröhler, D.
Betriebserfahrungen mit der 40-MW-Photovoltaik-Anlage Waldpolenz
25. Symposium Photovoltaische Solarenergie, 03.-05.03.2010, Staffelstein, Deutschland
25. Symposium Photovoltaische Solarenergie, Regensburg: Otti, 978-3-941785-23-6, 152-157

Rohde, U.; Baier, S.; Duerigen, S.; Fridman, E.; Merk, B.; Weiss, F.-P.
Development of the coupled 3D neutron kinetics/thermal-hydraulics code DYN3D-HTR for the simulation of transients in block-type HTGR
5th Topical Meeting on High Temperature Reactor Technology, 18.-20.10.2010, Pargue, Czech Republic
Conference Website http://www.htr2010.eu/authors-area/upload/docs/htr2010_pdfonly.rar, Paper #036

Rohde, U.; Merk, B.; Baier, S.; Fridman, E.; Dürigen, S.; Kliem, S.; Weiss, F.-P.
Development of a reactor dynamics code for block-type HTR at Forschungszentrum Dresden-Rossendorf
Fachtag der KTG: "Aktuelle Themen der Reaktorsicherheitsforschung in Deutschland", 07.-08.10.2010, Dresden, Deutschland, 07.-08.10.2010, Dresden, Deutschland
Tagungsband des Fachtages der KTG: "Aktuelle Themen der Reaktorsicherheitsforschung in Deutschland", CDROM

Schmidtke, M.; Krepper, E.; Lucas, D.; Beyer, M.
CFD-simulations and experiments on steam condensation in polydisperse bubbly flows
Jahrestagung Kerntechnik 2010, 04.-06.05.2010, Berlin, Deutschland

Schubert, M.; Fischer, F.; Hampel, U.
Detection of gas-liquid dynamics in monolithic channels using ultra-fast x-ray tomography
6th World Congress On Industrial Process Tomography (WCIPT6), 06.-09.09.2010, Bejing, China

Sharaf, S.; Azzopardi, B.; Hampel, U.; Zippe, C.; Beyer, M.; Da Silva, M. J.
Comparison between wire mesh sensor technology and gamma densitometry
6th World Congress On Industrial Process Tomography (WCIPT6), 06.-09.09.2010, Bejing, China
Proceedings of the 6th World Congress On Industrial Process Tomography, 1464-1472

Terzija, N.; Yin, W.; Peyton, A.; Gerbeth, G.; Stefani, F.; Timmel, K.; Wondrak, T.
Use of electromagnetic induction tomography for monitoring liquid metal/gas flow regimes on a model of an industrial steel caster
6th World Congress on Industrial Process Tomography, 06.-9.9.2010, Peking, China, 1033-1041

Timmel, K.; Eckert, S.; Gerbeth, G.
Ultrasonic flow measurements in a low temperature liquid metal model of the continuous steel casting process
6th Annual European Rheology Conference (AERC2010), ISUD7, 07.-09.04.10, Göteborg, Schweden
Proceedings of the 7th International Symposium on Ultrasonic Doppler Methods for Fluid Mechanics and Fluid Engineering, 93-96

Timmel, K.; Galindo, V.; Miao, X.; Eckert, S.; Gerbeth, G.
Physikalische Modellierung des Stranggussprozesses mit niedrig schmelzenden Legierungen
Symposium Stranggießen, 15.-17.11.2010, Neu-Ulm, Deutschland

Tobisch, S.; Krug, D.; Mäbert, M.; Bieberle, A.
Möglichkeiten und Potentiale einer modernen Faserstoffherstellung
14. Holztechnologisches Kolloquium - Werkstoffe aus Holz und Holzverarbeitung im Fokus von Forschung und Entwicklung, 08.-09.04.2010, Dresden, Deutschland
Möglichkeiten und Potentiale einer modernen Faserstoff-herstellung

Tselishcheva, Elena A.; Podowski, Michael Z.; Antal, Steven P.; Post Guillen, D.; Beyer, M.; Lucas, D.
Analysis of developing gas/liquid two-phase flows
7th International Conference on Multiphase Flow, ICMF 2010, 30.05.-04.06.2010, Tampa, USA
Analysis of developing gas/liquid two-phase flows

Tusheva, P.; Altstadt, E.; Weiss, F.-P.
Investigations on in-vessel melt retention for VVER-1000 reactors
Jahrestagung Kerntechnik 2010, 04.-06.05.2010, Berlin, Germany
Tagungsband JTKT2010, CD-ROM

Tusheva, P.; Schäfer, F.; Reinke, N.; Weiss, F.-P.
Assessment of early-phase accident management strategies in a station backout scenario for VVER-1000 Reactors
ICONE 18, 17.-21.05.2010, Xi'an, China

Vallée, C.; Seidel, T.; Lucas, D.; Tomiyama, A.; Murase, M.
Comparison of countercurrent flow limitation experiments performed in two different models of the hot leg of a PWR with rectangular cross-section
18th International Conference on Nuclear Engineering (ICONE18), 17.-21.05.2010, Xi'an, China, Paper ICONE18-30089

Viehrig, H.-W.
The Master Curve approach an approved fracture mechanics test method for more than one decade
COMAT 2010 RECENT TRENDS IN STRUCTURAL MATERIALS, 25.-26.11.2010, Plzen, Czech Republic
Proceedings of COMAT 2010 Recent Trends in Structural Materials, Plzen: COMTES FHT a.s.

Viehrig, H.-W.; Houska, M.; Arora, K. S.; Rindelhardt, U.
What one learns from reactor pressure vessels of decommissioned nuclear power plants.
International Symposium FONTEVRAUD 7: Contribution of Materials Investigations to Improve the Safety and Performance of LWRs, 26.-30.09.2010, Avignon, France
Proceedings of the International Symposium FONTEVRAUD 7: French Nuclear Energy Society

Viehrig, H.-W.; Houska, M.; Arora, K. S.; Rindelhardt, U.
Post Mortem Investigations of Greifswald WWER-440 Reactor Pressure Vessels
11th International Conference "Material Issues in Design, Manufacturing and Operation of Nuclear Power Plants Equipment, 14.-18.06.2010, St. Petersburg, Russia
Proceedings of the 11th International Conference Material Issues in Design, Manufacturing and Operation of Nuclear Power Plants Equipment, St. Petersburg

Viehrig, H.-W.; Zurbuchen, C.; Schindler, H.-J.; Kalkhof, D.
Effects of specimen size, initial crack acuity and test temperature on the master curve reference temperature
18th European Conference on Fracture, 30.08.-03.09.2010, Dresden, Germany
Proceedings of the 18th European Conference on Fracture: 18th European Conference on Fracture

Weiss, F.-P.; Schaefer, F.; Kliem, S.; Tusheva, P.
Analysis of Design Basis Accidents
Analysis of Design Basis Accidents, 24.-26.08.2010, Aix-en Provence, Frankreich

Willschütz, H.-G.; Diercks, F.; Leyer, S.; Krüssenberg, A.-K.; Schäfer, F.; Hristov, H. V.
Experimentelle und analytische Untersuchungen zu passiven Komponenten des KERENA TM Konzeptes im Versuchsstand INKA
42. Kraftwerkstechnisches Kolloquium 2010, 12.-13.10.2010, Congress Center Dresden, Deutschland
Experimentelle und analytische Untersuchungen zu passiven Komponenten des KERENA TM Konzeptes im Versuchsstand INKA

Willschütz, H.-G.; Leyer, S.; Krüssenberg, A.-K.; Schäfer, F.
Calculation of the operation mode of the emergency condenser (EC) of the INKA test facility with ATHLET
Annual Meeting on Nuclear Technology (Jahrestagung Kerntechnik), 04.-06.05.2010, Berlin, Deutschland
Jahrestagung Kerntechnik - Annual Meeting on Nuclear Technology, 04.-06. Mai 2010

Wondrak, T.; Stefani, F.; Timmel, K.; Galindo, V.; Gundrum, T.; Gerbeth, G.
Contactless inductive flow tomography: principles and application to a model of continuous casting
6th World Congress on Industrial Process Tomography, 06.-9.9.2010, Peking, China
6th World Congress on Industrial Process Tomography, 1051-1066

Zheng, G.; Schubert, M.; Hampel, U.; Grünewald, M.
Monitoring of multi-phase distribution in packing columns using wire-mesh sensor
6th World Congress on Industrial Process Tomography (WCIPT6), 06.-09.09.2010, Bejing, China

FZD reports and other reports

Bärtling, Y.; Hoppe, D.; Hampel, U.
Preliminary investigations on high energy electron beam tomography
Wissenschaftlich-Technische Berichte / Forschungszentrum Dresden-Rossendorf; FZD-544 2010

Bergner, F.; Birkenheuer, U.; Ulbricht, A.
Validierung von Software-Komponenten zur Voraussage der strahleninduzierten Schädigung von RDB-Stahl
Wissenschaftlich-Technische Berichte / Forschungszentrum Dresden-Rossendorf; FZD-533 2010

Bieberle, M.
Bildrekonstruktion für die ultraschnelle Limited-Angle-Röntgen-Computertomographie von Zweiphasenströmungen
Dresden: TUDpress, 2010

Kliem, S.
Ein Modell zur Beschreibung der Kühlmittelvermischung und seine Anwendung auf die Analyse von Borverdünnungstransienten in Druckwasserreaktoren
Wissenschaftlich-Technische Berichte / Forschungszentrum Dresden-Rossendorf; FZD-539 2010

Rohde, U.; Kozmenkov, Y.; Matveev, Y.; Pivovarov, V.
WTZ mit Russland - Transientenanalysen für Kernreaktoren - Abschlussbericht
Wissenschaftlich-Technische Berichte / Forschungszentrum Dresden-Rossendorf; FZD-543 2010

Seidel, T.; Vallée, C.; Lucas, D.; Beyer, M.; Deendarlianto,.
Two-phase flow experiments in a model of the hot leg of a pressurised water reactor
Wissenschaftlich-Technische Berichte / Forschungszentrum Dresden-Rossendorf; FZD-531 2010

Viehrig, H.-W.; Zurbuchen, C.; Schindler, H.-J.; Kalkhof, D.
Application of the Master Curve approach to fracture mechanics characterisation of reactor pressure vessel steel
Wissenschaftlich-Technische Berichte / Forschungszentrum Dresden-Rossendorf; FZD-536 2010

Weiss, F.-P.; Schäfer, F. (Editors)
Annual Report 2009 - Institute of Safety Research
Wissenschaftlich-Technische Berichte / Forschungszentrum Dresden-Rossendorf; FZD-541 2010

Granted patents

Eckert, S.; Räbiger, D.; Willers, B.; Gerbeth, G.; Nikrityuk, Petr A.; Eckert, K.; Grundmann, R.
Verfahren und Einrichtung zum elektromagnetischen Rühren von elektrisch leitenden Flüssigkeiten
Patent DE102007037340B4 2010/02/25

Hampel, U.
Anordnung zur Elektronenstrahltomographie
Anmeldung: DE 10 2009 002 114 A1 2010.10.14

Pietruske, H.; Sühnel, T.; Prasser, H.
Gittersensor
Patent US 7,795,883 B2 - 2010/09/14

PhD and diploma theses

PhD theses

Zhang, Chaojie
Liquid Metal flows Driven by Gas Bubbles in a Static Magnetic Field
Technische Universität Dresden

Kliem, Sören
Ein Modell zur Beschreibung der Kühlmittelvermischung und seine Anwendung auf die Analyse von Borverdünnungstransienten in Druckwasserreaktoren
Technische Universität Dresden

Steffen Böhlke
Analyse der Reaktivitätswirksamkeit von Bor in SWR-Brennelementen bei transienten Kernzuständen
Technische Universität Dresden

Diploma theses

Alexander Dick
Modellierung der Nachkühlkette eines Siedewasserreaktors mit ATHLET
Hochschule Zittau/Görlitz

Bever, Thomas
Untersuchungen zum Einfluss der Vernetzung der Rissspitze in Local-Approach Modellen
Technische Universität Dresden

Awards

Martina Bieberle

Doktorandenpreis 2010

Bildrekonstruktion für die ultraschnelle Limited-Angle-Röntgen-Computertomographie von Zweiphasenströmungen

Date of award: April 2011

Cornelia Heintze

Kompetenzpreis

2. Preis im Siempelkamp-Kompetenzworkshop „Kompetenzerhaltung in der Kerntechnik“ zur Jahrestagung Kerntechnik 2010

Date of award: May 2010

Iurii Bilodid

Best Presentation Competition, ICONE 18 2010, Xi’an/China
Modeling the Spectral History in the Depletion of a PWR Core

Date of award: May 2010

Andre Bieberle

Commerzbank-Preis 2009

Räumlich hoch auflösende Computertomografie mit Gammastrahlung zur Untersuchung von Mehrphasenströmungen

Date of award: June 2010

Guests

Zidouni, Faiza
31 January 2010 – 30 April 2010
Nuclear Research Energy Center of Birine / Algerien

Grants, Ilmars Dr.
25 May 2010 – 11 June 2010
29 November 2010 – 31 December 2010
Institute of Physics, Riga / Lettland

Li, Donggang Dr.
19 May – 31 May 2010
Northeastern University Shenyang / China

Gokhman, Oleksander Prof.
01 August 2010 – 30 September 2010
Southukrainian State University of Education, Odessa / Ukraine

Ieremenko, Maksym
08 August 2010 – 14 August 2010
Scientific-Technical Centre for Nuclear and Radiation Safety of the Ukraine, Kiew / Ukraine

Ovdiyenko, Yurii
08 August 2010 – 14 August 2010
Scientific-Technical Centre for Nuclear and Radiation Safety of the Ukraine, Kiew / Ukraine

Plevachuk, Yuri
02 November 2010 – 05 November 2010
Ivan Franko National University, Lviv / Ukraine

Gailitis, Agris Prof.
20 November 2010 . 27 November 2010
Institute of Physics, Riga / Lettland

Karule, Erna Dr.
20 November 2010 – 27 November 2010
Institute of Physics, Riga / Lettland

Priede, Janis
21 November 2010 – 23 November 2010
Coventry University / United Kingdom

Jain, Nitin
02 December 2010 – 31 December 2010
Indian Institute of Kanpur / India

Meetings and workshops

Kick-Off-Meeting of the EU Integrated Project LONGLIFE
Treatment of long term irridation embrittlement effects in RPV safety assessment
27 participants
Rossendorf, 25-26 February 2010

ANSYS-FZD Workshop
Multi-Phase Flow: Simulation, Experiment and Application
85 participants
Rossendorf, 22-24 June 2010

Sitzung der Reaktorsicherheits-Kommission
67. Sitzung des RSK-Ausschusses Anlagen- und Systemtechnik
25 participants
Rossendorf, 06 October 2010

Fachtag der Kerntechnischen Gesellschaft (KTG)
Fachtagung der KTG-Fachgruppen: Aktuelle Themen der Reaktorsicherheitsforschung in Deutschland
100 participants
Rossendorf, 07-08 October 2010

13th MHD-Days 2010
70 participants
Rossendorf, 22-23 November 2010

Seminars of the institute

Dr. Lorenzo Malerba (SCK CEN Mol, Belgien)
Modelling nanostructural changes in metals under irridation
12 January 2010

Dr. Tom Weier
Elektrochemische Energiespeicher – Was könnte die MHD beitragen?
27 January 2010

Dr. Frank Schäfer
Simulation des Betriebs- und Störfallverhaltens von Siedewasserreaktoren
11 February 2010

Dr. R. Jacqmin (Reactor Physics Division Cadarache / CEA)
Innovative fast reactor core physics studies at CEA
04 March 2010

Dr. Emil Fridman
Use of thorium in Pressurized Water Reactors
17 March 2010

Dr. D. Hoppe
Gammatomographische Dampfgehaltsmessungen in elektrisch beheizten Stabbündeln
08 April 2010

E. Schleicher
Zweiphaseninstrumentierung zur Untersuchung des Kühlverhaltens des KERENA-Notkondensators
29 April 2010

Dr. A. Giesecke
Simulationen der kinematischen Induktionsgleichung für das VKS-Dynamo Experiment
20 May 2010

C. Heintze, Dr. F. Bergner
Irridation behaviour of Fe-Cr alloys
03 June 2010

C.-L. Chen (I-Sou University Kaosiung, Taiwan)
Irradiation damage in dual beam irradiated nanostructured FeCrAl oxide dispersion strengthened steel
19 August 2010

Dr. D. Struwe (KIT Karlsruhe)
Sicherheitseigenschaften Natrium-gekühlter Reaktorsysteme
02 September 2010

Dr. H.-V. Hristov, Dr. F. Schäfer
Modelling of the passive cooling systems of the KERENA^{TM} boiling water reactor with ATHLETH
16 September 2010

St. Wissel (IER Stuttgart)
Ganzheitliche Bewertung der Kernenergie im Hinblick auf eine nachhaltige Energieversorgung
21 October 2010

Dr. H.-G. Sonnenburg (Gesellschaft für Anlagen- und Reaktorsicherheit)
Neuere Erkenntnisse und sicherheitstechnische Aspekte zu Brennstab-Phänomenen
28 October 2010

V. Glivici-Cotruta
Development and evaluation of analytical solutions for improved analysis of YALINA experiments
12 November 2010

Dr. W. Hoffmann, Dr. H. Kryk
Untersuchungen von Korrosionsprozessen bei Kühlmittelverluststörfällen
25 November 2010

M. Beyer
Experimentelle Untersuchung polydisperser Dampf/Wasser-Strömungen mit Phasenübergang in einer vertikalen DN200-Teststrecke
09 December 2010

Lecture courses

Frank-Peter Weiß
Zuverlässigkeit und Sicherheit technischer Systeme
TU Dresden, Fakultät Maschinenwesen
Summer semester 2010 and winter semester 2010

Matthias Werner
Zuverlässigkeit und Sicherheit technischer Systeme
TU Dresden, Fakultät Maschinenwesen
Summer semester 2010 and winter semester 2010

Udo Rindelhardt
Erneuerbare Energien I und II
Technische Universität Chemnitz, Fakultät für Elektrotechnik/Informationstechnik
Summer semester 2010 and winter semester 2010

Uwe Hampel
Computertomographie in der Medizin und Prozessdiagnostik
TU Dresden, Fakultät Elektro- und Informationstechnik
Summer semester 2010 and winter semester 2010

Departments of the institute

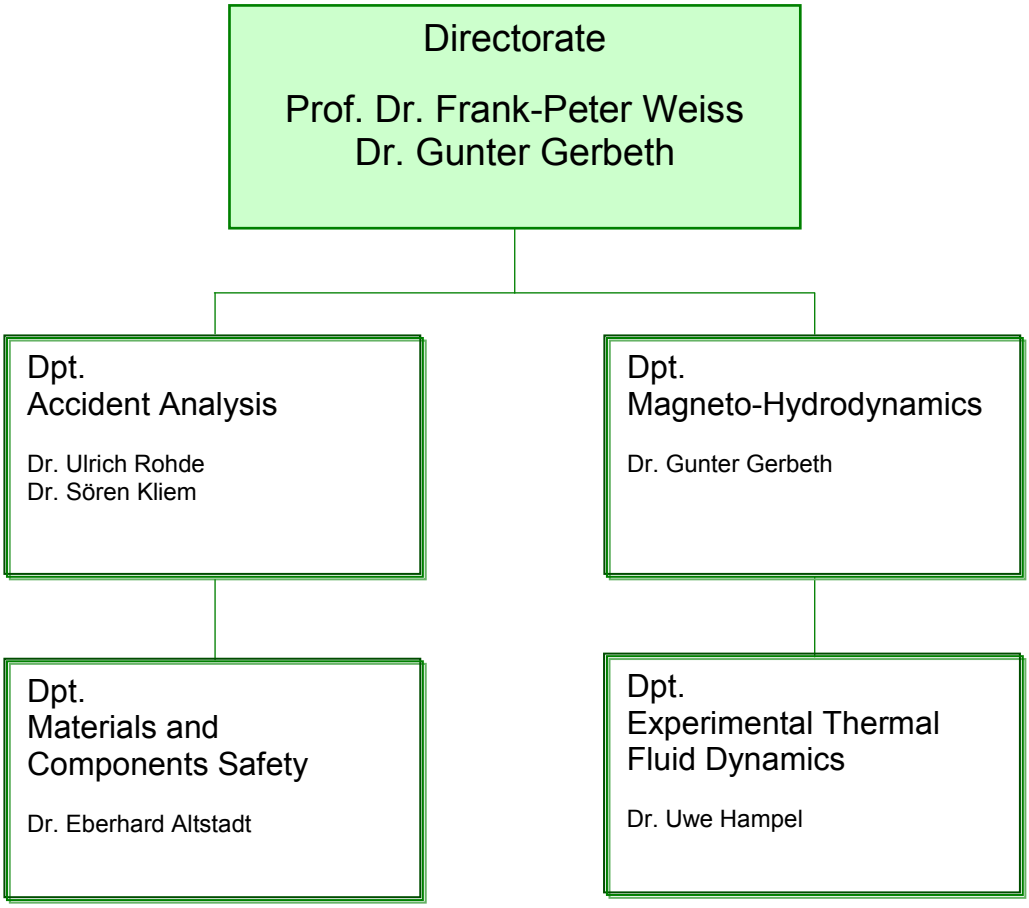

Personnel

Director: Prof. Dr. Frank-Peter Weiß (01.01.2010-31.10.2010)
Acting Director: Dr. Gunter Gerbeth (01.11.2010-31.12.2010)

Scientific Staff

Altstadt, Eberhard Dr.
Apanasevich, Pavel
Arifin, Defiar Nur
Arora, Kanwer Shing
Baier, Silvio Dr.
Barth, Thomas
Bergner, Frank Dr.
Beyer, Matthias
Bieberle, André Dr.
Bieberle, Martina Dr.
Birkenheuer, Uwe Dr.
Carl, Helmar Dr.
Cartland-Glover, Gregory Dr.
Cramer, Andreas Dr.
Eckert, Sven Dr.
Ferrari, Anna Dr.
Fridman, Emil Dr.
Galindo, Vladimir Dr.
Gerbeth, Gunter Dr.
Giesecke, Andre
Grahn, Alexander Dr.
Gundrum, Thomas
Günther, Uwe Dr.
Hampel, Uwe Dr.
Hoffmann, Wolfgang Dr.
Hoppe, Dietrich Dr.
Höhne, Thomas Dr.
Holt, Lars
Houska, Mario
Kliem, Sören Dr.
Konheiser, Jörg
Kozmenkov, Yroslav Dr.
Krepper, Eckhard Dr.
Kryk, Holger Dr.
Küchler, Roland Dr.
Leonhardt, Monika
Lucas, Dirk Dr.
Merk, Bruno Dr.
Mittag, Siegfried Dr.
Pal, Josef Dr.
Rindelhardt, Udo Prof. Dr.
Rohde, Ulrich Dr.
Rzehak, Roland Dr.
Schäfer, Frank Dr.
Schleicher, Eckhard
Schmidtke, Martin Dr.
Schubert, Markus Dr.
Shatrov, Viktor Dr.
Shevchenko, Natalia Dr.
Springer, Richard
Stefani, Frank Dr.
Talati, Minaben Dr.
Thiele, Marlen
Tietze, Henrik
Timmel, Klaus
Ulbricht, Andreas Dr.
Viehrig, Hans-Werner Dr.
Weier, Tom Dr.
Werner, Matthias Dr.
Zhang, Dongsheng Dr.
Zippe, Cornelius Dr.

PhD Students

Al-Asqalani, Ahmed Tamer
Baldova, Daniela
Barthel, Frank
Bärtling, Yves
Bilodid, Yuri
Boden, Stephan
Buchenau, Dominique
Danciu, Dana-Veronica
Dürigen, Susan
Heintze, Cornelia
Glivici-Cotruta, Varvara
Houenouvo, Hermann A.T.
Liao, Yixiang
Miao, Xincheng
Räbiger, Dirk
Reinecke, Sebastian
Seidel, Tobias
Seilmeyer, Martin
Tusheva, Polina
Valleé, Christophe
Wagner, Arne
Wondrak, Thomas
Xie, Miao

Technical Staff

Albrecht, Thomas
Berger, Ronny
Berger, Torsten
Bombis, Doris
Borchardt, Steffen
Erlebach, Stephan
Franz, Ronald
Futterschneider, Hein
Gommlich, André
Kunadt, Heiko
Lindner, Klaus
Losinski, Claudia
Löschau, Marcel
Mitreuter, Marcel
Müller, Gudrun Dr.
Nehring, Harald
Nowak, Bernd
Paul, Sebastian
Pietzsch, Jens
Pietruske, Heiko
Richter, Annett
Richter, Henry
Roßner, Michaela
Rott, Sonja
Röder, Michael
Ruhland, Henry
Rußig, Heiko
Schleßiger, Heike
Schütz, Peter
Skorupa, Ulrich
Sprewitz, Uwe
Szalinski, Lutz
Tamme, Marko
Thiel, Andre
Tschofen, Martin
Vetter, Petra
Webersinke, Wolfgang
Weichelt, Steffen
Weiß, Rainer
Zimmermann, Wilfried